Microscopic approach to high-temperature superconductors within the t-J model

S. Sykora and K. W. Becker
Institut für Theoretische Physik, Technische Universität Dresden, 01062 Dresden, Germany
(Received 3 March 2009; published 14 July 2009)

Despite the intense theoretical and experimental effort, an understanding of the superconducting pairing mechanism of the high-temperature superconductors leading to an unprecedented high transition temperature T_c is still lacking. An additional puzzle is the unknown connection between the superconducting gap and the so-called pseudogap which is a central property of the most unusual normal state. Angle-resolved photoemission spectroscopy (ARPES) measurements have revealed a gaplike behavior on parts of the Fermi surface, leaving a nongapped segment known as Fermi arc around the diagonal of the Brillouin zone. Two main interpretations of the origin of the pseudogap have been proposed: either the pseudogap is a precursor to superconductivity, or it arises from another order competing with superconductivity. Starting from the t-J model, in this paper we present a microscopic approach to investigate physical properties of the pseudogap phase as well as the superconducting phase in the framework of a renormalization scheme called projector-based renormalization method. This approach is based on a stepwise elimination of high-energy transitions using unitary transformations. We arrive at renormalized "free" Hamiltonians for correlated electrons for both phases. Our microscopic approach allows us to explain the experimental findings in the underdoped as well as in the optimal hole doping regime. The ARPES spectral function along the Fermi surface turns out to be in good agreement with experiment: For the pseudogap phase we find well-defined excitation peaks around $\omega=0$ near the nodal direction, which become strongly suppressed around the antinodal point. The origin of the pseudogap can be traced back to a suppression of spectral weight from incoherent excitations in a small ω range around the Fermi energy. In the superconducting phase, the order parameter turns out to have d-wave symmetry with a coherence length of a few lattice constants. In good agreement with experiments, we find no superconducting solutions for very small hole doping.

DOI: 10.1103/PhysRevB.80.014511 PACS number(s): 71.10.Fd, 71.30.+h

I. INTRODUCTION

Since the discovery of superconductivity in the cuprates,[1] enormous theoretical and experimental effort has been made to investigate the superconducting pairing mechanism which leads to an unprecedented high transition temperature T_c.[2–6] The generic phase diagram of the cuprates shows a wide variety of different behavior as a function of temperature and level of hole doping. In particular, with increasing hole doping away from half-filling, the physical properties completely change at the transition to the superconducting phase. An additional puzzle is the unknown connection between the superconducting gap and the so-called pseudogap which is a central property of the most unusual normal state of the cuprates. In particular, the pseudogap has been subject to intense debates.

Studies using angle resolved photoemission spectroscopy (ARPES) have revealed several key features of the pseudogap and the superconducting gap in the cuprates by elucidating the detailed momentum and temperature dependence.[7–13] It was found that the pseudogap opens on a part of the Fermi surface (FS) around the antinodal point, leaving a nongapped FS segment known as a Fermi arc around the nodal direction. The pseudogap also smoothly evolves with decreasing temperature into the SC gap and was, therefore, interpreted in favor of a "precursor pairing" scenario.[14,15] On the other hand, there are several experimental and theoretical reports which suggest a different origin for the pseudogap, such as caused by another order which competes with the superconducting order.[8] Superconductivity is usually understood as an instability from a nonsuperconducting state. Therefore, often in theoretical investigations, the starting point was either the Fermi-liquid or the antiferromagnetic phase at large or low doping. In this paper, we take a different approach and only consider hole fillings, in which either a superconducting or a pseudogap phase is present.

A generally accepted model for the cuprates is the t-J model which describes the electronic degrees of freedom in the copper-oxide planes for low energies. Alternatively, one could also start from a one-band Hubbard Hamiltonian as a minimal model. However, for low-energy excitations, the latter model reduces to the t-J model so that both models are equivalent. As our theoretical approach, we use a recently developed projector-based renormalization method which is called PRM.[16] The approach is based on a stepwise elimination of high-energy transitions using unitary transformations. We thus arrive at a renormalized "free" Hamiltonian for correlated electrons which can describe the pseudogap as well as the superconducting phase. The obtained ARPES spectral function along the Fermi surface is in good agreement with experiment: For the pseudogap phase we find well-defined excitation peaks around $\omega=0$ near the nodal direction which are strongly suppressed around the antinodal point. However, in the superconducting state the spectra display peaklike structures which are caused alone by coherent excitations in a small range around the Fermi energy. The origin of the pseudogap can be traced back to a suppression of spectral weight of the incoherent excitations in a small ω range around the Fermi energy. Therefore, the usual interpretations of the pseudogap origin can not be held. Instead, the

pseudogap is an inherent property of the unusual normal state caused by incoherent excitations. The superconducting order parameter turns out to have d-wave symmetry with a coherence length of a few lattice constants. The basic feature for the understanding of the superconducting pairing mechanism in the underdoped regime is a characteristic electronic oscillation behavior between neighboring lattice sites. The oscillation becomes less important for larger δ which agrees with the weakening of the superconducting phase for larger hole doping.

First, after a short introduction of the model in Sec. II, it seems to be helpful to start from a short outline of the basic ideas of our theoretical approach (PRM) in Sec. III. A review of this approach has been given elsewhere.[16] Then, in Secs. IV and VI the PRM will be applied to the pseudogap phase and the superconducting phase. The numerical results for both phases will be discussed in Secs. V and VII, respectively.

II. MODEL

A generally accepted model for the cuprates is the t-J model. In particular, in the antiferromagnetic phase at small doping, it has turned out that it can be used to describe the electronic degrees of freedom at low energies. We adopt the same model also for somewhat larger hole concentrations, outside the antiferromagnetic phase, where the superconducting and the pseudogap phases appear,

$$\mathcal{H} = -\sum_{ij,\sigma} t_{ij}\hat{c}^{\dagger}_{i\sigma}\hat{c}_{j\sigma} - \mu\sum_{i\sigma}\hat{c}^{\dagger}_{i\sigma}\hat{c}_{i\sigma} + \sum_{ij} J_{ij}\mathbf{S}_i\mathbf{S}_j =: \mathcal{H}_t + \mathcal{H}_J. \tag{1}$$

The model consists of a hopping term $\mathcal{H}_t$ and an antiferromagnetic exchange $\mathcal{H}_J$. Here, t_{ij} stands for the hopping matrix elements between nearest (t) and next-nearest (t') neighbors. J_{ij} is the exchange coupling and μ is the chemical potential. The quantities

$$\hat{c}^{\dagger}_{i\sigma} = c^{\dagger}_{i\sigma}(1-n_{i,-\sigma}), \quad \hat{c}_{i\sigma} = c_{i\sigma}(1-n_{i,-\sigma}) \tag{2}$$

are Hubbard creation and annihilation operators. They enter the model since doubly occupancies of local sites are strictly forbidden due to the presence of strong electronic correlations. Note that the Hubbard operators restrict the unitary space to states with only either empty or singly occupied local sites. They obey nontrivial anticommutation relations

$$[\hat{c}^{\dagger}_{i\sigma},\hat{c}_{j\sigma'}]_+ = \delta_{ij}[\delta_{\sigma\sigma'}\mathcal{D}_{\sigma}(i) + \delta_{\sigma,-\sigma'}S^{\sigma}_i], \tag{3}$$

where the operator

$$\mathcal{D}_{\sigma}(i) = 1 - n_{i,-\sigma} \tag{4}$$

can be interpreted as a projector which projects on the local subspace at site i consisting of either an empty or a singly-occupied state with spin σ. Finally, $n_{i\sigma}=c^{\dagger}_{i\sigma}c_{i\sigma}$ is the local occupation number operator for spin σ, and S^{σ}_i is the $\sigma = \pm 1$ component of the local spin operator

$$\mathbf{S}_i = \frac{1}{2}\sum_{\alpha\beta}\vec{\sigma}_{\alpha\beta}\hat{c}^{\dagger}_{i\alpha}\hat{c}_{i\beta}, \tag{5}$$

where $\vec{\sigma}_{\alpha\beta}=\Sigma_{\nu}\sigma^{\nu}_{\alpha\beta}\mathbf{e}_{\nu}$ is the vector formed by the Pauli spin matrices. In Fourier notation, t-J model (1) reads

$$\mathcal{H} = \sum_{\mathbf{k},\sigma}(\varepsilon_{\mathbf{k}}-\mu)\hat{c}^{\dagger}_{\mathbf{k}\sigma}\hat{c}_{\mathbf{k}\sigma} + \sum_{\mathbf{q}} J_{\mathbf{q}}\mathbf{S}_{\mathbf{q}}\mathbf{S}_{-\mathbf{q}} = \mathcal{H}_t + \mathcal{H}_J,$$

$$\varepsilon_{\mathbf{k}} = -\sum_{i(\neq j)} t_{ij}e^{i\mathbf{k}(\mathbf{R}_i-\mathbf{R}_j)}, \quad J_{\mathbf{q}} = \sum_{i(\neq j)} J_{ij}e^{i\mathbf{q}(\mathbf{R}_i-\mathbf{R}_j)}. \tag{6}$$

Note that for convenience, we shall somewhat change the notation. From now on, all energies will be measured from the chemical potential, i.e., $\varepsilon_{\mathbf{k}}-\mu$ will be denoted by $\varepsilon_{\mathbf{k}}$.

III. PROJECTOR-BASED RENORMALIZATION METHOD

Let us start with a short introduction to the PRM,[17,16] which we shall use as our theoretical tool. The general idea is as follows: The method starts from a decomposition of a given many-particle Hamiltonian

$$\mathcal{H} = \mathcal{H}_0 + \mathcal{H}_1 \tag{7}$$

into an unperturbed part $\mathcal{H}_0$ and a perturbation $\mathcal{H}_1$. In $\mathcal{H}_1$, no parts should be contained which commute with $\mathcal{H}_0$. Therefore, $\mathcal{H}_1$ accounts for all transitions with *nonzero* energies between the eigenstates of $\mathcal{H}_0$. The aim of the PRM is to construct an effective Hamiltonian which has the same eigenspectrum as $\mathcal{H}$, and which can be solved. The first step is to construct a new renormalized Hamiltonian $\mathcal{H}_{\lambda}$ which depends on a given cutoff λ,

$$\mathcal{H}_{\lambda} = \mathcal{H}_{0,\lambda} + \mathcal{H}_{1,\lambda}, \tag{8}$$

with renormalized parts $\mathcal{H}_{0,\lambda}$ and $\mathcal{H}_{1,\lambda}$. Thereby, $\mathcal{H}_{\lambda}$ should have the following properties: (i) The eigenvalue problem of $\mathcal{H}_{0,\lambda}$ can be solved,

$$\mathcal{H}_{0,\lambda}|n^{\lambda}\rangle = E^{\lambda}_n|n^{\lambda}\rangle,$$

where E^{λ}_n and $|n^{\lambda}\rangle$ are the renormalized eigenenergies and eigenvectors. (ii) From $\mathcal{H}_{1,\lambda}$, all transition operators are eliminated which have transition energies (with respect to $\mathcal{H}_{0,\lambda}$) larger than the cutoff energy λ. As shown in Refs. 16 and 17, the renormalization step from $\mathcal{H}$ to $\mathcal{H}_{\lambda}$ can be done by use of a unitary transformation. Therefore, the eigenspectrum of $\mathcal{H}_{\lambda}$ is the same as that of $\mathcal{H}$.

The realization of the renormalization starts from the construction of $\mathcal{H}_{\lambda}$. Here, the knowledge of the eigenvalue problem of $\mathcal{H}_{0,\lambda}$ is crucial. It can be used to define generalized projection operators, P_{λ} and Q_{λ},

$$\mathsf{P}_{\lambda}\mathcal{A} = \sum_{m,n}|n^{\lambda}\rangle\langle m^{\lambda}|\langle n^{\lambda}|\mathcal{A}|m^{\lambda}\rangle\Theta(\lambda-|E^{\lambda}_n-E^{\lambda}_m|),$$

$$\mathsf{Q}_{\lambda}\mathcal{A} = (1-\mathsf{P}_{\lambda})\mathcal{A}, \tag{9}$$

which act on usual operators $\mathcal{A}$ of the Hilbert space. Note that in Eq. (9) the vectors $|n^{\lambda}\rangle$ and $|m^{\lambda}\rangle$ are necessarily nei-

ther low-nor high-energy eigenstates of $\mathcal{H}_{0,\lambda}$. P_λ projects on the part of $\mathcal{A}$ which consists of transition operators $|n^\lambda\rangle\langle m^\lambda|$ with excitation energies $|E_n^\lambda - E_m^\lambda|$ smaller than λ, whereas Q_λ projects on the high-energy transition operators of $\mathcal{A}$.

In terms of P_λ and Q_λ, the property of $\mathcal{H}_\lambda$, not to allow transitions between eigenstates of $\mathcal{H}_{0,\lambda}$ with energy differences larger than λ, reads

$$\mathsf{Q}_\lambda \mathcal{H}_\lambda = 0 \quad \text{or } \mathcal{H}_\lambda = \mathsf{P}_\lambda \mathcal{H}_\lambda. \tag{10}$$

The effective Hamiltonian $\mathcal{H}_\lambda$ is obtained from the original Hamiltonian $\mathcal{H}$ by use of a unitary transformation,

$$\mathcal{H}_\lambda = e^{X_\lambda} \mathcal{H} e^{-X_\lambda}, \tag{11}$$

where X_λ is the generator of the unitary transformation, and condition (10) has to be fulfilled. The renormalization procedure starts from the cutoff energy $\lambda = \Lambda$ of the original model $\mathcal{H}$ and proceeds in steps of width $\Delta\lambda$ to lower values of λ. Every renormalization step is performed by means of a new unitary transformation,

$$\mathcal{H}_{\lambda-\Delta\lambda} = e^{X_{\lambda,\Delta\lambda}} \mathcal{H}_\lambda e^{-X_{\lambda,\Delta\lambda}}. \tag{12}$$

Here, the generator $X_{\lambda,\Delta\lambda}$ of the transformation from cutoff λ to the reduced cutoff $(\lambda - \Delta\lambda)$ has to be chosen appropriately (see below). In this way, difference equations are derived which connect the parameters of $\mathcal{H}_\lambda$ with those of $\mathcal{H}_{\lambda-\Delta\lambda}$. They will be called renormalization equations. The limit $\lambda \to 0$ provides the desired effective Hamiltonian $\tilde{\mathcal{H}} = \mathcal{H}_{\lambda\to 0} = \mathcal{H}_{0,\lambda\to 0}$. The elimination of all transitions in the original perturbation $\mathcal{H}_1$ leads to renormalized parameters in $\mathcal{H}_{0,\lambda\to 0}$. Note that $\tilde{\mathcal{H}}$ is diagonal or at least quasidiagonal and allows to evaluate all relevant physical quantities. The final expression for $\tilde{\mathcal{H}}$ depends on the parameter values of the original Hamiltonian $\mathcal{H}$. Note that $\tilde{\mathcal{H}}$ and $\mathcal{H}$ have, in principle, the same eigenspectrum because both Hamiltonians are connected by a unitary transformation.

What is left is to find an appropriate expression for the generator $X_{\lambda,\Delta\lambda}$ of the unitary transformation which connects $\mathcal{H}_\lambda$ with $\mathcal{H}_{\lambda-\Delta\lambda}$. According to Eq. (10), $X_{\lambda,\Delta\lambda}$ is fixed by the condition $\mathsf{Q}_{\lambda-\Delta\lambda}\mathcal{H}_{\lambda-\Delta\lambda} = 0$. As is shown in Refs. 16 and 17, one can find a perturbation expansion for $X_{\lambda,\Delta\lambda}$ in terms of $\mathcal{H}_1$. The lowest nonvanishing order reads

$$X^{(1)}_{\lambda,\Delta\lambda} = \frac{1}{\mathsf{L}_{0,\lambda}} [\mathsf{Q}_{\lambda-\Delta\lambda} \mathcal{H}_{1,\lambda}] + \cdots. \tag{13}$$

Here, $\mathsf{L}_{0,\lambda}$ is the Liouville operator, defined by the commutator $\mathsf{L}_{0,\lambda}\mathcal{A} = [\mathcal{H}_{0,\lambda}, \mathcal{A}]$, for any operator quantity $\mathcal{A}$. Note that Eq. (13) can further be evaluated, in case the decomposition of $\mathsf{Q}_{\lambda-\Delta\lambda}\mathcal{H}_{1,\lambda}$ into eigenmodes of $\mathsf{L}_{0,\lambda}$ is known. Formally written, we decompose

$$\mathsf{Q}_{\lambda-\Delta\lambda}\mathcal{H}_{1,\lambda} = \sum_\nu \mathbf{F}^\nu_{\lambda,\Delta\lambda}, \quad \text{where } \mathsf{L}_{0,\lambda}\mathbf{F}^\nu_{\lambda,\Delta\lambda} = \omega^\nu_{\lambda,\Delta\lambda}\mathbf{F}^\nu_{\lambda,\Delta\lambda}, \tag{14}$$

so that $X^{(1)}_{\lambda,\Delta\lambda}$ is given by

$$X^{(1)}_{\lambda,\Delta\lambda} = \sum_\nu \frac{1}{\omega^\nu_{\lambda,\Delta\lambda}} \mathbf{F}^\nu_{\lambda,\Delta\lambda}. \tag{15}$$

IV. RENORMALIZATION APPROACH FOR THE PSEUDOGAP PHASE

A. Renormalization ansatz

Our aim is to apply the PRM to the t-J model which is a generally accepted model for the low-energy properties of the cuprate superconductors. We consider a regime with moderate hole dopings. The hole concentrations should be large enough for the system to be outside the antiferromagnetic phase but small enough to be in the metallic phase. Our first aim is to find the decomposition of the Hamiltonian into an "unperturbed" part $\mathcal{H}_0$ and into a "perturbation" $\mathcal{H}_1$. We assume that the hopping element t between nearest neighbors is large compared to the exchange coupling J. Therefore, $\mathcal{H}_t$ is the dominant part of the Hamiltonian in the metallic phase and should be included in $\mathcal{H}_0$. However, also $\mathcal{H}_J$ has a part, which commutes with the hopping term, and which will be called $\mathcal{H}_J^{(0)}$. Note that this part of $\mathcal{H}_J$ will not lead to transitions between the eigenstates of $\mathcal{H}_t$. Therefore, $\mathcal{H}_t$ and $\mathcal{H}_J^{(0)}$ together form the unperturbed Hamiltonian $\mathcal{H}_0$. The remaining part of $\mathcal{H}_J$ does not commute with $\mathcal{H}_t$ and forms the perturbation $\mathcal{H}_1$. Thus, we can write

$$\mathcal{H}_0 = \mathcal{H}_t + \mathcal{H}_J^{(0)}, \quad \mathcal{H}_1 = \mathcal{H}_J - \mathcal{H}_J^{(0)}.$$

In the framework of the PRM, the perturbation $\mathcal{H}_1$ will be integrated out by use of a unitary transformation. In lowest-order perturbation theory, the generator of the unitary transformation $X_{\lambda,\Delta\lambda}$ is given by Eq. (15) and relies on the decomposition of $\mathcal{H}_J$ into the eigenmodes of L_0. However, it will be impossible to find the exact decomposition of $\mathcal{H}_J$ due to the presence of Hubbard operators in $\mathcal{H}_t$. Therefore, we have to apply approximations. For this purpose, we start by decomposing the electronic spin operator

$$\mathbf{S}_\mathbf{q} = \frac{1}{\sqrt{N}} \sum_{\alpha\beta} \frac{\vec{\sigma}_{\alpha\beta}}{2} \sum_i e^{i\mathbf{q}\mathbf{R}_i} \hat{c}^\dagger_{i\alpha} \hat{c}_{i\beta} \tag{16}$$

into eigenmodes of L_t instead of into eigenmodes of L_0. Here, L_t is the Liouville operator corresponding to the hopping part $\mathcal{H}_t$ of $\mathcal{H}_0$. The exchange $\mathcal{H}_J$ is given by a sum over products of spin operators $\mathbf{S}_\mathbf{q} \cdot \mathbf{S}_{-\mathbf{q}}$. Therefore, the decomposition of $\mathbf{S}_\mathbf{q}$ into eigenmodes of L_t can be used to find an equivalent decomposition of $\mathcal{H}_J$.

The easiest way to decompose $\mathbf{S}_\mathbf{q}$ is to derive an equation of motion for the time-dependent operator $\mathbf{S}_\mathbf{q}(t)$, where the time dependence is governed by $\mathcal{H}_t$,

$$\mathbf{S}_\mathbf{q}(t) = e^{i\mathcal{H}_t t} \mathbf{S}_\mathbf{q} e^{-i\mathcal{H}_t t} = e^{i\mathsf{L}_t t} \mathbf{S}_\mathbf{q}. \tag{17}$$

Due to Eq. (3), the first time derivative reads

$$\frac{d}{dt}\mathbf{S}_\mathbf{q} = -\frac{i}{\sqrt{N}} \sum_{\alpha\beta} \frac{\vec{\sigma}_{\alpha\beta}}{2} \sum_{i\neq l} t_{il} e^{i\mathbf{q}\mathbf{R}_i} (\hat{c}^\dagger_{l\alpha}\hat{c}_{i\beta} - \hat{c}^\dagger_{i\alpha}\hat{c}_{l\beta}),$$

$$= \frac{i}{\sqrt{N}} \sum_{\alpha\beta} \frac{\vec{\sigma}_{\alpha\beta}}{2} \sum_{i\neq l} t_{il} e^{i\mathbf{q}\mathbf{R}_i} (1 - e^{i\mathbf{q}(\mathbf{R}_l - \mathbf{R}_i)}) \hat{c}^\dagger_{i\alpha}\hat{c}_{l\beta}. \tag{18}$$

It can be interpreted as the hopping of a hole from some site l to a neighboring site i and vice versa. The second derivative is characterized by a twofold hopping,

$$\frac{d^2}{dt^2}\mathbf{S_q} = -\frac{1}{\sqrt{N}}\sum_{i\neq l} t_{il}^2(e^{i\mathbf{qR}_l} - e^{i\mathbf{qR}_i})[\mathbf{S}_l\mathcal{P}_0(i) - \mathbf{S}_i\mathcal{P}_0(l)]$$
$$-\frac{1}{2\sqrt{N}}\sum_{\alpha\beta}\sum_{i\neq j}\sum_{j(\neq i\neq l)} t_{il}t_{lj}(e^{i\mathbf{qR}_i} - e^{i\mathbf{qR}_l})$$
$$\times\{\vec{\sigma}_{\alpha\beta}[\hat{c}_{j\alpha}^{\dagger}\mathcal{D}_{\alpha}(l)\hat{c}_{i\beta} + \hat{c}_{j,-\alpha}^{\dagger}S_l^{\alpha}\hat{c}_{i\beta}]$$
$$+\vec{\sigma}_{\alpha\beta}^{*}[\hat{c}_{i\beta}^{\dagger}\mathcal{D}_{\alpha}(l)\hat{c}_{j\alpha} + c_{i\beta}^{\dagger}S_l^{-\alpha}\hat{c}_{m,-\alpha}]\}. \quad (19)$$

It has two different contributions. The first one describes the hopping of the hole from i back to site l from which it originally came and, equivalently, the hopping from l back to i. The second term in Eq. (19) stands for a twofold hopping away from the starting site.

Let us discuss the first contribution to Eq. (19) in more detail. The operators

$$\mathcal{P}_0(i) = (1 - n_{i,\uparrow})(1 - n_{i,\downarrow}) \quad (20)$$

and $\mathcal{P}_0(l)$ can be interpreted as local projectors on the empty state at site i and site l, respectively. They assure that the original sites i and l were empty before the first hop. Their presence results from the fact that doubly occupancies of local sites are strictly forbidden which is a consequence of the strong correlations in the t-J model. In a further approximation, let us replace $\mathcal{P}_0(i)$ and $\mathcal{P}_0(l)$ by their expectation values,

$$\mathcal{P}_0(i) \Rightarrow \langle(1 - n_{i,\uparrow})(1 - n_{i,\downarrow})\rangle_0 =: P_0, \quad (21)$$

which can be interpreted as the probability for a local site to be empty. Without the second term in Eq. (19), we are led to the following equation of motion for $\mathbf{S_q}(t)$:

$$\frac{d^2}{dt^2}\mathbf{S_q} = -\hat{\omega}_{\mathbf{q}}^2\mathbf{S_q}. \quad (22)$$

Obviously, differential equation (22) describes an oscillatory motion of $\mathbf{S_q}(t)$ with frequency $\hat{\omega}_{\mathbf{q}}$, where

$$\hat{\omega}_{\mathbf{q}}^2 = 2P_0(t_{\mathbf{q}=0}^2 - t_{\mathbf{q}}^2) = \hat{\omega}_{-\mathbf{q}}^2 \geqslant 0, \quad t_{\mathbf{q}}^2 = \sum_{l(\neq i)} t_{il}^2 e^{i\mathbf{q}(\mathbf{R}_l - \mathbf{R}_i)}. \quad (23)$$

Note that the averaged projector $P_0 = 1 - n$ also agrees with the hole concentration δ away from half-filling, i.e., $P_0 = \delta = 1 - n$, where n is the electron filling.

Before carrying on with the physical implications of Eqs. (22) and (23), let us discuss the influence of the hole (or electron) hopping in Eq. (19) to second-nearest neighbors and also to more distant sites. As long as the dynamics of $\mathbf{S_q}(t)$ is alone governed by the hopping Hamiltonian $\mathcal{H}_t$, all these hopping processes are important and would have to be taken into account. For instance, for a state close to half-filling outside the antiferromagnetic regime, a hole and a neighboring electron can freely interchange their positions for a system governed alone by $\mathcal{H}_t$. The hole can easily move through the lattice. However, the situation is different from the case for which the dynamics is governed by $\mathcal{H}_0 = \mathcal{H}_t + \mathcal{H}_J^{(0)}$. Then, we have to decompose the perturbation $\mathcal{H}_1$ into eigenstates of L_0, where L_0 is the Liouville operator corresponding to $\mathcal{H}_0$. Thus, the dynamics of $\mathbf{S_q}$ is not governed alone by the hopping Hamiltonian $\mathcal{H}_t$ but also by the yet unknown commuting part $\mathcal{H}_J^{(0)}$ of $\mathcal{H}_J$. However, in Appendix A, it is shown that local antiferromagnetic spin fluctuations due to $\mathcal{H}_J^{(0)}$ restrict the hole motion to neighboring sites. The hopping to more distant sites is strongly suppressed by spin fluctuations. Therefore, the former equation of motion [Eq. (22)] for $\mathbf{S_q}(t)$ turns out to be a good approximation for the case that the dynamics is determined by the full unperturbed Hamiltonian $\mathcal{H}_0$ including the exchange part.

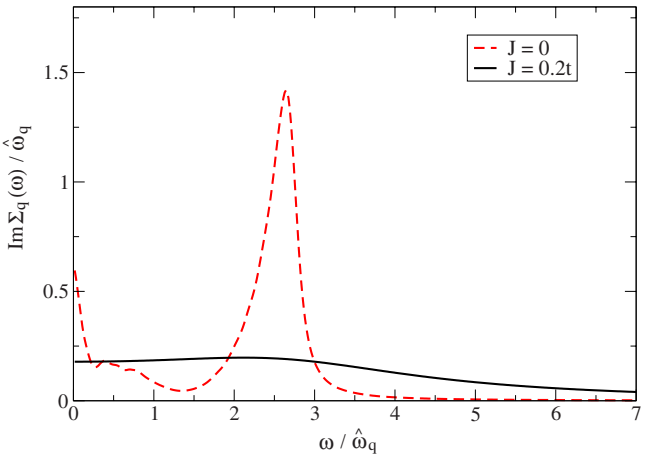

FIG. 1. (Color online) Imaginary part of the self-energy $\Im\Sigma_{\mathbf{q}}(\omega)$ from Eq. (25) in the presence of spin fluctuations ($J = 0.2t$, solid line) and in the absence of spin fluctuations ($J = 0$, dashed line). The $\mathbf{q}$ vector is fixed to $\mathbf{q} = (\pi/20, \pi/20)$.

The arguments in Appendix A are based on the evaluation of the dynamical spin susceptibility $\chi(\mathbf{q}, \omega)$ as follows. Using the Mori-Zwanzig projection formalism $\chi(\mathbf{q}, \omega)$ can be written as

$$\chi(\mathbf{q}, \omega) = \frac{-\omega_{\mathbf{q}}^2}{\omega^2 - \omega_{\mathbf{q}}^2 - \omega\Sigma_{\mathbf{q}}(\omega)}\chi_{\mathbf{q}}. \quad (24)$$

Here, $\omega_{\mathbf{q}}^2 \approx \hat{\omega}_{\mathbf{q}}^2$ is approximately the frequency, given in Eq. (23), and $\Sigma_{\mathbf{q}}(\omega)$ is the self-energy. The exact expression of $\Sigma_{\mathbf{q}}(\omega)$ in terms of the Mori scalar product reads

$$\Sigma_{\mathbf{q}}(\omega) = \frac{1}{(\dot{\mathbf{S}}_{\mathbf{q}}|\dot{\mathbf{S}}_{\mathbf{q}})}\left(\mathsf{Q}\ddot{\mathbf{S}}_{\mathbf{q}}\middle|\frac{1}{\omega - \mathsf{QL}_0\mathsf{Q} - i\eta}\mathsf{Q}\ddot{\mathbf{S}}_{\mathbf{q}}\right). \quad (25)$$

Here, Q is a generalized projection operator which projects perpendicular to $\mathbf{S_q}$ and $\dot{\mathbf{S}}_{\mathbf{q}}$ (for details see Appendix D). Due to construction, the operator $\mathsf{Q}\ddot{\mathbf{S}}_{\mathbf{q}}$ in the "bra" and "ket" of Eq. (25) corresponds to the second line in Eq. (19), and describes a twofold hopping away from the original site. Therefore, the self-energy $\Sigma_{\mathbf{q}}(\omega)$ provides information about the hopping processes between next-nearest-neighbor sites and to more distant sites. In Appendix A the self-energy $\Sigma_{\mathbf{q}}(\omega)$ is evaluated in a factorization approximation by including the spin fluctuations from $\mathcal{H}_J^{(0)}$. The result is shown in Fig. 1, where the imaginary part of $\Sigma_{\mathbf{q}}(\omega)$ for a small $\mathbf{q}$ vector is plotted (solid line) in the presence of spin fluctuations due to $\mathcal{H}_J^{(0)}$. As is seen, $\Sigma_{\mathbf{q}}(\omega)$ is rather small and almost ω independent over a wide frequency range. Thus, the only effect of $\Sigma_{\mathbf{q}}(\omega)$ is to give rise to a small damping and

lineshift of the resonances of $\chi(\mathbf{q},\omega)$. We have also repeated the same calculation for $\Im\Sigma_{\mathbf{q}}(\omega)$ in the absence of $\mathcal{H}_J^{(0)}$, i.e., when $\mathcal{H}_0$ is replaced by $\mathcal{H}_t$ (dashed line in Fig. 1). A strong ω dependence is found for small $\mathbf{q}$ values around $\omega=0$. This shows that long reaching hopping processes are important in this case. From these findings, one can conclude that the hopping to more distant than nearest neighbors is of minor importance as long as the exchange part $\mathcal{H}_J^{(0)}$ is not neglected in $\mathcal{H}_0$. A possible explanation would be that local antiferromagnetic correlations are still present at moderate hole doping outside the antiferromagnetic phase. They lead locally to strings of spin defects which are well known from the hole motion in the antiferromagnetic phase.

Let us come back to the discussion of the oscillation behavior in Eq. (19) which can be understood as follows. When an electron hops to a neighboring site, it preferably hops back to the original site since this was definitely empty after the first hop. In contrast, the hopping to next-nearest-neighbor sites is energetically unfavorable due to local antiferromagnetic order. As will be shown below, the proportionality of $\hat{\omega}_{\mathbf{q}}^2 \sim \delta$ turns out to be the basic feature for the understanding of the superconducting pairing mechanism in the cuprates. The oscillation becomes less important for larger δ which agrees with the weakening of the superconducting phase for larger hole doping.

The solution of Eq. (22) is easily found,

$$\mathbf{S}_{\mathbf{q}}(t) = \mathbf{S}_{\mathbf{q}} \cos\,\hat{\omega}_{\mathbf{q}} t + \frac{1}{\hat{\omega}_{\mathbf{q}}} \dot{\mathbf{S}}_{\mathbf{q}} \sin\,\hat{\omega}_{\mathbf{q}} t,$$

$$= \frac{1}{2}\left(\mathbf{S}_{\mathbf{q}} - \frac{i}{\hat{\omega}_{\mathbf{q}}}\dot{\mathbf{S}}_{\mathbf{q}}\right) e^{i\hat{\omega}_{\mathbf{q}} t} + \frac{1}{2}\left(\mathbf{S}_{\mathbf{q}} + \frac{i}{\hat{\omega}_{\mathbf{q}}}\dot{\mathbf{S}}_{\mathbf{q}}\right) e^{-i\hat{\omega}_{\mathbf{q}} t}, \tag{26}$$

where $\mathbf{S}_{\mathbf{q}}=\mathbf{S}_{\mathbf{q}}(t=0)$ and $\dot{\mathbf{S}}_{\mathbf{q}}=\frac{d}{dt}\mathbf{S}_{\mathbf{q}}(t=0)$ was used. From Eq. (26), the decomposition of $\mathbf{S}_{\mathbf{q}}$ into eigenmodes of L_0 can immediately be identified,

$$\mathsf{L}_0\left[\frac{1}{2}\left(\mathbf{S}_{\mathbf{q}} \mp \frac{i}{\hat{\omega}_{\mathbf{q}}}\dot{\mathbf{S}}_{\mathbf{q}}\right)\right] = \pm\,\hat{\omega}_{\mathbf{q}}\left[\frac{1}{2}\left(\mathbf{S}_{\mathbf{q}} \mp \frac{i}{\hat{\omega}_{\mathbf{q}}}\dot{\mathbf{S}}_{\mathbf{q}}\right)\right], \tag{27}$$

which leads to the intended decomposition of the exchange $\mathcal{H}_J$ as follows:

$$\mathcal{H}_J = \sum_{\mathbf{q}} J_{\mathbf{q}} \mathbf{S}_{\mathbf{q}}\mathbf{S}_{-\mathbf{q}} = \sum_{\mathbf{q}} J_{\mathbf{q}}[\mathcal{A}_0(\mathbf{q}) + \mathcal{A}_1(\mathbf{q}) + \mathcal{A}_1^\dagger(\mathbf{q})], \tag{28}$$

where

$$\mathcal{A}_0(\mathbf{q}) = \frac{1}{2}\left(\mathbf{S}_{\mathbf{q}}\mathbf{S}_{-\mathbf{q}} + \frac{1}{\hat{\omega}_{\mathbf{q}}^2}\dot{\mathbf{S}}_{\mathbf{q}}\dot{\mathbf{S}}_{-\mathbf{q}}\right),$$

$$\mathcal{A}_1(\mathbf{q}) = \frac{1}{4}\left(\mathbf{S}_{\mathbf{q}} - \frac{i}{\hat{\omega}_{\mathbf{q}}}\dot{\mathbf{S}}_{\mathbf{q}}\right)\left(\mathbf{S}_{-\mathbf{q}} - \frac{i}{\hat{\omega}_{\mathbf{q}}}\dot{\mathbf{S}}_{-\mathbf{q}}\right),$$

$$\mathcal{A}_1^\dagger(\mathbf{q}) = \frac{1}{4}\left(\mathbf{S}_{\mathbf{q}} + \frac{i}{\hat{\omega}_{\mathbf{q}}}\dot{\mathbf{S}}_{\mathbf{q}}\right)\left(\mathbf{S}_{-\mathbf{q}} + \frac{i}{\hat{\omega}_{\mathbf{q}}}\dot{\mathbf{S}}_{-\mathbf{q}}\right), \tag{29}$$

and

$$\mathsf{L}_0\mathcal{A}_0(\mathbf{q}) = 0, \quad \mathsf{L}_0\mathcal{A}_1(\mathbf{q}) = 2\hat{\omega}_{\mathbf{q}}\mathcal{A}_1(\mathbf{q}),$$

$$\mathsf{L}_0\mathcal{A}_1^\dagger(\mathbf{q}) = -2\hat{\omega}_{\mathbf{q}}\mathcal{A}_1^\dagger(\mathbf{q}). \tag{30}$$

Here, an additional approximation was used. In deriving Eqs. (30), the eigenmodes of the two spin operators $\mathbf{S}_{\mathbf{q}}\cdot\mathbf{S}_{-\mathbf{q}}$ in the expression for $\mathcal{H}_J$ were taken separately from Eq. (27). In this way, all local configurations were disregarded, where two spin operators in local space are located on neighboring sites. Thereby, a possible hopping between the two sites would be obstructed. The inclusion of these processes would need additional considerations. However, they would not change our results substantially.

With Eqs. (29), we have arrived at the intended decomposition of the t-J model. The Hamiltonian

$$\mathcal{H} = \sum_{\mathbf{k}\sigma} \varepsilon_{\mathbf{k}} \hat{c}_{\mathbf{k}\sigma}^\dagger \hat{c}_{\mathbf{k}\sigma} + \sum_{\mathbf{q}} J_{\mathbf{q}} \mathbf{S}_{\mathbf{q}}\mathbf{S}_{-\mathbf{q}} \tag{31}$$

can be decomposed into an unperturbed part $\mathcal{H}_0$ and into a perturbation $\mathcal{H}_1$. It reads

$$\mathcal{H}_0 = \mathcal{H}_t + \mathcal{H}_{0,J} =: \sum_{\mathbf{k}\sigma} \varepsilon_{\mathbf{k}} \hat{c}_{\mathbf{k}\sigma}^\dagger \hat{c}_{\mathbf{k}\sigma} + \sum_{\mathbf{q}} J_{\mathbf{q}} \mathcal{A}_0(\mathbf{q}),$$

$$\mathcal{H}_1 = \sum_{\mathbf{q}} J_{\mathbf{q}}[\mathcal{A}_1(\mathbf{q}) + \mathcal{A}_1^\dagger(\mathbf{q})]. \tag{32}$$

The aim of the PRM is to eliminate all transitions between the eigenstates of $\mathcal{H}_0$ which are induced by $\mathcal{H}_1$. Let us assume that all excitations with energies larger than a given cutoff λ have already been eliminated. Then, the renormalized Hamiltonian $\mathcal{H}_\lambda$ should have the form

$$\mathcal{H}_\lambda = \sum_{\mathbf{k}\sigma} \varepsilon_{\mathbf{k},\lambda} \hat{c}_{\mathbf{k}\sigma}^\dagger \hat{c}_{\mathbf{k}\sigma} + \sum_{\mathbf{q}} J_{\mathbf{q},\lambda} \mathsf{P}_\lambda \mathbf{S}_{\mathbf{q}}\mathbf{S}_{-\mathbf{q}}, \tag{33}$$

however, with λ-dependent prefactors $\varepsilon_{\mathbf{k},\lambda}$ and $J_{\mathbf{q},\lambda}$. Moreover, a projector P_λ was introduced which acts on operator variables. It guarantees that only transitions with excitation energies smaller than λ remain from $\mathbf{S}_{\mathbf{q}}\mathbf{S}_{-\mathbf{q}}$.

The separation of $\mathcal{H}_\lambda$ into an unperturbed part $\mathcal{H}_{0,\lambda}$ and a perturbation $\mathcal{H}_{1,\lambda}$ reads in analogy to Eq. (32), $\mathcal{H}_\lambda=\mathcal{H}_{0,\lambda}+\mathcal{H}_{1,\lambda}$, with

$$\mathcal{H}_{0,\lambda} = \mathcal{H}_{t,\lambda} + \sum_{\mathbf{q}} J_{\mathbf{q},\lambda}\mathcal{A}_{0,\lambda}(\mathbf{q}) + E_\lambda,$$

$$\mathcal{H}_{1,\lambda} = \sum_{\mathbf{q}} J_{\mathbf{q},\lambda}\Theta(\lambda - |2\hat{\omega}_{\mathbf{q},\lambda}|)[\mathcal{A}_{1,\lambda}(\mathbf{q}) + \mathcal{A}_{1,\lambda}^\dagger(\mathbf{q})], \tag{34}$$

where we have used the λ-dependent extension of relation (30) in order to exploit the properties of P_λ. Note that the Θ function $\Theta(\lambda-|2\hat{\omega}_{\mathbf{q},\lambda}|)$ in $\mathcal{H}_{1,\lambda}$ guarantees that only excitations with transition energies $|2\hat{\omega}_{\mathbf{q},\lambda}|$ smaller than λ contribute to $\mathcal{H}_{1,\lambda}$. In Eq. (34), $\mathcal{H}_{t,\lambda}$ is the renormalized hopping term from Eq. (33), $\mathcal{H}_{t,\lambda}=\Sigma_{\mathbf{k}\sigma}\varepsilon_{\mathbf{k},\lambda}\hat{c}_{\mathbf{k}\sigma}^\dagger\hat{c}_{\mathbf{k}\sigma}$. Also, the parameters $J_{\mathbf{q},\lambda}$, $\hat{\omega}_{\mathbf{q},\lambda}$ and E_λ in Eqs. (34) now depend on λ. Moreover, the new operators $\mathcal{A}_{\alpha,\lambda}(\mathbf{q})(\alpha=0,\pm1)$ depend on λ,

$$\mathcal{A}_{0,\lambda}(\mathbf{q}) = \frac{1}{2}\left(\mathbf{S}_{\mathbf{q}}\mathbf{S}_{-\mathbf{q}} + \frac{1}{\hat{\omega}_{\mathbf{q},\lambda}^2}\dot{\mathbf{S}}_{\mathbf{q},\lambda}\dot{\mathbf{S}}_{-\mathbf{q},\lambda}\right),$$

$$\mathcal{A}_{1,\lambda}(\mathbf{q}) = \frac{1}{4}\left(\mathbf{S}_{\mathbf{q}} - \frac{i}{\hat{\omega}_{\mathbf{q},\lambda}}\dot{\mathbf{S}}_{\mathbf{q},\lambda}\right)\left(\mathbf{S}_{-\mathbf{q}} - \frac{i}{\hat{\omega}_{\mathbf{q},\lambda}}\dot{\mathbf{S}}_{-\mathbf{q},\lambda}\right),$$

$$\mathcal{A}_{1,\lambda}^{\dagger}(\mathbf{q}) = \frac{1}{4}\left(\mathbf{S}_{\mathbf{q}} + \frac{i}{\hat{\omega}_{\mathbf{q},\lambda}}\dot{\mathbf{S}}_{\mathbf{q},\lambda}\right)\left(\mathbf{S}_{-\mathbf{q}} + \frac{i}{\hat{\omega}_{\mathbf{q},\lambda}}\dot{\mathbf{S}}_{-\mathbf{q},\lambda}\right), \quad (35)$$

where $\hat{\omega}_{\mathbf{q},\lambda}$ and $\dot{\mathbf{S}}_{\mathbf{q},\lambda}$ are defined by

$$\hat{\omega}_{\mathbf{q},\lambda}^2 = 2P_0(t_{\mathbf{q}=0,\lambda}^2 - t_{\mathbf{q},\lambda}^2), \quad t_{\mathbf{q},\lambda}^2 = \sum_{i(\neq j)} t_{ij,\lambda}^2 e^{i\mathbf{q}(\mathbf{R}_i - \mathbf{R}_j)},$$

$$\dot{\mathbf{S}}_{\mathbf{q},\lambda} = \frac{i}{\hbar}[\mathcal{H}_{0,\lambda}, \mathbf{S}_{\mathbf{q}}] \approx \frac{i}{\hbar}[\mathcal{H}_{t,\lambda}, \mathbf{S}_{\mathbf{q}}]. \quad (36)$$

B. Generator of the unitary transformation

To derive renormalization equations for the parameters of $\mathcal{H}_\lambda$, we have to apply unitary transformation (12) to $\mathcal{H}_\lambda$ in order to eliminate excitations within a new energy shell between λ and $\lambda-\Delta\lambda$. We use lowest-order expression (15) for the new generator $X_{\lambda,\Delta\lambda}$,

$$X_{\lambda,\Delta\lambda} = \sum_{\mathbf{q}} \frac{J_{\mathbf{q},\lambda}}{2\hat{\omega}_{\mathbf{q},\lambda}}\Theta_{\mathbf{q}}(\lambda,\Delta\lambda)[\mathcal{A}_{1,\lambda}(\mathbf{q}) - \mathcal{A}_{1,\lambda}^{\dagger}(\mathbf{q})]. \quad (37)$$

Here, $\Theta_{\mathbf{q}}(\lambda,\Delta\lambda)$ denotes a product of two Θ functions,

$$\Theta_{\mathbf{q}}(\lambda,\Delta\lambda) = \Theta(\lambda - |2\hat{\omega}_{\mathbf{q},\lambda}|)\Theta[|2\omega_{\mathbf{q},\lambda-\Delta\lambda}| - (\lambda-\Delta\lambda)],$$

which confines the elimination range to excitations with $|2\omega_{\mathbf{q},\lambda-\Delta\lambda}|$ larger than $\lambda-\Delta\lambda$ and $|2\hat{\omega}_{\mathbf{q},\lambda}|$ smaller than λ. Roughly speaking, for the case of a weak λ dependence of $|\omega_{\mathbf{q},\lambda}|$, the elimination is restricted to all transitions within an energy shell between $\lambda-\Delta\lambda$ and λ. With Eq. (35), the generator $X_{\lambda,\Delta\lambda}$ can also be expressed by

$$X_{\lambda,\Delta\lambda} = -i\sum_{\mathbf{q}} \frac{J_{\mathbf{q},\lambda}}{4\hat{\omega}_{\mathbf{q},\lambda}^2}\Theta_{\mathbf{q}}(\lambda,\Delta\lambda)(\mathbf{S}_{\mathbf{q}}\dot{\mathbf{S}}_{-\mathbf{q},\lambda} + \dot{\mathbf{S}}_{\mathbf{q},\lambda}\mathbf{S}_{-\mathbf{q}}). \quad (38)$$

In the following, we restrict ourselves to the lowest-order renormalization processes. Then, $J_{\mathbf{q},\lambda}$ will not be renormalized by higher orders in J, and we can use $J_{\mathbf{q},\lambda}=J_{\mathbf{q}}$ from the beginning.

C. Renormalization equations

Unitary transformation (12), applied to the renormalization step between λ and $\lambda-\Delta\lambda$, will be evaluated in perturbation theory in second order in $J_{\mathbf{q}}$,

$$\mathcal{H}_{\lambda-\Delta\lambda} = e^{X_{\lambda,\Delta\lambda}}\mathcal{H}_\lambda e^{-X_{\lambda,\Delta\lambda}} = \mathcal{H}_{\lambda-\Delta\lambda}^{(0)} + \mathcal{H}_{\lambda-\Delta\lambda}^{(1)} + \mathcal{H}_{\lambda-\Delta\lambda}^{(2)} + \cdots, \quad (39)$$

where

$$\mathcal{H}_{\lambda-\Delta\lambda}^{(0)} = \sum_{\mathbf{k}\sigma} \varepsilon_{\mathbf{k},\lambda}\hat{c}_{\mathbf{k}\sigma}^{\dagger}\hat{c}_{\mathbf{k}\sigma} + E_\lambda = \mathcal{H}_{t,\lambda} + E_\lambda,$$

$$\mathcal{H}_{\lambda-\Delta\lambda}^{(1)} = \sum_{\mathbf{q}} J_{\mathbf{q}}\mathcal{A}_{0,\lambda}(\mathbf{q}) + [X_{\lambda,\Delta\lambda}, \mathcal{H}_{t,\lambda}] + \sum_{\mathbf{q}} J_{\mathbf{q}}\Theta(\lambda - |2\hat{\omega}_{\mathbf{q},\lambda}|)[\mathcal{A}_{1,\lambda}(\mathbf{q}) + \mathcal{A}_{1,\lambda}^{\dagger}(\mathbf{q})],$$

$$\mathcal{H}_{\lambda-\Delta\lambda}^{(2)} = \frac{1}{2}[X_{\lambda,\Delta\lambda}, [X_{\lambda,\Delta\lambda}, \mathcal{H}_{t,\lambda}]] + \sum_{\mathbf{q}} J_{\mathbf{q}}[X_{\lambda,\Delta\lambda}, \mathcal{A}_{0,\lambda}(\mathbf{q})] + \sum_{\mathbf{q}} J_{\mathbf{q}}\Theta(\lambda - |2\hat{\omega}_{\mathbf{q},\lambda}|)[X_{\lambda,\Delta\lambda}, \mathcal{A}_{1,\lambda}(\mathbf{q}) + \mathcal{A}_{1,\lambda}^{\dagger}(\mathbf{q})]. \quad (40)$$

Let us first evaluate $\mathcal{H}_{\lambda-\Delta\lambda}^{(2)}$ from second-order processes. The commutators in Eq. (40) are explicitly evaluated in Appendix A. Then, we can compare the obtained result with the formal expression for $\mathcal{H}_{\lambda-\Delta\lambda}$ which has the same operator structure as $\mathcal{H}_\lambda$, with λ is replaced by $\lambda-\Delta\lambda$. One obtains the following renormalization equation from the second-order contributions in $J_{\mathbf{q}}$:

$$\begin{aligned}\varepsilon_{\mathbf{k},\lambda-\Delta\lambda} - \varepsilon_{\mathbf{k},\lambda} = {} & \frac{1}{16N}\sum_{\mathbf{q}} \frac{J_{\mathbf{q}}^2}{\hat{\omega}_{\mathbf{q},\lambda}^4}\Theta_{\mathbf{q}}(\lambda,\Delta\lambda) \\ & \times(\varepsilon_{\mathbf{k}+\mathbf{q},\lambda} + \varepsilon_{\mathbf{k}-\mathbf{q},\lambda} - 2\varepsilon_{\mathbf{k},\lambda})\langle\dot{\mathbf{S}}_{\mathbf{q},\lambda}\dot{\mathbf{S}}_{-\mathbf{q},\lambda}\rangle \\ & + \frac{3}{2N}\sum_{\mathbf{q}\sigma}\left(\frac{J_{\mathbf{q}}}{4\hat{\omega}_{\mathbf{q}}^2}\right)^2\Theta_{\mathbf{q}}(\lambda,\Delta\lambda)(\varepsilon_{\mathbf{k},\lambda} - \varepsilon_{\mathbf{k}-\mathbf{q},\lambda})^2 \\ & \times\left[\frac{1}{N}\sum_{\mathbf{k}'\sigma'}(2\varepsilon_{\mathbf{k}',\lambda} - \varepsilon_{\mathbf{k}'+\mathbf{q},\lambda} - \varepsilon_{\mathbf{k}'-\mathbf{q},\lambda})\right. \\ & \left.\times\langle\hat{c}_{\mathbf{k}'\sigma'}^{\dagger}\hat{c}_{\mathbf{k}'\sigma'}\rangle\right]n_{\mathbf{k}-\mathbf{q}\alpha}^{(NL)}, \end{aligned} \quad (41)$$

where we have defined

$$n_{\mathbf{k},\sigma}^{(NL)} = \langle\hat{c}_{\mathbf{k}\sigma}^{\dagger}\hat{c}_{\mathbf{k}\sigma}\rangle - \frac{1}{N}\sum_{\mathbf{k}'}\langle\hat{c}_{\mathbf{k}'\sigma}^{\dagger}\hat{c}_{\mathbf{k}'\sigma}\rangle \quad (42)$$

as nonlocal part of the one-particle occupation number per spin direction. An equivalent equation also exists for $E_{\lambda-\Delta\lambda}$. Note that in Eq. (41) an additional factorization approximation was used in order to extract all terms which have the same operator structure as $\mathcal{H}_\lambda$. The quantity $\langle\dot{\mathbf{S}}_{\mathbf{q},\lambda}\dot{\mathbf{S}}_{-\mathbf{q},\lambda}\rangle$ is a correlation function of the time derivatives of $\mathbf{S}_{\mathbf{q}}$ which can easily be evaluated from Eq. (B3). Note that an additional contribution to $\varepsilon_{\mathbf{k},\lambda-\Delta\lambda}$, proportional to the correlation function $\langle\mathbf{S}_{\mathbf{q}}\cdot\mathbf{S}_{-\mathbf{q}}\rangle$, has been neglected. The remaining expectation values in Eq. (41) have to be calculated separately. In principle, they should be defined with the λ-dependent Hamiltonian $\mathcal{H}_\lambda$ because the factorization approximation was employed for the renormalization step from $\mathcal{H}_\lambda$ to $\mathcal{H}_{\lambda-\Delta\lambda}$. However, $\mathcal{H}_\lambda$ still contains interactions which prevent a straight evaluation of λ-dependent expectation values. The best way to circumvent this difficulty is to calculate the expectation values with the full Hamiltonian $\mathcal{H}$ instead of with

$\mathcal{H}_\lambda$. In this case, the renormalization equations can be solved self-consistently, as will be discussed below.

Note that renormalization (41) of $\varepsilon_{\mathbf{k},\lambda}$ was evaluated from the second-order part $\mathcal{H}^{(2)}_{\lambda-\Delta\lambda}$ of Hamiltonian (40). Thus, we are led to

$$\mathcal{H}_{\lambda-\Delta\lambda} = \mathcal{H}_{t,\lambda-\Delta\lambda} + \mathcal{H}^{(1)}_{\lambda-\Delta\lambda} + E_{\lambda-\Delta\lambda}, \tag{43}$$

where $\mathcal{H}_{t,\lambda-\Delta\lambda}=\Sigma_{\mathbf{k},\sigma}\varepsilon_{\mathbf{k},\lambda-\Delta\lambda}\hat{c}^\dagger_{\mathbf{k}\sigma}\hat{c}_{\mathbf{k}\sigma}$. What remains is to evaluate the renormalization part $\mathcal{H}^{(1)}_{\lambda-\Delta\lambda}$ in first order in $J_\mathbf{q}$ to $\mathcal{H}_{\lambda-\Delta\lambda}$. First, the second term on the right-hand side of Eq. (40) can be rewritten since

$$[X_{\lambda,\Delta\lambda},\mathcal{H}_{t,\lambda}] = -\sum_\mathbf{q} J_\mathbf{q}\Theta_\mathbf{q}(\lambda,\Delta\lambda)[\mathcal{A}_{1,\lambda}(\mathbf{q}) + \mathcal{A}^\dagger_{1,\lambda}(\mathbf{q})].$$

Then, by combining the second and third terms, we find

$$\mathcal{H}^{(1)}_{\lambda-\Delta\lambda} = \sum_\mathbf{q} J_\mathbf{q}\mathcal{A}_{0,\lambda}(\mathbf{q}) + \sum_\mathbf{q} J_\mathbf{q}\Theta(\lambda - |2\hat{\omega}_{\mathbf{q},\lambda}|) \times\Theta(\lambda-\Delta\lambda-|2\hat{\omega}_{\mathbf{q},\lambda-\Delta\lambda}|)[\mathcal{A}_{1,\lambda}(\mathbf{q}) + \mathcal{A}^\dagger_{1,\lambda}(\mathbf{q})]. \tag{44}$$

The excitation energies of $\mathcal{A}_{1,\lambda}(\mathbf{q})$ and $\mathcal{A}^\dagger_{1,\lambda}(\mathbf{q})$ are restricted to $|2\hat{\omega}_{\mathbf{q},\lambda}|\leqslant\lambda$ by the first Θ function in Eq. (44). This condition is automatically fulfilled by the second Θ function, in the case that $|2\hat{\omega}_{\mathbf{q},\lambda-\Delta\lambda}|$ only weakly depends on λ and we can replace λ by $\lambda-\Delta\lambda$. By introducing the projector $\mathsf{P}_{\lambda-\Delta\lambda}$ on all low-energy transition operators with energies smaller than $\lambda-\Delta\lambda$, we find

$$\mathcal{H}^{(1)}_{\lambda-\Delta\lambda} = \sum_\mathbf{q} J_\mathbf{q}\mathsf{P}_{\lambda-\Delta\lambda}[\mathcal{A}_{0,\lambda}(\mathbf{q}) + \mathcal{A}_{1,\lambda}(\mathbf{q}) + \mathcal{A}^\dagger_{1,\lambda}(\mathbf{q})],$$

$$= \sum_\mathbf{q} J_\mathbf{q}\mathsf{P}_{\lambda-\Delta\lambda}\mathbf{S}_\mathbf{q}\cdot\mathbf{S}_{-\mathbf{q}}, \tag{45}$$

where we have used representation (28) for the scalar product $\mathbf{S}_\mathbf{q}\cdot\mathbf{S}_{-\mathbf{q}}$,

$$\mathbf{S}_\mathbf{q}\cdot\mathbf{S}_{-\mathbf{q}} = \mathcal{A}_{0,\lambda}(\mathbf{q}) + \mathcal{A}_{1,\lambda}(\mathbf{q}) + \mathcal{A}^\dagger_{1,\lambda}(\mathbf{q}). \tag{46}$$

Finally, for the total Hamiltonian $\mathcal{H}_{\lambda-\Delta\lambda}$, we obtain according to Eq. (43)

$$\mathcal{H}_{\lambda-\Delta\lambda} = \sum_{\mathbf{k},\sigma}\varepsilon_{\mathbf{k},\lambda-\Delta\lambda}\hat{c}^\dagger_{\mathbf{k}\sigma}\hat{c}_{\mathbf{k}\sigma} + \sum_\mathbf{q} J_\mathbf{q}\mathsf{P}_{\lambda-\Delta\lambda}\mathbf{S}_\mathbf{q}\cdot\mathbf{S}_{-\mathbf{q}} + E_{\lambda-\Delta\lambda}. \tag{47}$$

Note that this expression completely agrees with the Hamiltonian at cutoff λ, when λ is replaced by $\lambda-\Delta\lambda$. The required decomposition into $\mathcal{H}_{0,\lambda-\Delta\lambda}$ and $\mathcal{H}_{1,\lambda-\Delta\lambda}$ is found as follows. We use again relation (46), with λ replaced by $\lambda-\Delta\lambda$, and rewrite $\mathcal{H}^{(1)}_{\lambda-\Delta\lambda}$ as

$$\mathcal{H}^{(1)}_{\lambda-\Delta\lambda} = \sum_\mathbf{q} J_\mathbf{q}\mathsf{P}_{\lambda-\Delta\lambda}[\mathcal{A}_{0,\lambda-\Delta\lambda}(\mathbf{q}) + \mathcal{A}_{1,\lambda-\Delta\lambda}(\mathbf{q}) + \mathcal{A}^\dagger_{1,\lambda-\Delta\lambda}(\mathbf{q})]. \tag{48}$$

Using again Eq. (45), we arrive at the renormalized Hamiltonian $\mathcal{H}_{\lambda-\Delta\lambda}=\mathcal{H}_{0,\lambda-\Delta\lambda}+\mathcal{H}_{1,\lambda-\Delta\lambda}$ in the following form,

$$\mathcal{H}_{0,\lambda-\Delta\lambda} = \mathcal{H}_{t,\lambda-\Delta\lambda} + \sum_\mathbf{q} J_\mathbf{q}\mathcal{A}_{0,\lambda-\Delta\lambda}(\mathbf{q}) + E_{\lambda-\Delta\lambda},$$

$$\mathcal{H}_{1,\lambda-\Delta\lambda} = \sum_\mathbf{q} J_\mathbf{q}\Theta(\lambda-\Delta\lambda-|2\hat{\omega}_{\mathbf{q},\lambda-\Delta\lambda}|) \times[\mathcal{A}_{1,\lambda-\Delta\lambda}(\mathbf{q}) + \mathcal{A}^\dagger_{1,\lambda-\Delta\lambda}(\mathbf{q})]. \tag{49}$$

As expected, the renormalized Hamiltonians $\mathcal{H}_{0,\lambda-\Delta\lambda}$ and $\mathcal{H}_{1,\lambda-\Delta\lambda}$ have the same operator structure as at cutoff λ. Therefore, we can formulate a renormalization scheme as follows: We start from the original t-J model, where the energy cutoff is denoted by $\lambda=\Lambda$. Starting from a guess for the unknown expectation values, which enter renormalization equation (41), we proceed by eliminating all excitations in steps $\Delta\lambda$ from $\lambda=\Lambda$ down to $\lambda=0$. Thereby, the parameters of the Hamiltonian change in steps according to renormalization equation (41). In this way, we obtain the following model at $\lambda=0$:

$$\mathcal{H}_{\lambda=0} = \mathcal{H}_{t,\lambda=0} + \sum_\mathbf{q} J_\mathbf{q}\mathsf{P}_{\lambda=0}\mathbf{S}_\mathbf{q}\cdot\mathbf{S}_{-\mathbf{q}} + E_{\lambda=0},$$

$$= \sum_{\mathbf{k}\sigma}\varepsilon_{\mathbf{k},\lambda=0}\hat{c}^\dagger_{\mathbf{k}\sigma}\hat{c}_{\mathbf{k}\sigma} + \sum_\mathbf{q} J_\mathbf{q}\mathcal{A}_{0,\lambda=0}(\mathbf{q}) + E_{\lambda=0}. \tag{50}$$

Note that in Eq. (50) the perturbation $\mathcal{H}_1$ is completely integrated out. Only the part of the exchange, which commutes with the hopping term, remains.

Unfortunately, due to the presence of the $\mathcal{A}_0$ term, the Hamiltonian $\mathcal{H}_{\lambda=0}$ can not be diagonalized. It does not yet allow us to recalculate the expectation values. Therefore, a further approximation is necessary which consists of a factorization of the second term

$$\sum_\mathbf{q} J_\mathbf{q}\mathcal{A}_{0,\lambda=0}(\mathbf{q}) = \sum_\mathbf{q}\frac{J_\mathbf{q}}{2}\left(\mathbf{S}_\mathbf{q}\mathbf{S}_{-\mathbf{q}} + \frac{1}{\hat{\omega}^2_{\mathbf{q},\lambda=0}}\dot{\mathbf{S}}_{\mathbf{q},\lambda=0}\dot{\mathbf{S}}_{-\mathbf{q},\lambda=0}\right). \tag{51}$$

According to Appendix B, $\mathcal{H}_{\lambda=0}$ can finally be replaced by a modified Hamiltonian which will be denoted by $\tilde{\mathcal{H}}^{(1)}$,

$$\tilde{\mathcal{H}}^{(1)} = \sum_{\mathbf{k}\sigma}\tilde{\varepsilon}^{(1)}_\mathbf{k}\hat{c}^\dagger_{\mathbf{k}\sigma}\hat{c}_{\mathbf{k}\sigma} + \sum_\mathbf{q}\frac{J_\mathbf{q}}{2}\mathbf{S}_\mathbf{q}\mathbf{S}_{-\mathbf{q}} + \tilde{E}^{(1)}, \tag{52}$$

where the electron energy is modified according to

$$\tilde{\varepsilon}^{(1)}_\mathbf{k} = \varepsilon_{\mathbf{k},\lambda=0} - \frac{1}{N}\sum_\mathbf{q}\frac{3J_\mathbf{q}}{4\hat{\omega}^2_{\mathbf{q},\lambda=0}}(\varepsilon_{\mathbf{k},\lambda=0}-\varepsilon_{\mathbf{k}-\mathbf{q},\lambda=0})^2 n^{(NL)}_{\mathbf{k}-\mathbf{q},\sigma}, \tag{53}$$

and $n^{(NL)}_{\mathbf{k},\sigma}$ is defined in Eq. (42). Note that the operator structure of $\tilde{\mathcal{H}}^{(1)}$ agrees with that of the original t-J model of Eq. (31). However, the parameters have changed. Most important, the strength of the exchange coupling in Eq. (52) is decreased by a factor 1/2. This property allows us to start the whole renormalization procedure again. We consider the modified t-J model of Eq. (52) as our new initial Hamiltonian, which has to be renormalized again. The initial values of $\tilde{\mathcal{H}}^{(1)}$ at cutoff $\lambda=\Lambda$ are $\tilde{\varepsilon}^{(1)}_\mathbf{k}$ and $J_\mathbf{q}/2$. After the new

renormalization cycle the exchange coupling of the new renormalized Hamiltonian $\tilde{\mathcal{H}}^{(2)}$ is again decreased by a factor 1/2, until after a sufficiently large number of renormalization cycles ($n \to \infty$) the exchange operator completely disappears. Thus, we finally arrive at a free model,

$$\tilde{\mathcal{H}} = \sum_{\mathbf{k}\sigma} \tilde{\varepsilon}_{\mathbf{k}} \hat{c}^{\dagger}_{\mathbf{k}\sigma} \hat{c}_{\mathbf{k}\sigma} + \tilde{E}, \tag{54}$$

where we have introduced as new notations $\tilde{\mathcal{H}} = \tilde{\mathcal{H}}^{(n\to\infty)}$, $\tilde{\varepsilon}_{\mathbf{k}} = \tilde{\varepsilon}^{(n\to\infty)}_{\mathbf{k}}$, and $\tilde{E} = \tilde{E}^{(n\to\infty)}$. Note that the Hamiltonian $\tilde{\mathcal{H}}$ now allows us to recalculate the unknown expectation values. With the new values, the whole renormalization procedure can be started again until, after a sufficiently large number of such overall cycles, the expectation values have converged. The renormalization equations are solved self-consistently. However, note that fully renormalized Hamiltonian (54) is actually not a free model. Instead, it is still subject to strong electronic correlations which are built in by the presence of the Hubbard operators. Therefore, to evaluate the expectation values, further approximations have to be made.

D. Evaluation of expectation values

The expectation values in Eqs. (41) and (42) are formed with the full Hamiltonian. To evaluate expectation values for operator variables $\mathcal{A}$, we have to apply the unitary transformation also on $\mathcal{A}$. According to Eq. (55), we have

$$\langle \mathcal{A} \rangle = \frac{\mathrm{Tr}(\mathcal{A} e^{-\beta \mathcal{H}})}{\mathrm{Tr} e^{-\beta \mathcal{H}}} = \langle \mathcal{A}(\lambda) \rangle_{\mathcal{H}_\lambda} = \langle \tilde{\mathcal{A}} \rangle_{\tilde{\mathcal{H}}}, \tag{55}$$

where we have defined $\mathcal{A}(\lambda) = e^{X_\lambda} \mathcal{A} e^{-X_\lambda}$ and $\tilde{\mathcal{A}} = \mathcal{A}(\lambda \to 0)$. Thus, additional renormalization equations for $\mathcal{A}(\lambda)$ have to be derived.

As an example, let us consider the angle-resolved photoemission (ARPES) spectral function. It is defined by

$$A(\mathbf{k},\omega) = \frac{1}{2\pi} \int_{-\infty}^{\infty} \langle \hat{c}^{\dagger}_{\mathbf{k}\sigma}(-t) \hat{c}_{\mathbf{k}\sigma} \rangle e^{i\omega t} dt = \langle \hat{c}^{\dagger}_{\mathbf{k}\sigma} \delta(\mathsf{L} + \omega) \hat{c}_{\mathbf{k}\sigma} \rangle \tag{56}$$

and can be rewritten by use of the dissipation-fluctuation theorem as

$$A(\mathbf{k},\omega) = \frac{1}{1 + e^{\beta\omega}} \Im G(\mathbf{k},\omega), \tag{57}$$

where $\Im G(\mathbf{k},\omega)$ is the dissipative part of the anticommutator Green's function

$$\Im G(\mathbf{k},\omega) = \frac{1}{2\pi} \int_{-\infty}^{\infty} \langle [\hat{c}^{\dagger}_{\mathbf{k}\sigma}(-t), \hat{c}_{\mathbf{k}\sigma}]_+ \rangle e^{i\omega t} dt$$

$$= \langle [\hat{c}^{\dagger}_{\mathbf{k}\sigma}, \delta(\mathsf{L} + \omega) \hat{c}_{\mathbf{k}\sigma}]_+ \rangle.$$

The time dependence and the expectation value are formed with the full Hamiltonian $\mathcal{H}$, and L is the Liouville operator corresponding to $\mathcal{H}$. According to Eq. (55), the anticommutator Green's function can be expressed by

$$\Im G(\mathbf{k},\omega) = \langle [\hat{c}^{\dagger}_{\mathbf{k}\sigma}(\lambda), \delta(\mathsf{L}_\lambda + \omega) \hat{c}_{\mathbf{k}\sigma}(\lambda)]_+ \rangle_\lambda, \tag{58}$$

where now the creation and annihilation operators are also subject to the unitary transformation. To evaluate $A(\mathbf{k},\omega)$, we have to derive renormalization equations for $\hat{c}_{\mathbf{k}\sigma}(\lambda)$ and $\hat{c}^{\dagger}_{\mathbf{k}\sigma}(\lambda)$. According to Appendix C, the following *ansatz* for $\hat{c}_{\mathbf{k}\sigma}(\lambda)$ can be used:

$$\hat{c}_{\mathbf{k}\sigma}(\lambda) = u_{\mathbf{k},\lambda} \hat{c}_{\mathbf{k}\sigma} + \frac{1}{2N} \sum_{\mathbf{q}\mathbf{k}'} v_{\mathbf{k},\mathbf{q},\lambda} \frac{J_{\mathbf{q}}}{4\hat{\omega}^2_{\mathbf{q},\lambda}} \sum_{\alpha\beta\gamma} (\vec{\sigma}_{\alpha\beta} \cdot \vec{\sigma}_{\sigma\gamma})$$

$$\times (\varepsilon_{\mathbf{k}',\lambda} - \varepsilon_{\mathbf{k}'+\mathbf{q},\lambda}) \hat{c}^{\dagger}_{\mathbf{k}'+\mathbf{q}\alpha} \hat{c}_{\mathbf{k}'\beta} \hat{c}_{\mathbf{k}+\mathbf{q}\gamma}. \tag{59}$$

It can be justified from lowest-order perturbation theory. Note that the λ-dependence is transferred to the parameters $u_{\mathbf{k},\lambda}$ and $v_{\mathbf{k},\mathbf{q},\lambda}$. Also the quantities $\hat{\omega}_{\mathbf{q},\lambda}$ and $\varepsilon_{\mathbf{k},\lambda}$ depend on λ. However, having in mind perturbation theory in J, this λ-dependence will be neglected in the numerical evaluation of Sec. V below. According to Appendix C, the renormalization equations for $u_{\mathbf{k},\lambda}$ and $v_{\mathbf{k},\mathbf{q},\lambda}$ read

$$u^2_{\mathbf{k},\lambda-\Delta\lambda} = u^2_{\mathbf{k},\lambda} - \frac{3}{2N^2} \sum_{\mathbf{q}\mathbf{k}'} \left(\frac{J_{\mathbf{q}}}{4\hat{\omega}^2_{\mathbf{q}}} \right)^2$$

$$\times \Theta_{\mathbf{q}}(\lambda, \Delta\lambda) (\varepsilon_{\mathbf{k}',\lambda} - \varepsilon_{\mathbf{k}'+\mathbf{q},\lambda})^2$$

$$\times \left\{ \left(\frac{u_{\mathbf{k},\lambda}}{2} \right)^2 + u_{\mathbf{k},\lambda} v_{\mathbf{k},\mathbf{q},\lambda} \right\}$$

$$\times \{ n_{\mathbf{k}'+\mathbf{q}} m_{\mathbf{k}'} + n_{\mathbf{k}+\mathbf{q}} (D + n_{\mathbf{k}'} - n_{\mathbf{k}'+\mathbf{q}}) \}$$

$$+ \frac{3}{4N^2} \sum_{\mathbf{q}\mathbf{q}'} \frac{J_{\mathbf{q}}}{4\hat{\omega}^2_{\mathbf{q}}} \frac{J_{\mathbf{q}'}}{4\hat{\omega}^2_{\mathbf{q}'}}$$

$$\times (\varepsilon_{\mathbf{k}+\mathbf{q}',\lambda} - \varepsilon_{\mathbf{k}+\mathbf{q}+\mathbf{q}',\lambda}) (\varepsilon_{\mathbf{k}+\mathbf{q},\lambda} - \varepsilon_{\mathbf{k}+\mathbf{q}+\mathbf{q}',\lambda})$$

$$\times \{ v_{\mathbf{k},\mathbf{q}',\lambda} \Theta_{\mathbf{q}}(\lambda, \Delta\lambda) + v_{\mathbf{k},\mathbf{q},\lambda} \Theta_{\mathbf{q}'}(\lambda, \Delta\lambda) \} \frac{u_{\mathbf{k},\lambda}}{2}$$

$$\times \{ n_{\mathbf{k}+\mathbf{q}'} (n_{\mathbf{k}+\mathbf{q}+\mathbf{q}'} - n_{\mathbf{k}+\mathbf{q}} - D) - m_{\mathbf{k}+\mathbf{q}} n_{\mathbf{k}+\mathbf{q}+\mathbf{q}'} \} \tag{60}$$

and

$$v_{\mathbf{k},\mathbf{q},\lambda-\Delta\lambda} = v_{\mathbf{k},\mathbf{q},\lambda} + u_{\mathbf{k},\lambda} \Theta_{\mathbf{q}}(\lambda, \Delta\lambda). \tag{61}$$

The quantities $n_{\mathbf{k}}$ and $m_{\mathbf{k}}$ in Eq. (60) are the $\mathbf{k}$-dependent occupation numbers for electrons and holes per spin direction, which are formed with the full Hamiltonian $\mathcal{H}$,

$$n_{\mathbf{k}} = \langle \hat{c}^{\dagger}_{\mathbf{k}\sigma} \hat{c}_{\mathbf{k}\sigma} \rangle, \quad m_{\mathbf{k}} = \langle \hat{c}_{\mathbf{k}\sigma} \hat{c}^{\dagger}_{\mathbf{k}\sigma} \rangle. \tag{62}$$

In the following, we simplify the notation by suppressing the spin index σ in Eq. (62). Renormalization equations (60) and (61) for $u^2_{\mathbf{k},\lambda}$ and $v_{\mathbf{k},\mathbf{q},\lambda}$, together with ansatz (59) for $\hat{c}_{\mathbf{k},\sigma}(\lambda)$, enable us to evaluate $n_{\mathbf{k}}$ and $m_{\mathbf{k}}$ and also the ARPES spectral function. With some initial guess for $n_{\mathbf{k}}$ and $m_{\mathbf{k}}$, we start from the parameter values of the original model at $\lambda = \Lambda$,

$$u_{\mathbf{k},\Lambda} = 1, \quad v_{\mathbf{k},\mathbf{q},\Lambda} = 0, \tag{63}$$

and eliminate all excitations in steps $\Delta\lambda$ from $\lambda = \Lambda$ to $\lambda = 0$. We end up with renormalized parameters which obey

$$u_{\mathbf{k},\lambda=0} \neq 1, \quad v_{\mathbf{k},\mathbf{q},\lambda=0} \neq 0.$$

Thus, after the renormalization, the annihilation operator $\hat{c}_{\mathbf{k}}(\lambda=0) := \hat{c}^{(1)}_{\mathbf{k}\sigma}$ at $\lambda=0$ has the final form

$$\hat{c}^{(1)}_{\mathbf{k}\sigma} = u_{\mathbf{k},\lambda=0}\hat{c}_{\mathbf{k}\sigma} + \frac{1}{2N}\sum_{\mathbf{q}\mathbf{k}'} v_{\mathbf{k},\mathbf{q},\lambda=0}\frac{J_{\mathbf{q}}}{4\hat{\omega}^2_{\mathbf{q}}}\sum_{\alpha\beta\gamma}(\vec{\sigma}_{\alpha\beta}\cdot\vec{\sigma}_{\sigma\gamma}) \times(\varepsilon_{\mathbf{k}',\lambda=0} - \varepsilon_{\mathbf{k}'+\mathbf{q},\lambda=0})\hat{c}^{\dagger}_{\mathbf{k}'+\mathbf{q}\alpha}\hat{c}_{\mathbf{k}'\beta}\hat{c}_{\mathbf{k}+\mathbf{q}\gamma}.$$

As was discussed before, the Hamiltonian after the first renormalization $\tilde{\mathcal{H}}^{(1)}$ can not directly be used to recalculate the expectation values $n_{\mathbf{k}}$ and $m_{\mathbf{k}}$. In $\tilde{\mathcal{H}}^{(1)}$, there is still a part of the exchange present, which is, however, reduced by a factor $1/2$. Therefore, the renormalization has to be done again by starting from $\tilde{\mathcal{H}}^{(1)}$ as the new initial Hamiltonian. Similarly, $\hat{c}^{(1)}_{\mathbf{k}\sigma}$ can be considered as the new initial annihilation operator, i.e., $\hat{c}^{(1)}_{\mathbf{k}\sigma}=\hat{c}^{(1)}_{\mathbf{k}\sigma}(\lambda=\Lambda)$, with

$$u^{(1)}_{\mathbf{k},\lambda=\Lambda} = u_{\mathbf{k},\lambda=0}, \quad v^{(1)}_{\mathbf{k},\mathbf{q},\lambda=\Lambda} = v_{\mathbf{k},\mathbf{q},\lambda=0}.$$

After n renormalization cycles, the exchange is scaled down by a factor $(1/2)^n$. For the renormalization equation for $u^{(n)}_{\mathbf{k},\lambda}$ and $v^{(n)}_{\mathbf{k},\mathbf{q},\lambda}$, we obtain

$$\begin{aligned}(u^{(n)}_{\mathbf{k},\lambda-\Delta\lambda})^2 = (u^{(n)}_{\mathbf{k},\lambda})^2 &- \frac{3}{2N^2}\sum_{\mathbf{q}\mathbf{k}'}\left(\frac{J_{\mathbf{q}}}{4\hat{\omega}^2_{\mathbf{q}}}\right)^2 \times\Theta_{\mathbf{q}}(\lambda,\Delta\lambda)(\varepsilon_{\mathbf{k}',\lambda}-\varepsilon_{\mathbf{k}'+\mathbf{q},\lambda})^2 \\ &\times\left\{\left(\frac{u^{(n)}_{\mathbf{k},\lambda}}{2^n}\right)^2 + \frac{u^{(n)}_{\mathbf{k},\lambda}}{2^{n-1}}v^{(n)}_{\mathbf{k},\mathbf{q},\lambda}\right\} \\ &\times\{n_{\mathbf{k}'+\mathbf{q}}m_{\mathbf{k}'} + n_{\mathbf{k}+\mathbf{q}}(D+n_{\mathbf{k}'}-n_{\mathbf{k}'+\mathbf{q}})\} \\ &+ \frac{3}{4N^2}\sum_{\mathbf{q}\mathbf{q}'}\frac{J_{\mathbf{q}}}{4\hat{\omega}^2_{\mathbf{q}}}\frac{J_{\mathbf{q}'}}{4\hat{\omega}^2_{\mathbf{q}'}} \\ &\times(\varepsilon_{\mathbf{k}+\mathbf{q}',\lambda}-\varepsilon_{\mathbf{k}+\mathbf{q}+\mathbf{q}',\lambda})(\varepsilon_{\mathbf{k}+\mathbf{q},\lambda}-\varepsilon_{\mathbf{k}+\mathbf{q}+\mathbf{q}',\lambda}) \\ &\times\{v^{(n)}_{\mathbf{k},\mathbf{q}',\lambda}\Theta_{\mathbf{q}}(\lambda,\Delta\lambda) + v^{(n)}_{\mathbf{k},\mathbf{q},\lambda}\Theta_{\mathbf{q}'}(\lambda,\Delta\lambda)\}\frac{u^{(n)}_{\mathbf{k},\lambda}}{2^n} \\ &\times\{n_{\mathbf{k}+\mathbf{q}'}(n_{\mathbf{k}+\mathbf{q}+\mathbf{q}'}-n_{\mathbf{k}+\mathbf{q}}-D) - m_{\mathbf{k}+\mathbf{q}}n_{\mathbf{k}+\mathbf{q}+\mathbf{q}'}\}\end{aligned} \tag{64}$$

and

$$v^{(n)}_{\mathbf{k},\mathbf{q},\lambda-\Delta\lambda} = v^{(n)}_{\mathbf{k},\mathbf{q},\lambda} + \frac{u^{(n)}_{\mathbf{k},\lambda}}{2^n}\Theta_{\mathbf{q}}(\lambda,\Delta\lambda). \tag{65}$$

Note that the factor $1/2^n$ was incorporated in $v^{(n)}_{\mathbf{k},\mathbf{q},\sigma}$, in order to keep the shape of *ansatz* (59) unchanged,

$$\hat{c}^{(n)}_{\mathbf{k}\sigma}(\lambda) = u^{(n)}_{\mathbf{k},\lambda}\hat{c}_{\mathbf{k}\sigma} + \frac{1}{2N}\sum_{\mathbf{q}\mathbf{k}'} v^{(n)}_{\mathbf{k},\mathbf{q},\lambda}\frac{J_{\mathbf{q}}}{4\hat{\omega}^2_{\mathbf{q}}}\sum_{\alpha\beta\gamma}(\vec{\sigma}_{\alpha\beta}\cdot\vec{\sigma}_{\sigma\gamma}) \times(\varepsilon_{\mathbf{k}',\lambda}-\varepsilon_{\mathbf{k}'+\mathbf{q},\lambda})\hat{c}^{\dagger}_{\mathbf{k}'+\mathbf{q}\alpha}\hat{c}_{\mathbf{k}'\beta}\hat{c}_{\mathbf{k}+\mathbf{q}\gamma}. \tag{66}$$

For $n\to\infty$, we arrive at the fully renormalized operator

$$\hat{c}^{(n\to\infty)}_{\mathbf{k}\sigma}(\lambda=0) = \tilde{u}_{\mathbf{k}}\hat{c}_{\mathbf{k}\sigma} + \frac{1}{2N}\sum_{\mathbf{q}\mathbf{k}'}\tilde{v}_{\mathbf{k},\mathbf{q}}\frac{J_{\mathbf{q}}}{4\hat{\omega}^2_{\mathbf{q}}}\sum_{\alpha\beta\gamma}(\vec{\sigma}_{\alpha\beta}\cdot\vec{\sigma}_{\sigma\gamma}) \times(\tilde{\varepsilon}_{\mathbf{k}'}-\tilde{\varepsilon}_{\mathbf{k}'+\mathbf{q}})\hat{c}^{\dagger}_{\mathbf{k}'+\mathbf{q}\alpha}\hat{c}_{\mathbf{k}'\beta}\hat{c}_{\mathbf{k}+\mathbf{q}\gamma}, \tag{67}$$

where $\tilde{u}_{\mathbf{k}}=u^{(n\to\infty)}_{\mathbf{k},\lambda=0}$ and $\tilde{v}_{\mathbf{k},\mathbf{q}}=v^{(n\to\infty)}_{\mathbf{k},\mathbf{q},\lambda=0}$. Using $\tilde{\mathcal{H}}$, the expectation values $n_{\mathbf{k}}$ and $m_{\mathbf{k}}$ as well as the spectral function $\Im G(\mathbf{k},\omega)$ can be evaluated. However, due to the strong correlations in $\tilde{\mathcal{H}}$, additional approximations will still be necessary.

To evaluate the spectral function $\Im G(\mathbf{k},\omega)$, we start from Eq. (58) for $n\to\infty$, $\lambda=0$

$$\Im G(\mathbf{k},\omega) = \langle[\hat{c}^{(n\to\infty)\dagger}_{\mathbf{k}\sigma}(\lambda=0), \delta(\tilde{\mathsf{L}}+\omega)\hat{c}^{(n\to\infty)}_{\mathbf{k}\sigma}(\lambda=0)]_+\rangle_{\tilde{\mathcal{H}}}. \tag{68}$$

Here $\hat{c}^{(n\to\infty)}_{\mathbf{k}\sigma}(\lambda\to 0)$ is given by Eq. (67). The time dependence and the expectation value are defined with $\tilde{\mathcal{H}}$, and $\tilde{\mathsf{L}}$ is the Liouville operator to $\tilde{\mathcal{H}}$. For a state close to half-filling, the following relation is approximately valid according to Appendix B:

$$\tilde{\mathsf{L}}\hat{c}_{\mathbf{k}\sigma} = [\tilde{\mathcal{H}},\hat{c}_{\mathbf{k}\sigma}] = -\tilde{\varepsilon}_{\mathbf{k}}\hat{c}_{\mathbf{k}\sigma}. \tag{69}$$

It means, in the case that the dynamics is governed by the Hamiltonian $\tilde{\mathcal{H}}$, in which no magnetic interactions are present, a hole can move almost freely through the lattice. Using Eqs. (67) and (68), the spectral function $\Im G(\mathbf{k},\omega)$ then reads

$$\begin{aligned}\Im G(\mathbf{k},\omega) &= \tilde{u}^2_{\mathbf{k}}D\,\delta(\omega-\tilde{\varepsilon}_{\mathbf{k}}) + \frac{3D}{2N^2}\sum_{\mathbf{q}\mathbf{q}'}\left[\left(\frac{J_{\mathbf{q}}\tilde{v}_{\mathbf{k},\mathbf{q}}}{4\hat{\omega}^2_{\mathbf{q}}}\right)^2(\tilde{\varepsilon}_{\mathbf{k}+\mathbf{q}'}-\tilde{\varepsilon}_{\mathbf{k}+\mathbf{q}+\mathbf{q}'})^2\right. \\ &\times\{\tilde{n}_{\mathbf{k}+\mathbf{q}+\mathbf{q}'}\tilde{m}_{\mathbf{k}+\mathbf{q}'} + \tilde{n}_{\mathbf{k}+\mathbf{q}}(D+\tilde{n}_{\mathbf{k}+\mathbf{q}'}-\tilde{n}_{\mathbf{k}+\mathbf{q}+\mathbf{q}'})\} \\ &-\frac{1}{2}\frac{J_{\mathbf{q}}}{4\hat{\omega}^2_{\mathbf{q}}}\frac{J_{\mathbf{q}'}}{4\hat{\omega}^2_{\mathbf{q}'}}\tilde{v}_{\mathbf{k},\mathbf{q}}\tilde{v}_{\mathbf{k},\mathbf{q}'}(\tilde{\varepsilon}_{\mathbf{k}+\mathbf{q}'}-\tilde{\varepsilon}_{\mathbf{k}+\mathbf{q}+\mathbf{q}'})(\tilde{\varepsilon}_{\mathbf{k}+\mathbf{q}}-\tilde{\varepsilon}_{\mathbf{k}+\mathbf{q}+\mathbf{q}'}) \\ &\left.\times\{(\tilde{n}_{\mathbf{k}+\mathbf{q}'}-\tilde{m}_{\mathbf{k}+\mathbf{q}})\tilde{n}_{\mathbf{k}+\mathbf{q}+\mathbf{q}'} - \tilde{n}_{\mathbf{k}+\mathbf{q}'}(\tilde{n}_{\mathbf{k}+\mathbf{q}}+D)\}\right] \\ &\times\delta(\omega+\tilde{\varepsilon}_{\mathbf{k}+\mathbf{q}+\mathbf{q}'}-\tilde{\varepsilon}_{\mathbf{k}+\mathbf{q}'}-\tilde{\varepsilon}_{\mathbf{k}+\mathbf{q}}).\end{aligned} \tag{70}$$

Note that in deriving Eq. (70), an additional factorization approximation was used. Thereby, an expectation value, formed with six fermion operators, was replaced by a product of three two-fermion expectation values. The new quantities $\tilde{n}_{\mathbf{k}}$ and $\tilde{m}_{\mathbf{k}}$ in Eq. (70),

$$\tilde{n}_{\mathbf{k}} = \langle\hat{c}^{\dagger}_{\mathbf{k}\sigma}\hat{c}_{\mathbf{k}\sigma}\rangle_{\tilde{\mathcal{H}}}, \quad \tilde{m}_{\mathbf{k}} = \langle\hat{c}_{\mathbf{k}\sigma}\hat{c}^{\dagger}_{\mathbf{k}\sigma}\rangle_{\tilde{\mathcal{H}}}$$

are again $\mathbf{k}$-dependent occupation numbers for electrons and holes per spin direction, However, they are defined with the fully renormalized model $\tilde{\mathcal{H}}$ instead of with $\mathcal{H}$ as in Eqs. (62). For $\tilde{n}_{\mathbf{k}}$ and $\tilde{m}_{\mathbf{k}}$, we use the Gutzwiller approximation[18]

$$\tilde{n}_{\mathbf{k}} = (D-q) + qf(\tilde{\varepsilon}_{\mathbf{k}}),$$

$$\tilde{m}_{\mathbf{k}} = q[1-f(\tilde{\varepsilon}_{\mathbf{k}})] \quad \text{with } q = \frac{1-n}{1-n/2} = \frac{\delta}{1-n/2}, \tag{71}$$

where $f(\tilde{\varepsilon}_{\mathbf{k}})$ is the Fermi function, $f(\tilde{\varepsilon}_{\mathbf{k}})=\Theta(-\tilde{\varepsilon}_{\mathbf{k}})$ for $T=0$. Note that $\tilde{m}_{\mathbf{k}}$ is proportional to the hole filling $\delta=1-n$. Obviously, the application of $\hat{c}^{\dagger}_{\mathbf{k}\sigma}$ on a Hilbert space vector is nonzero only when holes are present. In contrast, $\tilde{n}_{\mathbf{k}\sigma}$ does not vanish even at half-filling.

According to Eq. (70), the spectral function $\mathcal{J}G(\mathbf{k},\omega)$ consists of two parts: The first one is a coherent excitation of energy $\tilde{\varepsilon}_{\mathbf{k}}$ with the weight $\tilde{u}^2_{\mathbf{k}}D$. The second part describes three-particle excitations. Also note that the sum rule

$$\int_{-\infty}^{\infty} d\omega \mathcal{J}G(\mathbf{k},\omega) = \langle [\hat{c}^{\dagger}_{\mathbf{k}\sigma}, \hat{c}_{\mathbf{k}\sigma}]_+ \rangle = 1 - \frac{n}{2} = D \tag{72}$$

is automatically fulfilled by Eq. (70). The sum rule is built in by the construction of the renormalization equations for $u_{\mathbf{k},\lambda}$ and $v_{\mathbf{k},\mathbf{q},\lambda}$ in Appendix C.

For finite temperature, a phenomenological extension of the Gutzwiller approximation according to Ref. 19 will later be used. Here, the Fermi function is replaced by

$$f(\tilde{\varepsilon}_{\mathbf{k}}) = \frac{1}{1+\exp[\beta q \tilde{\varepsilon}_{\mathbf{k}}/w(\mathbf{k},n)]}, \tag{73}$$

where $w(\mathbf{k},n)$ is a weighting function in $\mathbf{k}$ space. It was introduced in Ref. 19 in order to account for an overcompleteness in the Gutzwiller approximation. It plays the role of a $\mathbf{k}$-dependent effective mass and is a quantity of order 1.

Finally, note that the static expectation values $n_{\mathbf{k}}$ and $m_{\mathbf{k}}$, defined in Eq. (62), can also be evaluated from $A(\mathbf{k},\omega)$ or $\mathcal{J}G(\mathbf{k},\omega)$,

$$n_{\mathbf{k}} = \int_{-\infty}^{\infty} A(\mathbf{k},\omega) d\omega = \int_{-\infty}^{\infty} \frac{1}{1+e^{\beta\omega}} \mathcal{J}G(\mathbf{k},\omega) d\omega, \quad m_{\mathbf{k}} = D - n_{\mathbf{k}}. \tag{74}$$

V. NUMERICAL EVALUATION FOR THE PSEUDOGAP PHASE

Renormalization equations (41), (53), (64), and (65) together with Eq. (74) form a closed system of equations, which could be solved self-consistently. However, to simplify the numerical evaluation, we calculate the expectation values in Eqs. (41) and (53) with the renormalized Hamiltonian $\tilde{\mathcal{H}}$ instead of with $\mathcal{H}$. Within this approximation and Gutzwiller approximation (71), the renormalization equation for the energy $\varepsilon_{\mathbf{k},\lambda}$ reads

$$\begin{aligned}\varepsilon_{\mathbf{k},\lambda-\Delta\lambda} - \varepsilon_{\mathbf{k},\lambda} = {} & \frac{1}{16N}\sum_{\mathbf{q}} \frac{J^2_{\mathbf{q}}}{\hat{\omega}^4_{\mathbf{q},\lambda}} \Theta_{\mathbf{q}}(\lambda,\Delta\lambda)(\varepsilon_{\mathbf{k}+\mathbf{q},\lambda} + \varepsilon_{\mathbf{k}-\mathbf{q},\lambda} \\ & - 2\varepsilon_{\mathbf{k},\lambda})\langle \dot{\mathbf{S}}_{\mathbf{q}}\dot{\mathbf{S}}_{-\mathbf{q}}\rangle + \frac{3q^2}{8N}\sum_{\mathbf{q}} \frac{J^2_{\mathbf{q}}}{\hat{\omega}^4_{\mathbf{q},\lambda}} \Theta_{\mathbf{q}}(\lambda,\Delta\lambda) \\ & \times \left[\frac{1}{N}\sum_{\mathbf{k}'} (2\varepsilon_{\mathbf{k}',\lambda} - \varepsilon_{\mathbf{k}'+\mathbf{q},\lambda} - \varepsilon_{\mathbf{k}'-\mathbf{q},\lambda}) f^{(NL)}_{\mathbf{k}'} \right] \\ & \times (\varepsilon_{\mathbf{k},\lambda} - \varepsilon_{\mathbf{k}-\mathbf{q},\lambda})^2 f^{(NL)}_{\mathbf{k}-\mathbf{q}},\end{aligned} \tag{75}$$

with

$$\langle \dot{\mathbf{S}}_{\mathbf{q}}\dot{\mathbf{S}}_{-\mathbf{q}}\rangle = -\frac{3q^2}{2}\frac{1}{N}\sum_{\mathbf{k}'} (\tilde{\varepsilon}_{\mathbf{k}'} - \tilde{\varepsilon}_{\mathbf{k}'+\mathbf{q}})^2 f^{(NL)}_{\mathbf{k}'} f^{(NL)}_{\mathbf{k}'+\mathbf{q}}.$$

Here, $f^{(NL)}_{\mathbf{k}}$ is the nonlocal part of the Fermi distribution, $f^{(NL)}_{\mathbf{k}} = 1/(1+e^{\beta\tilde{\varepsilon}_{\mathbf{k}}}) - (1/N)\Sigma_{\mathbf{k}} 1/(1+e^{\beta\tilde{\varepsilon}_{\mathbf{k}}})$. Remember that the factor q as well as $\hat{\omega}^2_{\mathbf{q},\lambda}$ are proportional to the hole concentration $\delta=1-n$. Therefore, the renormalization contributions to Eq. (75) are almost independent of δ and turn out to be very small. Therefore, from now on, the λ dependence of $\varepsilon_{\mathbf{k},\lambda}$ and also of $\hat{\omega}_{\mathbf{q},\lambda}$ will be neglected.

A. Zero-temperature results

For the evaluation of the renormalization scheme, we have used a sufficiently large number of renormalization cycles in order to obtain self-consistency. We have considered a square lattice with $N=40\times 40$ sites and a moderate hole doping, such that the system is outside the antiferromagnetic phase but not yet in the Fermi-liquid phase. Possible superconducting solutions are not considered.

The main feature of the normal state is the appearance of a pseudogap which is experimentally observed in ARPES measurements. A small next-nearest-neighbor hopping $t'=0.1t$ and an exchange constant $J=0.2t$ between nearest neighbors are assumed. The inclusion of a nonzero t' leads to a Fermi surface (FS), as sketched in the inset of Fig. 3. It closely resembles the Fermi surface of noninteracting electrons. The FS is determined from the condition $\tilde{\varepsilon}_{\mathbf{k}}=0$ for a fixed value of the electron filling $n=1-\delta$. The temperature is set equal to $T=0$. Let us first concentrate on the ω dependence of the spectral function $\mathcal{J}G(\mathbf{k},\omega)$. In all figures, the symmetrized function will be plotted in order to remove the effects of the Fermi function on the spectra.

Figure 2 shows the PRM result for $\mathcal{J}G(\mathbf{k},\omega)$ for two different hole concentrations in the underdoped regime (a) $\delta=0.03$ and (b) $\delta=0.075$, for several $\mathbf{k}$ values on the FS between the nodal point near $(\pi/2,\pi/2)$ and the antinodal near $(\pi,0)$. As the most important finding, one recognizes the opening of a pseudogap for both hole concentrations, when one proceeds from the nodal towards the antinodal direction. On a substantial part of the FS, the spectra show a peaklike behavior around $\omega=0$, indicating a Fermi arc of gapless excitations. Note that our analytical results show a remarkable agreement with findings from ARPES experiments in high-temperature superconductors.[9–12] Also additional peaks are found in the nodal direction at lower binding energies which are enhanced for $\delta=0.075$. In Fig. 3, the pseudogap on the

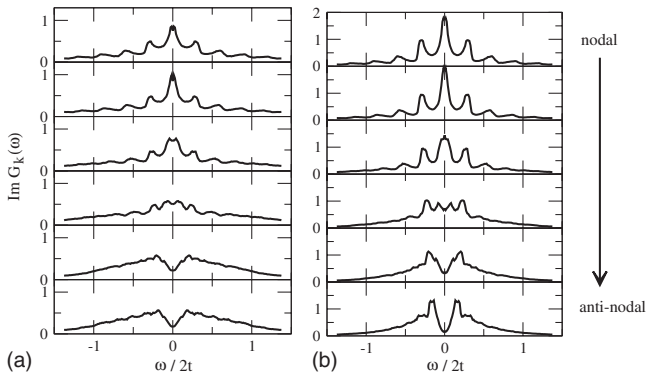

FIG. 2. Symmetrized spectral function $\Im G(\mathbf{k},\omega)$ in units of $(2t)^{-1}$ at $T=0$ for two hole fillings (a) $\delta=0.03$ and (b) $\delta=0.075$ along the Fermi surface. The top $\Im G(\mathbf{k},\omega)$ is at the node, whereas the bottom is at the antinode, as defined in the inset of Fig. 3.

FS is shown as a function of the angle ϕ, where ϕ is defined in the inset of Fig. 3. The results are taken from Figs. 2(a) and 2(b). Note that for the smaller hole filling, the length of the Fermi arc becomes smaller, whereas the pseudogap becomes larger. This behavior agrees with the known experimental feature of a characteristic pseudogap temperature T^* which increases with decreasing hole filling.[9,20]

The ω and $\mathbf{k}$ dependences of $\Im G(\mathbf{k},\omega)$ from Fig. 2 can easily be understood from equation (70),

$$\Im G(\mathbf{k},\omega) = |\tilde{u}_{\mathbf{k}}|^2 D\delta(\omega-\varepsilon_{\mathbf{k}}) + \frac{3D}{2N^2}\sum_{\mathbf{q}\mathbf{k}'}\left\{\left(\frac{J_{\mathbf{q}}}{4\hat{\omega}_{\mathbf{q}}^2}\right)^2|\tilde{v}_{\mathbf{k},\mathbf{q}}|^2 \times(\varepsilon_{\mathbf{k}'}-\varepsilon_{\mathbf{k}'+\mathbf{q}})^2[\tilde{n}_{\mathbf{k}'+\mathbf{q}}\tilde{m}_{\mathbf{k}'}+\tilde{n}_{\mathbf{k}+\mathbf{q}}(D+\tilde{n}_{\mathbf{k}'} - \tilde{n}_{\mathbf{k}'+\mathbf{q}})]+\cdots\right\}\delta(\omega+\varepsilon_{\mathbf{k}'+\mathbf{q}}-\varepsilon_{\mathbf{k}'}-\varepsilon_{\mathbf{k}+\mathbf{q}}), \tag{76}$$

where the dots $+\cdots$ indicate additional terms which are less important. First, from renormalization equation (60) for $u^2_{\mathbf{k},\lambda}$, one finds that its original value $u^2_{\mathbf{k}}=1$ at $\lambda=\Lambda$ is reduced by renormalization contributions of order δ^{-2} according to $u^2_{\mathbf{k},\lambda-\Delta\lambda}-u^2_{\mathbf{k},\lambda}=-\alpha_\lambda/\delta^2$. Thus, the weight of the coherent excitation $|\tilde{u}_{\mathbf{k}}|^2$ becomes small for small δ so that the spectral function $\Im G(\mathbf{k},\omega)$ is dominated by the incoherent excitations in Eq. (76). What remains is to show that the different behavior of $\Im G(\mathbf{k},\omega)$ in the nodal and in the antinodal region can be understood solely from the incoherent part of Eq. (76):

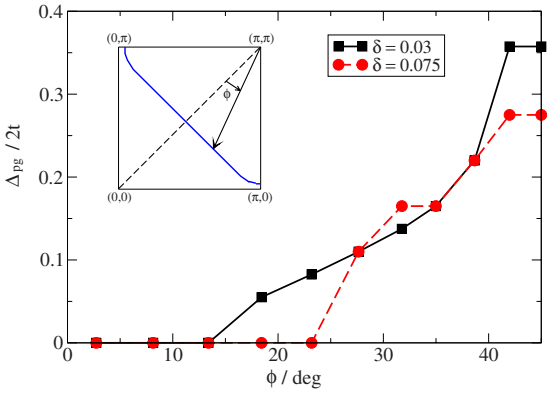

FIG. 3. (Color online) Pseudogap size Δ_{pg} from Fig. 2 as function of the Fermi surface angle ϕ for $\delta=0.03$ (black) and $\delta=0.075$ (red).

First note that the dominant contribution in Eq. (76) at small ω arises from the small $\mathbf{q}$ terms in the sum over $\mathbf{q}$ since in the denominator $\hat{\omega}^2_{\mathbf{q}}\sim\mathbf{q}^2$. In the numerator, the factor $(\varepsilon_{\mathbf{k}'}-\varepsilon_{\mathbf{k}'+\mathbf{q}})^2$ is also proportional to q^2 so that the combined prefactor $(J_{\mathbf{q}}/4\hat{\omega}^2_{\mathbf{q}})^2(\varepsilon_{\mathbf{k}'}-\varepsilon_{\mathbf{k}'+\mathbf{q}})^2$ behaves as $\sim\mathbf{q}^{-2}$. However, the small $\mathbf{q}$ terms do not lead to a divergency in Eq. (76) since the additional renormalization parameter $\tilde{v}^2_{\mathbf{k},\mathbf{q}}$ also vanishes for $\mathbf{q}\to 0$. This behavior can be verified by a close inspection of the renormalization equations (60) and (61) for $u_{\mathbf{k},\lambda}$ and $v_{\mathbf{k},\mathbf{q},\lambda}$. Next, let us use the small $\mathbf{q}$ expansion for the energy difference

$$\varepsilon_{\mathbf{k}'}-\varepsilon_{\mathbf{k}'+\mathbf{q}} = -2t(q_x\sin k'_x + q_y\sin k'_y). \tag{77}$$

The excitations from the δ function in Eq. (76) are given by

$$\omega = \varepsilon_{\mathbf{k}'}-\varepsilon_{\mathbf{k}'+\mathbf{q}}+\varepsilon_{\mathbf{k}+\mathbf{q}} \approx \varepsilon_{\mathbf{k}}+2t\{q_x(\sin k_x-\sin k'_x)+q_y(\sin k_y-\sin k'_y)\}, \tag{78}$$

which still depend on $\mathbf{k}'$. There is also a $\mathbf{k}'$-dependent factor in the numerator which contributes to the intensity,

$$(\varepsilon_{\mathbf{k}'}-\varepsilon_{\mathbf{k}'+\mathbf{q}})^2 = 4t^2(q_x\sin k'_x+q_y\sin k'_y)^2+\mathcal{O}(q^4). \tag{79}$$

Now, we are able to discuss the small ω behavior of the spectral function $\Im G(\mathbf{k},\omega)$, when the wave vector $\mathbf{k}$ is varied:

(i) First, close to the antinodal point $\mathbf{k}=(0,\pi)$, the excitation energy [Eq. (78)] reduces to

$$\omega = \varepsilon_{\mathbf{k}'}-\varepsilon_{\mathbf{k}'+\mathbf{q}}+\varepsilon_{\mathbf{k}+\mathbf{q}} \approx \varepsilon_{\mathbf{k}}-2t(q_x\sin k'_x+q_y\sin k'_y). \tag{80}$$

By comparing Eq. (80) with Eq. (79), one realizes that the square of the frequency shift in Eq. (80) is identical to intensity factor (79). Thus, excitations with small shifts away from the Fermi surface $\varepsilon_{\mathbf{k}}=0$ also have small intensities, whereas those with large shifts have large intensities. This explains naturally the pseudogap behavior at the antinodal point, where a lack of intensity is found at $\omega=0$.

(ii) For the nodal point near $\mathbf{k}=(\pi/2,\pi/2)$, the excitations have energies

$$\omega = \varepsilon_{\mathbf{k}'}-\varepsilon_{\mathbf{k}'+\mathbf{q}}+\varepsilon_{\mathbf{k}+\mathbf{q}} \approx \varepsilon_{\mathbf{k}}+2t\{q_x(1-\sin k'_x)+q_y(1-\sin k'_y)\}, \tag{81}$$

whereas the intensity factor is again given by Eq. (79). The largest intensity is caused by terms in the sum over $\mathbf{k}'$ which either belong to the region around $\mathbf{k}'\approx(\pi/2,\pi/2)$ or around $\mathbf{k}'\approx(-\pi/2,-\pi/2)$. In the first case, the excitations [Eq. (81)] reduce to $\omega\approx\varepsilon_{\mathbf{k}}$, whereas intensity factor (79) is given by $4t^2(q_x+q_y)^2$. Thus, from this $\mathbf{k}'$ region, one obtains excitations directly at the Fermi surface. For the second $\mathbf{k}'$ region, the excitation energies are given by $\omega\approx\varepsilon_{\mathbf{k}}+4t(q_x+q_y)$. The intensity factor is the same as before. Thus, similar to the antinodal point, the square of the excitation shift away from the Fermi surface $\varepsilon_{\mathbf{k}}=0$ is proportional to the corre-

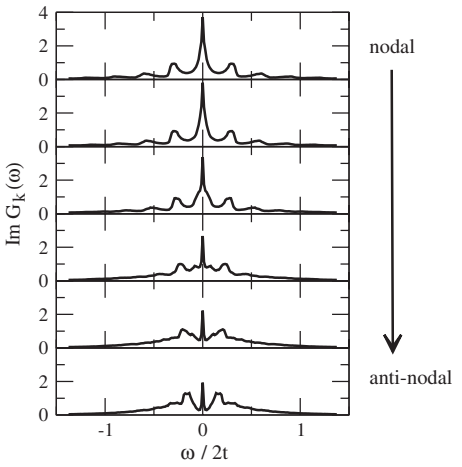

FIG. 4. Same quantity as in Figs. 2(a) and 2(b) for a larger hole doping of $\delta=0.09$.

sponding intensity. Therefore, from these $\mathbf{k}'$ terms no intensity is expected at $\omega=0$. To summarize, an excitation peak at $\omega=0$ is expected for wave vectors $\mathbf{k}$ at the antinodal point from the first $\mathbf{k}'$ regime, discussed above. In contrast, for wave vector $\mathbf{k}$ at the antinodal point a pseudogap arises. This explains the pseudogap behavior of the ARPES spectral function and leads to an understanding of the spectra of Fig. 2. In Fig. 4, the spectral function is plotted for a larger hole concentration $\delta=0.09$. The remarkable new feature is the occurrence of a narrow coherent excitation at $\omega=0$. Note that for this hole concentration, the weight $D|\tilde{u}_{\mathbf{k}}|^2$ of the coherent excitation is no longer negligible as in the preceding cases since the renormalization contributions $\sim 1/\delta^2$ to $u^2_{\mathbf{k},\lambda}$ are less important for larger δ. By increasing δ, the coherent peak gains weight at the expense of the incoherent excitations. We also expect a broadening of the coherent peak due to a coupling to other degrees of freedom such as phonons or impurities.

In Figs. 5(a) and 5(b), the spectral functions are shown for two different cuts in the Brillouin zone. In both figures, k_x is fixed and k_y is varied thereby crossing the FS. In panel (a), where $k_x=\pi$, the cut runs along the antinodal region through the FS at $\mathbf{k}_F \approx (\pi, 0.07\pi)$. Note that the pseudogap is restricted to a small $\mathbf{k}$ range around the antinodal point. It disappears for larger k_y values away from the antinodal point, in agreement with the earlier discussion on the origin of the pseudogap. The spectra along a cut in the nodal region are shown in panel (b), where $k_x=\pi/2$. Apart from the dominant excitation which corresponds to the gapless excitation on the FS in Fig. 2, also weaker excitations are found at lower binding energies. The complete peak structure is shifted almost unchanged through the FS, when k_y is varied. The energy distance between the primary and the secondary peak slowly decreases by proceeding along the FS from the nodal point to the antinodal point, until finally both peaks disappear when the antinodal region is reached. Such a double-peak structure with the same properties along the FS was observed in underdoped cuprate superconductors.[13] Finally, one point might still be worth mentioning. For fixed ω, the spectrum in $\mathbf{k}$ space is much broader than what one would expect for free electrons. Thus, the electron occupation $\langle \hat{c}^\dagger_{\mathbf{k}\sigma}\hat{c}_{\mathbf{k}\sigma}\rangle = \int d\omega (1+e^{\beta\omega})^{-1} \Im G(\mathbf{k},\omega)$ depends only weakly on $\mathbf{k}$. This feature is consistent with the former expression [Eq. (71)] for $\tilde{n}_{\mathbf{k}}$, where the Gutzwiller approximation was used. Remember that the expectation value $\tilde{n}_{\mathbf{k}}$ was defined with the renormalized Hamiltonian $\tilde{\mathcal{H}}$ and not with $\mathcal{H}$.

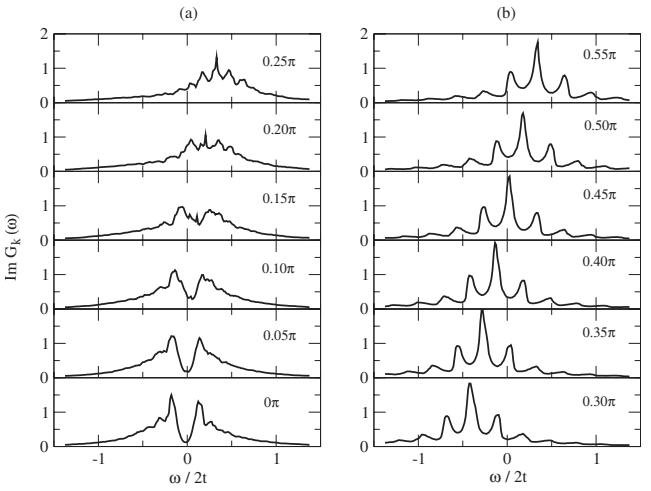

FIG. 5. Spectral functions $\Im G(\mathbf{k},\omega)$ for two fixed k_x values: (a) $k_x=\pi$ and (b) $k_x=\pi/2$ and different values of k_y, thereby crossing the Fermi surface. The hole filling $\delta=0.075$ is the same as in Fig. 2(b).

B. Finite temperature results

Next, we discuss the influence of the temperature on the one-particle spectra in the normal state. For the hopping to next-nearest neighbors, we use a somewhat larger value $t'=0.4t$. This leads to an enhanced curvature of the Fermi surface, as it is observed in most of the copper oxides superconductors. The other parameters remain unchanged. Figure 6 shows the symmetrized spectral function $\Im G(\mathbf{k},\omega)$ for two

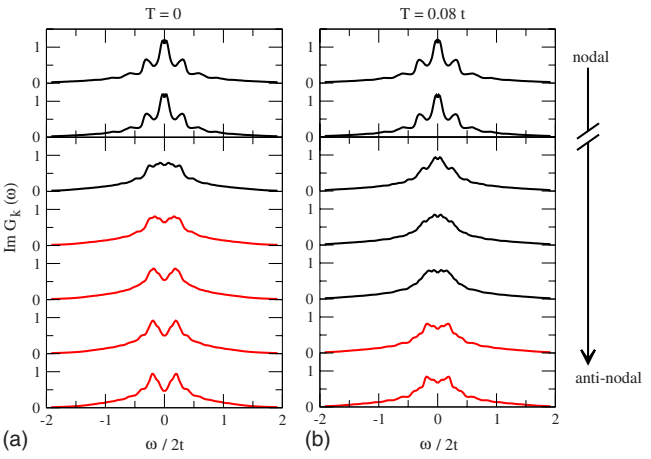

FIG. 6. (Color online) Symmetrized spectral function $\Im G(\mathbf{k},\omega)$ at doping $\delta=0.04$ for two temperatures (a) $T=0$ and (b) $T=0.08t$ for $\mathbf{k}$ values along the FS. The other parameters are $t'=0.4t$ and $J=0.2t$. The two top curves in each case are at the node, whereas the bottom curves show the pseudogap behavior in the vicinity of the antinode. A possible superconducting solution was suppressed.

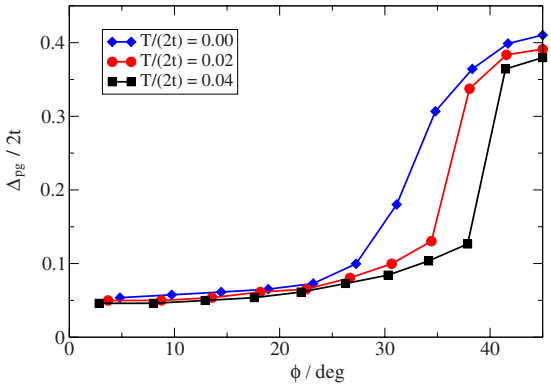

FIG. 7. (Color online) Pseudogap Δ_{pg} from Fig. 6 as a function of the Fermi surface angle ϕ for $T=0$ (blue), $T=0.04t$ (red), and $T=0.08t$ (black).

different temperatures (a) $T=0$ and (b) $T=0.08t$. The hole concentration for all curves is $\delta=0.04$. Possible superconducting solutions are again suppressed. The results are shown for different $\mathbf{k}$ vectors on the Fermi surface between the nodal (top) and the antinodal point (below). For all temperatures, a separation of the Fermi surface into two segments is found, as it was already discussed in the foregoing section: (i) For $\mathbf{k}$ vectors around the nodal points, $\Im G(\mathbf{k},\omega)$ shows strong excitations at $\omega=0$ (black curves). They form the Fermi arc. (ii) The other segment is given by $\mathbf{k}$ vectors, for which $\Im G(\mathbf{k},\omega)$ shows a pseudogap around $\omega=0$ (red curves). From Figs. 6(a) and 6(b), one can see that the length of the Fermi arc increases with increasing temperature. This increase is equivalent to a reduction of the pseudogap region. For instance, for the larger temperature $T=0.08t$, the pseudogap is restricted to a quite small region around the antinodal point. Note that this temperature behavior is in good agreement with recent ARPES experiments.[9] A comparison of the spectral functions at the antinodal point for the two different temperatures [lowest curves in Figs. 6(a) and 6(b)] shows the influence of T on the pseudogap: With increasing T, the pseudogap is filled up with additional spectral weight, whereas the magnitude of the gap (i.e., the distance between the maxima on the ω axis) remains almost constant. Also this temperature behavior is verified experimentally.[9] A characteristic temperature T^* can be defined at which the pseudogap is completely filled up, and the Fermi arc extends over the whole Fermi surface. This temperature T^* was already introduced above and is called pseudogap temperature. For the present case, T^* is approximately $T^*\approx 0.1t$.

The pseudogaps, taken over from Figs. 6(a) and 6(b), are shown in Fig. 7 for three different temperatures as function of the Fermi surface angle ϕ. Note the strong increase in the pseudogap at a finite Fermi angle which depends on the temperature. This particular angle marks the transition between the Fermi arc and the pseudogap section. At $T=0$, it is about 25 degrees and moves towards the antinodal point for higher temperatures. From Fig. 7, one may also deduce that the length of the Fermi arc approximately increases linearly with T. Also this feature is consistent with ARPES experiments.[9]

To discuss the influence of δ on the temperature dependence, in Fig. 8 the symmetrized spectral function $\Im G(\mathbf{k},\omega)$

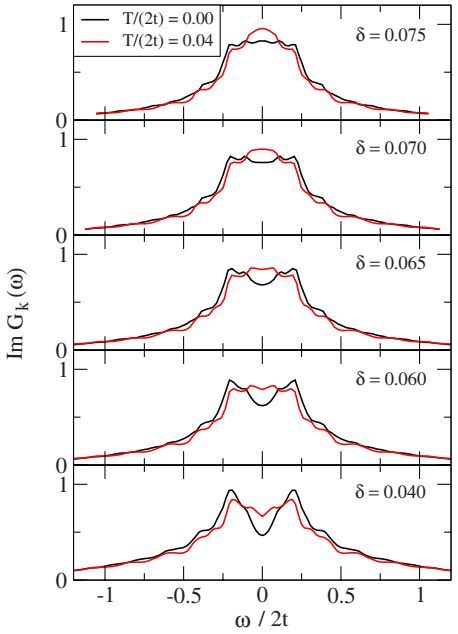

FIG. 8. (Color online) Symmetrized spectral function $\Im G(\mathbf{k},\omega)$ for fixed $\mathbf{k}$ value on the antinodal point for five different hole concentrations from $\delta=0.04$ (bottom curves) to $\delta=0.075$ (top curves). In each case, the results are shown for two different temperatures $T=0$ (black) and $T=0.08t$ (red). For the coherent excitations $\sim|\tilde{u}_{\mathbf{k}}|^2$, the same broadening has been taken for each δ value.

is shown as function of ω for two different temperatures $T=0$ (black) and $T=0.08t$ (red) and for five different hole concentrations between $\delta=0.04$ (bottom) and $\delta=0.075$ (top). The $\mathbf{k}$ vector is fixed to the antinodal point on the FS. The curves for $T=0$ (black) show a decrease in the pseudogap with increasing hole concentration until it vanishes at $\delta\approx 0.075$. For the higher temperature $T=0.08t$ (red), the pseudogap vanishes already at a lower hole concentration of $\delta\approx 0.06$. This verifies the experimentally known decrease in the pseudogap temperature T^* with increasing hole concentration.

The doping and temperature behavior of $\Im G(\mathbf{k},\omega)$ can be understood on the basis of the former result [Eq. (76)] for the spectral function. First, in Fig. 9, the parameter $\tilde{u}_{\mathbf{k}}$ is shown as a function of δ which shows a strong increase with the hole concentration. According to the first line in Eq. (76), $\tilde{u}_{\mathbf{k}}$ agrees with the amplitude of the coherent excitation. Therefore, in Fig. 6 for instance, the weight of the coherent excitation $\sim|\tilde{u}_{\mathbf{k}}|^2$ is negligibly small for the smallest hole concentration $\delta=0.04$, and the spectrum is dominated by the incoherent part of Eq. (76). In contrast, for sufficiently large δ, a coherent excitation at $\omega=0$ is expected, when $\mathbf{k}$ is fixed to the Fermi surface. This behavior is for instance realized in Fig. 4. Note that an additional broadening of the coherent excitation should be included, which follows from the scattering of the charge carriers at additional phonons or impurities. In Fig. 8, this broadening was assumed to be T independent and was set equal to $0.1t$. Therefore, the following doping behavior can be deduced from Fig. 8: For small hole concentrations $\delta(\delta\ll 0.07)$, the spectrum at $T=0$ is dominated by the incoherent excitations with a pronounced

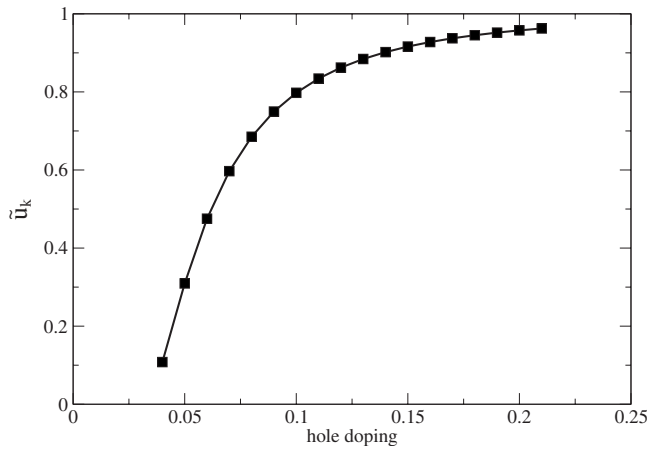

FIG. 9. The renormalized amplitude $\tilde{u}_{\mathbf{k}}$ of the coherent excitation in Eq. (76) is shown as a function of the hole concentration δ. The $\mathbf{k}$ vector is fixed to $(0,\pi)$.

pseudogap around the antinodal point. For intermediate hole doping ($\delta \approx 0.07$), the spectrum is a superposition of a coherent and of incoherent excitations. Both parts are of the same order of magnitude for an intermediate doping. The incoherent part has still a pseudogap which is partly compensated by the broadening of the coherent excitation. For larger doping $\delta > 0.07$, the spectrum mainly consists of a coherent excitation around $\omega = 0$. With respect to temperature, the coherent excitation is almost unaffected by T, whereas the pseudogap is filled up due to the temperature-dependent shift of the Fermi surface, as will be explained below.

To understand the T behavior of the spectral function, keep in mind that $\tilde{u}_{\mathbf{k}}$ and therefore the weight of the coherent excitation in $\Im G(\mathbf{k},\omega)$ is almost independent of T. Moreover, the total spectral weight, to which coherent and incoherent excitations contribute, is T independent. This follows from sum rule (72) since the total electron number is fixed. Thus, except of minor changes, the overall temperature dependence of $\Im G(\mathbf{k},\omega)$ is expected to be weak. Instead, the main reason for the T dependence can be traced back to a change in the Fermi surface with temperature. Consider a $\mathbf{k}$ vector on the Fermi surface at the antinodal point, $\mathbf{k}_F = (\pi, k_F^y)$, where the x component is fixed to $k_F^x = \pi$. By varying the temperature, one finds that the magnitude of the y component k_F^y increases almost linearly with T. Due to this shift of the Fermi energy with T, also the positions of the incoherent excitations at $\omega = 0$ are shifted. In this way, one understands that the pseudogap is less pronounced for higher temperatures, when k_F^x is fixed to $k_F^x = \pi$. A similar behavior of the pseudogap was found before in Fig. 5. There, the spectral function is shown for fixed $k_x = \pi$ and different values of k_y, when the temperature is fixed. Also in this case, the pseudogap is suppressed for larger values of k_y. Finally, note that k_F^y also strongly depends on the nearest-neighbor hopping t'. For small t', the pseudogap is more pronounced than for larger values of t'. This can be seen by comparing the spectrum in Fig. 2 (with $t' = 0.1t$) with that of Fig. 6, where $t' = 0.4t$.

VI. RENORMALIZATION APPROACH FOR THE SUPERCONDUCTING PHASE

A. Renormalization equations

In the preceding sections, we have investigated the pseudogap phase in the cuprates on the basis of the t-J model. We now adopt the same model also for the superconducting phase. As before, we restrict ourselves to moderate hole concentrations away from half-filling outside the antiferromagnetic phase. In Fourier notation, the t-J model (1) reads

$$\mathcal{H} = \sum_{\mathbf{k},\sigma} \varepsilon_{\mathbf{k}} \hat{c}^{\dagger}_{\mathbf{k}\sigma} \hat{c}_{\mathbf{k}\sigma} + \sum_{\mathbf{k}} (\Delta_{\mathbf{k},\Lambda} \hat{c}^{\dagger}_{\mathbf{k}\uparrow} \hat{c}^{\dagger}_{\mathbf{k}\downarrow} + \Delta^{*}_{\mathbf{k},\Lambda} \hat{c}_{\mathbf{k}\downarrow} \hat{c}_{\mathbf{k}\uparrow}) + \sum_{\mathbf{q}} J_{\mathbf{q}} \mathbf{S}_{\mathbf{q}} \mathbf{S}_{-\mathbf{q}}. \tag{82}$$

Here, $\varepsilon_{\mathbf{k}}$ measures the one-particle energy from the Fermi energy, i.e., $\varepsilon_{\mathbf{k}} = -\Sigma_{i \neq (j)} t_{ij} e^{i\mathbf{k}(\mathbf{R}_i - \mathbf{R}_j)} - \mu$. Note that in Eq. (82), we have introduced an infinitesimal field $\Delta_{\mathbf{k},\Lambda} \to 0$ which breaks the gauge symmetry in the superconducting phase.

As before, we can decompose the Hamiltonian into an unperturbed part $\mathcal{H}_0$ and into a perturbation $\mathcal{H}_1$,

$$\mathcal{H}_0 = \sum_{\mathbf{k}\sigma} \varepsilon_{\mathbf{k}} \hat{c}^{\dagger}_{\mathbf{k}\sigma} \hat{c}_{\mathbf{k}\sigma} + \sum_{\mathbf{k}} (\Delta_{\mathbf{k},\Lambda} \hat{c}^{\dagger}_{\mathbf{k}\uparrow} \hat{c}^{\dagger}_{\mathbf{k}\downarrow} + \Delta^{*}_{\mathbf{k},\Lambda} \hat{c}_{\mathbf{k}\downarrow} \hat{c}_{\mathbf{k}\uparrow}) + \sum_{\mathbf{q}} J_{\mathbf{q}} \mathcal{A}_0(\mathbf{q}),$$

$$\mathcal{H}_1 = \sum_{\mathbf{q}} J_{\mathbf{q}} [\mathcal{A}_1(\mathbf{q}) + \mathcal{A}_1^{\dagger}(\mathbf{q})]. \tag{83}$$

Decomposition (83) is an extension of the former decomposition for the pseudogap phase to the superconducting phase. It is based on a splitting of the exchange into two parts. The first one, containing $\mathcal{A}_0$, commutes with $\mathcal{H}_t$ and should, therefore, be a part of the unperturbed Hamiltonian $\mathcal{H}_0$. In contrast, the two operators $\mathcal{A}_1$ and $\mathcal{A}_1^{\dagger}$ do not commute with $\mathcal{H}_t$ and belong to $\mathcal{H}_1$. The operators $\mathcal{A}_\alpha(\mathbf{q})$ were defined before in Eqs. (29) and (30).

The derivation of the renormalization equations for the parameters of the Hamiltonian runs parallel to that for the pseudogap phase. The aim of the projector-based renormalization method (PRM) is to eliminate all transitions due to $\mathcal{H}_1$ between the eigenstates of $\mathcal{H}_0$ with nonzero transition energies. Let us again assume that all excitations with energies larger than a given cutoff λ have already been eliminated. Then, the *ansatz* for the renormalized Hamiltonian $\mathcal{H}_\lambda$ should have the following form:

$$\mathcal{H}_\lambda = \mathcal{H}_{0,\lambda} + \mathcal{H}_{1,\lambda} \tag{84}$$

with

$$\mathcal{H}_{0,\lambda} = \mathcal{H}_{t,\lambda} + \sum_{\mathbf{q}} J_{\mathbf{q},\lambda} \mathcal{A}_{0,\lambda}(\mathbf{q}) - \sum_{\mathbf{k}} (\Delta_{\mathbf{k},\lambda} \hat{c}^{\dagger}_{\mathbf{k},\uparrow} \hat{c}^{\dagger}_{-\mathbf{k},\downarrow} + \Delta^{*}_{\mathbf{k},\lambda} \hat{c}_{-\mathbf{k},\downarrow} \hat{c}_{\mathbf{k},\uparrow}) + E_\lambda,$$

$$\mathcal{H}_{1,\lambda} = \sum_{\mathbf{q}} J_{\mathbf{q},\lambda}\Theta(\lambda - |2\hat{\omega}_{\mathbf{q},\lambda}|)[\mathcal{A}_{1,\lambda}(\mathbf{q}) + \mathcal{A}^{\dagger}_{1,\lambda}(\mathbf{q})]. \quad (85)$$

$\mathcal{H}_{t,\lambda}=\Sigma_{\mathbf{k}\sigma}\varepsilon_{\mathbf{k},\lambda}\hat{c}^{\dagger}_{\mathbf{k}\sigma}\hat{c}_{\mathbf{k}\sigma}$ is the renormalized hopping term and depends on λ. The other parameters $\Delta_{\mathbf{k},\lambda}$, $\hat{\omega}_{\mathbf{q},\lambda}$, and $J_{\mathbf{q},\lambda}$ in Eq. (85) are also λ dependent. However, the λ dependence of $J_{\mathbf{q},\lambda}$ can be suppressed according to Sec. IV. The λ-dependent operators $\mathcal{A}_{\alpha,\lambda}(\mathbf{q})(\alpha=0,\pm 1)$ are defined by Eqs. (29), where $\dot{\mathbf{S}}_{\mathbf{q}}$ and $\hat{\omega}_{\mathbf{q}}$ are replaced by $\dot{\mathbf{S}}_{\mathbf{q},\lambda}$ and $\hat{\omega}_{\mathbf{q},\lambda}$. The latter quantities were given in Eq. (36).

In order to derive renormalization equations for the parameters of $\mathcal{H}_{\lambda}$, we eliminate all excitations within an additional energy shell between λ and a reduced cutoff $\lambda-\Delta\lambda$. This is done by applying the unitary transformation to $\mathcal{H}_{\lambda}$ according to Eq. (12). In the following, we shall restrict ourselves to a weak coupling theory. Therefore, all contributions to the unitary transformation from the symmetry-breaking fields can be neglected. Thus, the generator $X_{\lambda,\Delta\lambda}$ is the same as in the pseudogap phase. In lowest-order perturbation theory in $J_{\mathbf{q}}$, $X_{\lambda,\Delta\lambda}$ was given by Eq. (38). The explicit evaluation of the unitary transformation [Eq. (12)] follows that of the pseudogap phase. In perturbation theory to second order in $J_{\mathbf{q}}$, $\mathcal{H}_{\lambda-\Delta\lambda}$ reads $\mathcal{H}_{\lambda-\Delta\lambda}=\mathcal{H}^{(0)}_{\lambda-\Delta\lambda}+\mathcal{H}^{(1)}_{\lambda-\Delta\lambda}+\mathcal{H}^{(2)}_{\lambda-\Delta\lambda}+\cdots$, where all orders look the same as in Eq. (40), except that now in $\mathcal{H}^{(0)}_{\lambda-\Delta\lambda}$ the new symmetry breaking terms appear. Let us at first investigate the effect of the second order term $\mathcal{H}^{(2)}_{\lambda-\Delta\lambda}$. As before, the commutator expressions have to be reduced in a further factorization approximation to operator terms appearing in $\mathcal{H}_{\lambda}$. Thereby, also a reduction to operators $\hat{c}^{\dagger}_{\mathbf{k}\uparrow}\hat{c}^{\dagger}_{-\mathbf{k}\downarrow}$ and $\hat{c}_{-\mathbf{k}\downarrow}\hat{c}_{\mathbf{k}\uparrow}$ has to be included. The final result has to be compared with the formal expression for $\mathcal{H}_{\lambda-\Delta\lambda}$, which corresponds to the expression [Eq. (84)] for $\mathcal{H}_{\lambda}$, when λ is replaced by $\lambda-\Delta\lambda$. According to Appendix D, the following second-order renormalization to the order parameter $\Delta_{\mathbf{k},\lambda}$ is found:

$$\begin{aligned}\Delta_{\mathbf{k},\lambda-\Delta\lambda} - \Delta_{\mathbf{k},\lambda} &= -\frac{1}{16N}\sum_{\mathbf{q}}\frac{J_{\mathbf{q}}^2}{\hat{\omega}^4_{\mathbf{q},\lambda}}\Theta_{\mathbf{q}}(\lambda,\Delta\lambda)(\varepsilon_{\mathbf{k},\lambda}-\varepsilon_{\mathbf{k}+\mathbf{q},\lambda})^2\langle\hat{c}_{-(\mathbf{k}+\mathbf{q})\downarrow}\hat{c}_{\mathbf{k}+\mathbf{q}\uparrow}\rangle \\ &\times\frac{1}{N}\sum_{\mathbf{k}'}(\varepsilon_{\mathbf{k}'+\mathbf{q},\lambda}+\varepsilon_{\mathbf{k}'-\mathbf{q},\lambda}-2\varepsilon_{\mathbf{k}',\lambda})n^{(NL)}_{\mathbf{k}'\sigma}, \quad (86)\end{aligned}$$

whereas the renormalization for $\varepsilon_{\mathbf{k},\lambda}$ is the same as in the pseudogap phase. $n^{(NL)}_{\mathbf{k},\sigma}$ was already defined in Eq. (42) and is the nonlocal part of the one-particle occupation number per spin direction. The expectation values in Eq. (86) have to be calculated separately.

Up to now, only the renormalization contribution from the second-order term $\mathcal{H}^{(2)}_{\lambda-\Delta\lambda}$ of $\mathcal{H}_{\lambda-\Delta\lambda}$ was evaluated. With $\varepsilon_{\mathbf{k},\lambda-\Delta\lambda}$ and $\Delta_{\mathbf{k},\lambda-\Delta\lambda}$, we obtain for $\mathcal{H}_{\lambda-\Delta\lambda}$

$$\begin{aligned}\mathcal{H}_{\lambda-\Delta\lambda} &= \mathcal{H}_{t,\lambda-\Delta\lambda} - \sum_{\mathbf{k}}(\Delta_{\mathbf{k},\lambda-\Delta\lambda}\hat{c}^{\dagger}_{\mathbf{k},\uparrow}\hat{c}^{\dagger}_{-\mathbf{k},\downarrow} + \Delta^{*}_{\mathbf{k},\lambda-\Delta\lambda}\hat{c}_{-\mathbf{k},\downarrow}\hat{c}_{\mathbf{k},\uparrow}) \\ &+ \mathcal{H}^{(1)}_{\lambda-\Delta\lambda} + E_{\lambda-\Delta\lambda}, \quad (87)\end{aligned}$$

where the first-order term $\mathcal{H}^{(1)}_{\lambda-\Delta\lambda}$ has still to be evaluated. This can again be done along the procedure for the pseudogap phase. The final result for the renormalized Hamiltonian $\mathcal{H}_{\lambda-\Delta\lambda}$ reads $\mathcal{H}_{\lambda-\Delta\lambda}=\mathcal{H}_{0,\lambda-\Delta\lambda}+\mathcal{H}_{1,\lambda-\Delta\lambda}$, with

$$\begin{aligned}\mathcal{H}_{0,\lambda-\Delta\lambda} &= \mathcal{H}_{t,\lambda-\Delta\lambda} - \sum_{\mathbf{k}}(\Delta_{\mathbf{k},\lambda-\Delta\lambda}\hat{c}^{\dagger}_{\mathbf{k},\uparrow}\hat{c}^{\dagger}_{-\mathbf{k},\downarrow} + \Delta^{*}_{\mathbf{k},\lambda-\Delta\lambda}\hat{c}_{-\mathbf{k},\downarrow}\hat{c}_{\mathbf{k},\uparrow}) \\ &+ E_{\lambda-\Delta\lambda} + \sum_{\mathbf{q}} J_{\mathbf{q}}\mathcal{A}_{0,\lambda-\Delta\lambda}(\mathbf{q}), \\ \mathcal{H}_{1,\lambda-\Delta\lambda} &= \sum_{\mathbf{q}} J_{\mathbf{q}}\Theta(\lambda-\Delta\lambda-|2\hat{\omega}_{\mathbf{q},\lambda-\Delta\lambda}|) \\ &\times[\mathcal{A}_{1,\lambda-\Delta\lambda}(\mathbf{q}) + \mathcal{A}^{\dagger}_{1,\lambda-\Delta\lambda}(\mathbf{q})]. \quad (88)\end{aligned}$$

The renormalized Hamiltonian $\mathcal{H}_{\lambda-\Delta\lambda}$ has the same operator structure as $\mathcal{H}_{\lambda}$. Therefore, we can formulate the same renormalization procedure as before: We start from the original t-J model in the presence of a small gauge symmetry-breaking field. The energy cutoff of the original model is denoted by $\lambda=\Lambda$. Starting from a guess for the unknown expectation values, which enter the renormalization equations $\Delta_{\mathbf{k},\lambda}$ and $\varepsilon_{\mathbf{k},\lambda}$, we proceed by eliminating all excitations in steps $\Delta\lambda$ from $\lambda=\Lambda$ down to $\lambda=0$. Thereby, the parameters of the Hamiltonian change in steps according to the renormalization equations for $\Delta_{\mathbf{k},\lambda}$ and $\varepsilon_{\mathbf{k},\lambda}$. In this way, we obtain a final model at $\lambda=0$, in which the perturbation $\mathcal{H}_{1,\lambda}$ is completely integrated out. It reads

$$\begin{aligned}\mathcal{H}_{\lambda=0} &= \sum_{\mathbf{k}\sigma}\varepsilon_{\mathbf{k},\lambda=0}\hat{c}^{\dagger}_{\mathbf{k}\sigma}\hat{c}_{\mathbf{k}\sigma} - \sum_{\mathbf{k}}(\Delta_{\mathbf{k},\lambda=0}\hat{c}^{\dagger}_{\mathbf{k},\uparrow}\hat{c}^{\dagger}_{-\mathbf{k},\downarrow} \\ &+ \Delta^{*}_{\mathbf{k},\lambda=0}\hat{c}_{-\mathbf{k},\downarrow}\hat{c}_{\mathbf{k},\uparrow}) + \sum_{\mathbf{q}} J_{\mathbf{q}}\mathcal{A}_{0,\lambda=0}(\mathbf{q}) + E_{\lambda=0}. \quad (89)\end{aligned}$$

Unfortunately, due to the presence of the $\mathcal{A}_0$ term, result (89) does not yet allow us to recalculate the expectation values since the eigenvalue problem of $\mathcal{H}_{\lambda=0}$ can not be solved. Therefore, a further approximation is necessary. It consists of a factorization of the second term, defined in Eq. (59). According to Appendix D, we end up with a modified Hamiltonian which will be denoted by $\tilde{\mathcal{H}}^{(1)}$,

$$\begin{aligned}\tilde{\mathcal{H}}^{(1)} &= \sum_{\mathbf{k}\sigma}\tilde{\varepsilon}^{(1)}_{\mathbf{k}}\hat{c}^{\dagger}_{\mathbf{k}\sigma}\hat{c}_{\mathbf{k}\sigma} - \sum_{\mathbf{k}}(\tilde{\Delta}^{(1)}_{\mathbf{k}}\hat{c}^{\dagger}_{\mathbf{k},\uparrow}\hat{c}^{\dagger}_{-\mathbf{k},\downarrow} + \tilde{\Delta}^{(1)*}_{\mathbf{k}}\hat{c}_{-\mathbf{k},\downarrow}\hat{c}_{\mathbf{k},\uparrow}) \\ &+ \sum_{\mathbf{q}}\frac{J_{\mathbf{q}}}{2}\mathbf{S}_{\mathbf{q}}\mathbf{S}_{-\mathbf{q}} + \tilde{E}^{(1)}. \quad (90)\end{aligned}$$

Here, not only the electron energy $\varepsilon_{\mathbf{k},\lambda=0}$ but also the order parameter $\Delta_{\mathbf{k},\lambda=0}$ is modified according to

$$\begin{aligned}\tilde{\varepsilon}^{(1)}_{\mathbf{k}} &= \varepsilon_{\mathbf{k},\lambda=0} - \frac{1}{N}\sum_{\mathbf{q}}\frac{3J_{\mathbf{q}}}{4\hat{\omega}^2_{\mathbf{q},\lambda=0}}(\varepsilon_{\mathbf{k},\lambda=0}-\varepsilon_{\mathbf{k}+\mathbf{q},\lambda=0})^2 n^{(NL)}_{\mathbf{k}+\mathbf{q},\sigma}, \\ \tilde{\Delta}^{(1)}_{\mathbf{k}} &= \Delta_{\mathbf{k},\lambda=0} - \frac{1}{N}\sum_{\mathbf{q}}\frac{3J_{\mathbf{q}}}{4\hat{\omega}^2_{\mathbf{q},\lambda=0}}(\varepsilon_{\mathbf{k},\lambda=0}-\varepsilon_{\mathbf{k}+\mathbf{q},\lambda=0})^2 \\ &\times\langle\hat{c}_{-(\mathbf{k}+\mathbf{q})\downarrow}\hat{c}_{\mathbf{k}+\mathbf{q}\uparrow}\rangle. \quad (91)\end{aligned}$$

Note that the operator structure of $\tilde{\mathcal{H}}^{(1)}$ agrees with that of the original t-J model of Eq. (82) in the presence of the symmetry breaking field. Since the strength of the exchange coupling in Eq. (90) is decreased by a factor of 1/2, we can start the whole renormalization procedure again. We consider

modified t-J model (90) as our new initial Hamiltonian (at $\lambda=\Lambda$) which has to be renormalized. The initial values of the new Hamiltonian $\tilde{\mathcal{H}}^{(1)}$ at cutoff $\lambda=\Lambda$ are $\tilde{\varepsilon}_{\mathbf{k}}^{(1)}$, $\tilde{\Delta}_{\mathbf{k}}^{(1)}$, and $J_{\mathbf{q}}/2$. After the new renormalization cycle, the exchange coupling of the renormalized Hamiltonian $\tilde{\mathcal{H}}^{(2)}$ is again decreased by a factor of 1/2, until, after a sufficiently large number of renormalization cycles ($n\to\infty$), the exchange completely disappears. Thus, we finally arrive at a free model

$$\tilde{\mathcal{H}}=\sum_{\mathbf{k}\sigma}\tilde{\varepsilon}_{\mathbf{k}}\hat{c}_{\mathbf{k}\sigma}^{\dagger}\hat{c}_{\mathbf{k}\sigma}-\sum_{\mathbf{k}}(\tilde{\Delta}_{\mathbf{k}}\hat{c}_{\mathbf{k},\uparrow}^{\dagger}\hat{c}_{-\mathbf{k},\downarrow}^{\dagger}+\tilde{\Delta}_{\mathbf{k}}^{*}\hat{c}_{-\mathbf{k},\downarrow}\hat{c}_{\mathbf{k},\uparrow})+\tilde{E}, \tag{92}$$

with the new notation, $\tilde{\mathcal{H}}=\tilde{\mathcal{H}}^{(n\to\infty)}$, $\tilde{\varepsilon}_{\mathbf{k}}=\tilde{\varepsilon}_{\mathbf{k}}^{(n\to\infty)}$, $\tilde{\Delta}_{\mathbf{k}}=\tilde{\Delta}_{\mathbf{k}}^{(n\to\infty)}$, and $\tilde{E}=\tilde{E}^{(n\to\infty)}$. The Hamiltonian $\tilde{\mathcal{H}}$ allows us to recalculate the unknown expectation values. With these values, the whole renormalization procedure can be started again, until, after a sufficiently large number of such overall cycles, the expectation values converge. Then, the renormalization equations have been solved self-consistently. However, the fully renormalized Hamiltonian [Eq. (92)] is actually not a free model. Instead, it is still subject to strong electronic correlations which are built in by the presence of the Hubbard operators.

B. Evaluation of expectation values

The expectation values in Eqs. (86) and (91) are formed with the full Hamiltonian of Eq. (82). To evaluate an expectation value $\langle\mathcal{A}\rangle$, we have to apply the unitary transformation also on the operator variable $\mathcal{A}$,

$$\langle\mathcal{A}\rangle=\frac{\mathrm{Tr}(\mathcal{A}e^{-\beta\mathcal{H}})}{\mathrm{Tr}e^{-\beta\mathcal{H}}}=\langle\mathcal{A}(\lambda)\rangle_{\mathcal{H}_{\lambda}}=\langle\tilde{\mathcal{A}}\rangle_{\tilde{\mathcal{H}}}, \tag{93}$$

where we have defined as before $\mathcal{A}(\lambda)=e^{X_{\lambda}}\mathcal{A}e^{-X_{\lambda}}$ and $\tilde{\mathcal{A}}=\mathcal{A}(\lambda\to 0)$. Thus, additional renormalization equations for $\mathcal{A}(\lambda)$ have to be derived.

1. ARPES spectral functions

According to Eqs. (57) and (68) the spectral function from angle-resolved photoemission (ARPES) can be evaluated from

$$A(\mathbf{k},\omega)=\frac{1}{1+e^{\beta\omega}}\Im G(\mathbf{k},\omega). \tag{94}$$

Using relation (93), the dissipative part of the anticommutator Green's function, $\Im G(\mathbf{k},\omega)$, can be expressed by

$$\Im G(\mathbf{k},\omega)=\langle[\hat{c}_{\mathbf{k}\sigma}^{(n\to\infty)\dagger}(\lambda=0),\delta(\tilde{L}+\omega)\hat{c}_{\mathbf{k}\sigma}^{(n\to\infty)}(\lambda=0)]_{+}\rangle_{\tilde{\mathcal{H}}}, \tag{95}$$

where the Liouville operator $\tilde{\mathsf{L}}$ is related to $\tilde{\mathcal{H}}$. Also, the expectation value has to be evaluated with $\tilde{\mathcal{H}}$. The fully renormalized annihilation operator $\hat{c}_{\mathbf{k}\sigma}^{(n\to\infty)}(\lambda=0)$ can be taken over from Eq. (67),

$$\hat{c}_{\mathbf{k}\sigma}^{(n\to\infty)}(\lambda=0)=\tilde{u}_{\mathbf{k}}\hat{c}_{\mathbf{k}\sigma}+\frac{1}{2N}\sum_{\mathbf{q}\mathbf{k}'}\tilde{v}_{\mathbf{k},\mathbf{q}}\frac{J_{\mathbf{q}}}{4\tilde{\omega}_{\mathbf{q}}^{2}}\sum_{\alpha\beta\gamma}(\vec{\sigma}_{\alpha\beta}\cdot\vec{\sigma}_{\sigma\gamma})\times(\tilde{\varepsilon}_{\mathbf{k}'}-\tilde{\varepsilon}_{\mathbf{k}'+\mathbf{q}})\hat{c}_{\mathbf{k}'+\mathbf{q}\alpha}^{\dagger}\hat{c}_{\mathbf{k}'\beta}\hat{c}_{\mathbf{k}+\mathbf{q}\gamma}, \tag{96}$$

where $\tilde{u}_{\mathbf{k}}=u_{\mathbf{k},\lambda=0}^{(n\to\infty)}$, $\tilde{v}_{\mathbf{k},\mathbf{q}}=v_{\mathbf{k},\mathbf{q},\lambda=0}^{(n\to\infty)}$, and $\tilde{\varepsilon}_{\mathbf{k}}=\varepsilon_{\mathbf{k},\lambda=0}^{(n\to\infty)}$.

In order to evaluate the expectation value in Eq. (95), we introduce new approximate quasiparticle operators (Appendix E),

$$\alpha_{\mathbf{k}}^{\dagger}=\mathsf{U}_{\mathbf{k}}\hat{c}_{\mathbf{k},\uparrow}^{\dagger}-\mathsf{V}_{\mathbf{k}}\hat{c}_{-\mathbf{k},\downarrow},$$

$$\beta_{\mathbf{k}}^{\dagger}=\mathsf{U}_{\mathbf{k}}\hat{c}_{-\mathbf{k},\downarrow}^{\dagger}+\mathsf{V}_{\mathbf{k}}\hat{c}_{\mathbf{k},\uparrow}, \tag{97}$$

which fulfill the following relations: $\tilde{\mathsf{L}}\alpha_{\mathbf{k}}^{\dagger}=E_{\mathbf{k}}\alpha_{\mathbf{k}}^{\dagger}$ and $\tilde{\mathsf{L}}\beta_{\mathbf{k}}^{\dagger}=E_{\mathbf{k}}\beta_{\mathbf{k}}^{\dagger}$, where $E_{\mathbf{k}}=\sqrt{\tilde{\varepsilon}_{\mathbf{k}}^{2}+D^{2}\tilde{\Delta}_{\mathbf{k}}^{2}}$. Inserting Eq. (96) into Eq. (95) and replacing all $\hat{c}_{\mathbf{k}\sigma}^{(\dagger)}$ operators by the quasiparticle operators $\alpha_{\mathbf{k}}^{(\dagger)}$ and $\beta_{\mathbf{k}}^{(\dagger)}$, the δ functions can be evaluated. We restrict ourselves to the leading order in the superconducting order parameter. The resulting expression for $\Im G(\mathbf{k},\omega)$ reads

$$\begin{aligned}\Im G(\mathbf{k},\omega)=&\frac{D\tilde{u}_{\mathbf{k}}^{2}}{2}\left\{\left(1+\frac{\tilde{\varepsilon}_{\mathbf{k}}}{E_{\mathbf{k}}}\right)\delta(\omega-E_{\mathbf{k}})+\left(1-\frac{\tilde{\varepsilon}_{\mathbf{k}}}{E_{\mathbf{k}}}\right)\delta(\omega+E_{\mathbf{k}})\right\}\\&+\frac{3D}{2N^{2}}\sum_{\mathbf{q}\mathbf{q}'}\left[\left(\frac{J_{\mathbf{q}}\tilde{v}_{\mathbf{k},\mathbf{q}}}{4\hat{\omega}_{\mathbf{q}}^{2}}\right)^{2}(\varepsilon_{\mathbf{k}+\mathbf{q}'}-\varepsilon_{\mathbf{k}+\mathbf{q}+\mathbf{q}'})^{2}\right.\\&\times\{\tilde{n}_{\mathbf{k}+\mathbf{q}+\mathbf{q}'}\tilde{m}_{\mathbf{k}+\mathbf{q}'}+\tilde{n}_{\mathbf{k}+\mathbf{q}}(D+\tilde{n}_{\mathbf{k}+\mathbf{q}'}-\tilde{n}_{\mathbf{k}+\mathbf{q}+\mathbf{q}'})\}\\&-\frac{1}{2}\frac{J_{\mathbf{q}}}{4\hat{\omega}_{\mathbf{q}}^{2}}\frac{J_{\mathbf{q}'}}{4\hat{\omega}_{\mathbf{q}'}^{2}}\tilde{v}_{\mathbf{k},\mathbf{q}}\tilde{v}_{\mathbf{k},\mathbf{q}'}\\&\times(\varepsilon_{\mathbf{k}+\mathbf{q}'}-\varepsilon_{\mathbf{k}+\mathbf{q}+\mathbf{q}'})(\varepsilon_{\mathbf{k}+\mathbf{q}}-\varepsilon_{\mathbf{k}+\mathbf{q}+\mathbf{q}'})\\&\left.\times\{(\tilde{n}_{\mathbf{k}+\mathbf{q}'}-\tilde{m}_{\mathbf{k}+\mathbf{q}'})\tilde{n}_{\mathbf{k}+\mathbf{q}+\mathbf{q}'}-\tilde{n}_{\mathbf{k}+\mathbf{q}'}(\tilde{n}_{\mathbf{k}+\mathbf{q}}+D)\}\right]\\&\times\delta\{\omega+\mathrm{sign}(\tilde{\varepsilon}_{\mathbf{k}+\mathbf{q}+\mathbf{q}'})E_{\mathbf{k}+\mathbf{q}+\mathbf{q}'}\\&-\mathrm{sign}(\tilde{\varepsilon}_{\mathbf{k}+\mathbf{q}'})E_{\mathbf{k}+\mathbf{q}'}-\mathrm{sign}(\tilde{\varepsilon}_{\mathbf{k}+\mathbf{q}})E_{\mathbf{k}+\mathbf{q}}\},\end{aligned} \tag{98}$$

where $\tilde{n}_{\mathbf{k}}$ and $\tilde{m}_{\mathbf{k}}$ are defined by $\tilde{n}_{\mathbf{k}}=\langle\hat{c}_{\mathbf{k}\sigma}^{\dagger}\hat{c}_{\mathbf{k}\sigma}\rangle_{\tilde{\mathcal{H}}}$ and $\tilde{m}_{\mathbf{k}}=\langle\hat{c}_{\mathbf{k}\sigma}\hat{c}_{\mathbf{k}\sigma}^{\dagger}\rangle_{\tilde{\mathcal{H}}}$. For $\tilde{n}_{\mathbf{k}}$ and $\tilde{m}_{\mathbf{k}}$, we use again the Gutzwiller approximation,[18]

$$\tilde{n}_{\mathbf{k}}=(D-q)+qf(\tilde{\varepsilon}_{\mathbf{k}}),$$

$$\tilde{m}_{\mathbf{k}}=q[1-f(\tilde{\varepsilon}_{\mathbf{k}})]\quad\text{with } q=\frac{1-n}{1-n/2},$$

where $f(\tilde{\varepsilon}_{\mathbf{k}})$ is the Fermi function.

2. Pair correlation function

In order to evaluate the superconducting order parameter $\tilde{\Delta}_{\mathbf{k}}$, we have to know the superconducting pairing function $\langle\hat{c}_{-\mathbf{k}\downarrow}\hat{c}_{\mathbf{k}\uparrow}\rangle$. Here, the expectation value is defined with the full Hamiltonian for the superconducting phase. We first have to transform the pairing function, according to Eq. (93),

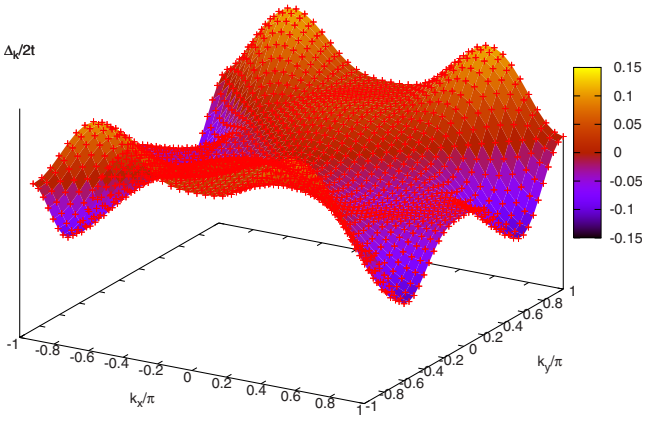

FIG. 10. (Color online) The superconducting gap function $\tilde{\Delta}_{\mathbf{k}}$ versus $\mathbf{k}$, as obtained from Eq. (108) for a square lattice with $N=40\times 40$ sites. The parameters are $\delta=0.08$, $t'=0.4t$, and $T=0$. Note that the gap function shows d-wave symmetry.

$$\langle \hat{c}_{-\mathbf{k}\downarrow}\hat{c}_{\mathbf{k}\uparrow}\rangle = \langle \hat{c}^{(n\to\infty)}_{-\mathbf{k}\downarrow}(\lambda\to 0)\hat{c}^{(n\to\infty)}_{\mathbf{k}\uparrow}(\lambda\to 0)\rangle_{\tilde{\mathcal{H}}}, \tag{99}$$

where the expectation value is formed with the Hamiltonian $\tilde{\mathcal{H}}$, given by Eq. (92). We can immediately take over our previous result [Eq. (96)] for $\hat{c}^{(n\to\infty)}_{\mathbf{k},\sigma}(\lambda\to 0)$. For the full renormalization, we obtain

$$\langle \hat{c}_{-\mathbf{k}\downarrow}\hat{c}_{\mathbf{k}\uparrow}\rangle = \tilde{u}^2_{\mathbf{k}}\langle \hat{c}_{-\mathbf{k}\downarrow}\hat{c}_{\mathbf{k}\uparrow}\rangle_{\tilde{\mathcal{H}}} + \frac{3}{2N^2}\sum_{\mathbf{q}\mathbf{k}'}\tilde{v}^2_{\mathbf{k},\mathbf{q}}\left(\frac{J_{\mathbf{q}}}{4\hat{\omega}^2_{\mathbf{q}}}\right)^2 \times(\varepsilon_{\mathbf{k}'}-\varepsilon_{\mathbf{k}'+\mathbf{q}})^2\tilde{m}_{\mathbf{k}'+\mathbf{q}}\tilde{n}_{\mathbf{k}'}\langle \hat{c}_{-(\mathbf{k}+\mathbf{q})\downarrow}\hat{c}_{(\mathbf{k}+\mathbf{q})\uparrow}\rangle_{\tilde{\mathcal{H}}}. \tag{100}$$

Contributions from third order in the superconducting order parameter have been neglected. The expectation values on the right-hand side are formed with the fully renormalized Hamiltonian $\tilde{\mathcal{H}}$ [Eq. (92)]. Using again the approximate Bogoliubov transformation of Appendix E, we find

$$\langle \hat{c}_{-\mathbf{k}\downarrow}\hat{c}_{\mathbf{k}\uparrow}\rangle_{\tilde{\mathcal{H}}} = \frac{D^2\tilde{\Delta}_{\mathbf{k}}}{2E_{\mathbf{k}}}\left(1-\frac{2}{1+e^{\beta E_{\mathbf{k}}}}\right). \tag{101}$$

VII. NUMERICAL EVALUATION FOR THE SUPERCONDUCTING STATE

Superconducting solutions have been obtained by evaluating self-consistently the full PRM renormalization scheme for a sufficiently large number of renormalization cycles. We have taken the same parameters as for the normal state in Sec. V B, $t'=0.4t$, $J=0.2t$.

A. Order parameter

1. Zero-temperature results

In Fig. 10, the superconducting gap function $\tilde{\Delta}_{\mathbf{k}}$ is plotted in $\mathbf{k}$ space for optimal doping, $\delta=0.08$. In agreement with experiment, the solution shows d-wave symmetry with nodal lines directed along the diagonals of the Brillouin zone from $(-\pi,-\pi)$ to (π,π) and from $(\pi,-\pi)$ to $(-\pi,\pi)$. No s-wave-like solutions were found.

In Fig. 11, both the superconduction gap function $\tilde{\Delta}_{\mathbf{k}}$ (left panel) and the pair correlation function $\langle \hat{c}_{-\mathbf{k}\downarrow}\hat{c}_{\mathbf{k}\uparrow}\rangle$ (right panel) are shown as a two-dimensional (2D) plot for the same parameter values as in Fig. 10. Again, in both functions, the nodal lines are clearly seen. Moreover, the absolute value of the pair correlation $|\langle \hat{c}_{-\mathbf{k}\downarrow}\hat{c}_{\mathbf{k}\uparrow}\rangle|$ has a pronounced maximum along the Fermi surface (FS). This behavior can easily be understood from Eq. (101). For $\mathbf{k}$ values close to the FS, $\mathbf{k}\approx\mathbf{k}_F$, where $\varepsilon_{\mathbf{k}}\leqslant\mathcal{O}(\tilde{\Delta}_{\mathbf{k}})$, the quantity $|\langle \hat{c}_{-\mathbf{k}\downarrow}\hat{c}_{\mathbf{k}\uparrow}\rangle|$ is of order $\mathcal{O}(1)$. In contrast, for $\mathbf{k}$ vectors away from the FS [with $\varepsilon_{\mathbf{k}}\gg\mathcal{O}(\tilde{\Delta}_{\mathbf{k}})$], the pair correlation function is of order $\mathcal{O}(\Delta/t)$. Note that the gap function $|\tilde{\Delta}_{\mathbf{k}}|$ has only a weak

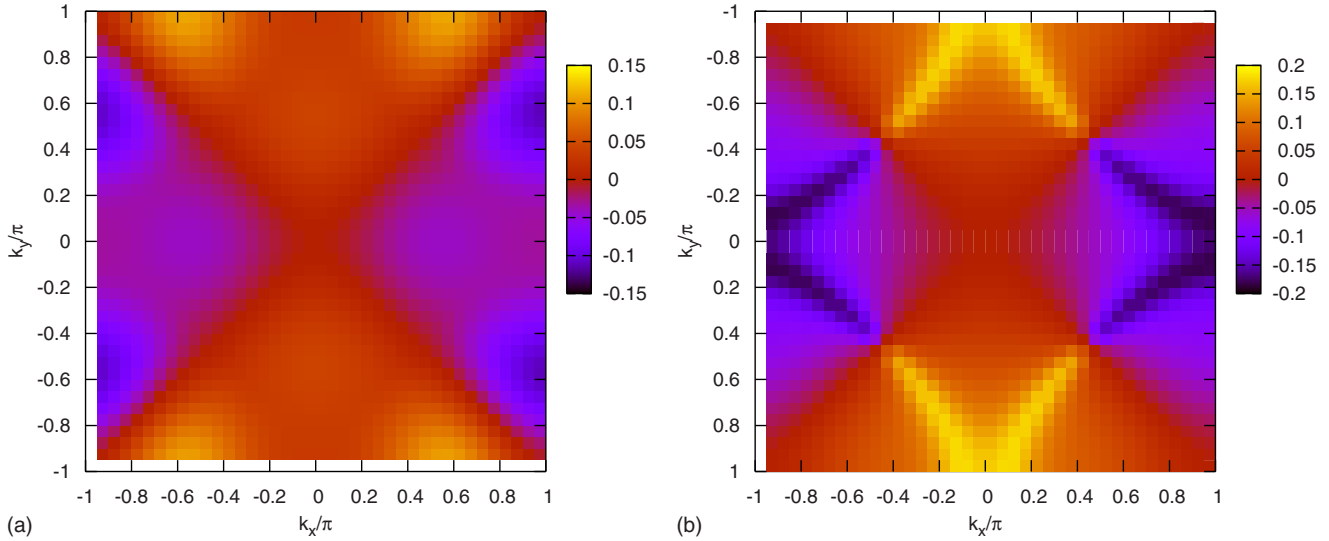

FIG. 11. (Color online) The superconducting gap $\tilde{\Delta}_{\mathbf{k}}$ (left panel) and the superconducting pairing function $\langle \hat{c}_{-\mathbf{k}\downarrow}\hat{c}_{\mathbf{k}\uparrow}\rangle$ for the same parameters as in Fig. 10 plotted as a 2D map.

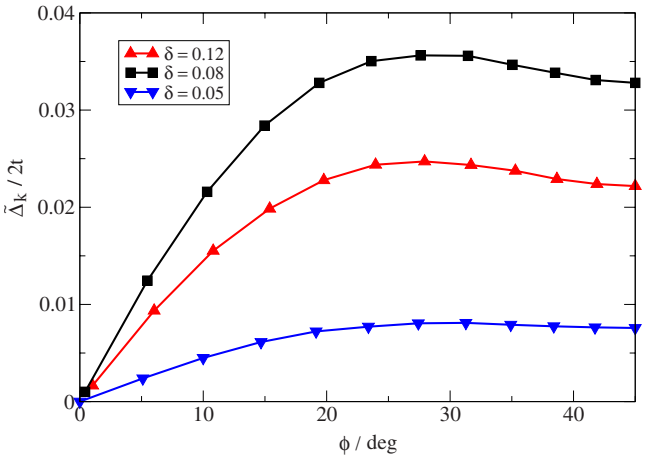

FIG. 12. (Color online) Superconducting gap function $\tilde{\Delta}_{\mathbf{k}}$ (in units of $2t$) as a function of the Fermi surface angle ϕ which was defined in the inset of Fig. 3 for three doping values, δ=0.05 (underdoped case, blue line), δ=0.08 (optimal doping, black line), and δ=0.12 (overdoped case, red line).

minimum at the Fermi surface. Additional weak maxima can be detected for the following $\mathbf{k}$ vectors: $(\pm\pi, \pm 0.55\pi)$, $(\pm 0.55\pi, \pm\pi)$, $(\pm 0.5\pi, 0)$, and $(0, \pm 0.5\pi)$.

Figure 12 shows the superconducting gap function $\tilde{\Delta}_{\mathbf{k}}$ on the Fermi surface as a function of the Fermi surface angle ϕ for three doping values, δ=0.05 (underdoped case, blue line), δ=0.08 (optimally doped, black line), and δ=0.12 (overdoped, red line). The angle ϕ was already defined in the inset of Fig. 3. In all three cases, $\tilde{\Delta}_{\mathbf{k}}$ shows a characteristic overall increase from the nodal (ϕ=0) to the antinodal point. Note, however, that the maximum value is already reached at a finite angle of about 27°, which is followed by a weak decrease in $\tilde{\Delta}_{\mathbf{k}}$.

According to Fig. 10, the gap function shows a pronounced $\mathbf{k}$ dependence in the whole Brillouin zone. By Fourier transforming $\tilde{\Delta}_{\mathbf{k}}$ to the local space,

$$\tilde{\Delta}_{ij} = \frac{1}{N}\sum_{i,j} \tilde{\Delta}_{\mathbf{k}}^{(\infty)} e^{i\mathbf{k}(\mathbf{R}_i - \mathbf{R}_j)}, \tag{102}$$

one finds the spatial dependence shown in Fig. 13. The figure again reveals the d-wave character of the superconducting order parameter. Note that the strong $\mathbf{k}$ dependence of $\tilde{\Delta}_{\mathbf{k}}$ maps on a short-range behavior in local space. As is clearly seen, the local order parameter decays in space within a few lattice constants. This feature is consistent with the experimentally found superconducting coherence length in the cuprates of the order of a few lattice constants. The order parameter changes its sign by proceeding along the x or y axis. This can be seen for various hole fillings in Fig. 14, where $\tilde{\Delta}_{ij}$ is shown as a function of R_{ij}^x (for fixed R_{ij}^y=0). Here R_{ij}^x and R_{ij}^y are the components of the difference vector $\mathbf{R}_{ij}=\mathbf{R}_i-\mathbf{R}_j$ between lattice sites $\mathbf{R}_i$ and $\mathbf{R}_j$. The alternating sign of $\tilde{\Delta}_{ij}$ seems to be reminiscent of the sign behavior of antiferromagnetic correlations. However, the sign change is a property of the superconducting state and not of antiferromagnetic correlations.

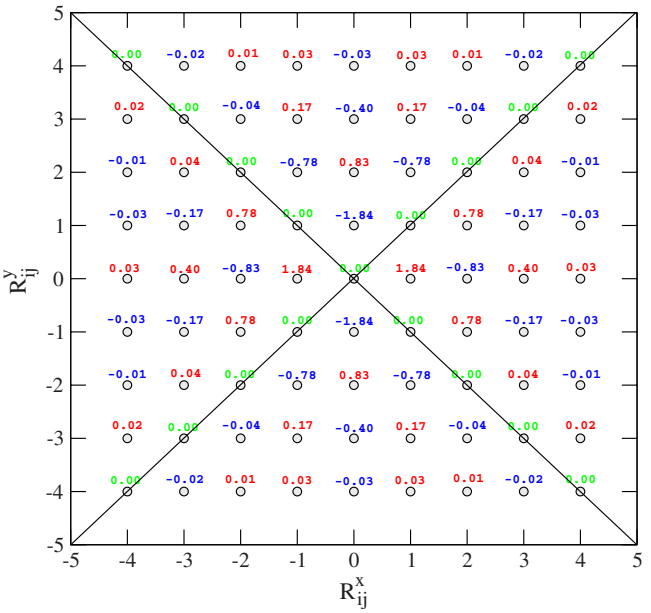

FIG. 13. (Color online) Superconducting order parameter in local space $\tilde{\Delta}_{ij}$ [in units of $10^{-2}(2t)$] for optimal doping δ=0.08 and T=0. The hopping parameter t' between next-nearest neighbors is given by $t'=0.4t$. R_{ij}^x and R_{ij}^y denote the x and y components of $\mathbf{R}_i-\mathbf{R}_j$.

2. Finite-temperature results

In Fig. 15, the local order parameter $\tilde{\Delta}_{ij}$ is plotted as a function of T for different values of the distance between local sites, $\kappa=|\mathbf{R}_{ij}|$. The curves are obtained from Fourier back transforming Eq. (102) together with the temperature-dependent expression for $\langle \hat{c}_{-\mathbf{k}\downarrow}\hat{c}_{\mathbf{k}\uparrow}\rangle$ from Sec. IV B. All

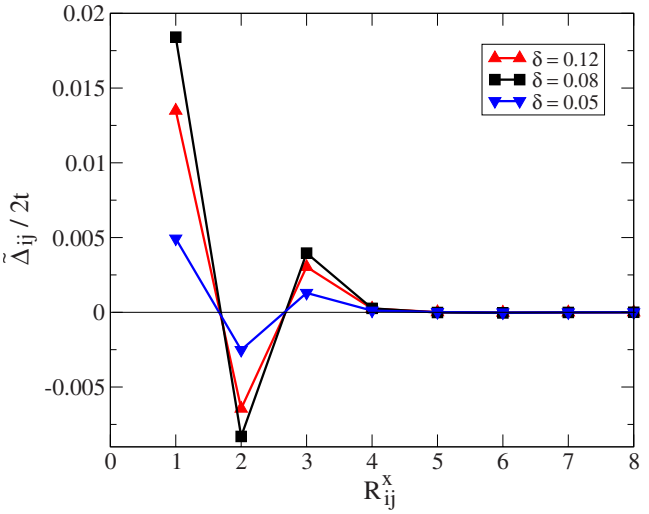

FIG. 14. (Color online) Superconducting order parameter $\tilde{\Delta}_{ij}$ (in units of $2t$) in local space along the x direction (for R_{ij}^y=0) for three different hole fillings δ=0.05 (blue), 0.08 (black), and 0.12 (red). The parameters t' and T are the same as in Fig. 10.

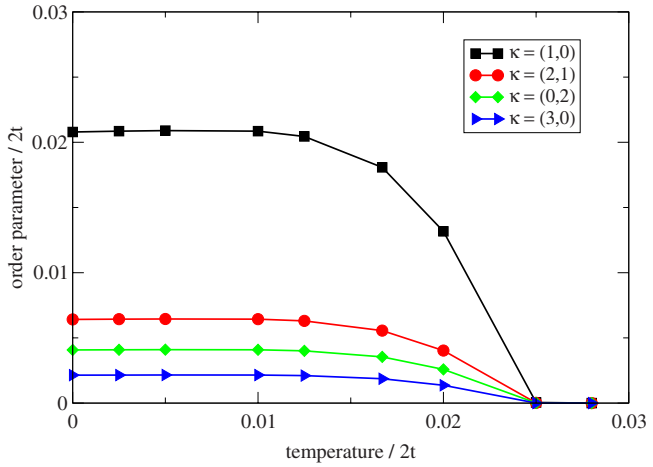

FIG. 15. (Color online) Local order parameter $\tilde{\Delta}_{ij}(T)$ as function of T (both in units of $2t$) for different values of the distance $\kappa = |\mathbf{R}_{ij}|$. Note that all curves vanish at the same critical temperature T_c.

curves vanish at the same temperature $T/2t \approx 0.026$, which defines the critical temperature T_c. Note that the temperature dependence of $\tilde{\Delta}_{ij}$ and thus of the gap function $\tilde{\Delta}_{\mathbf{k}}$ resembles that of the order parameter in usual BCS superconductors.[21] This property can be traced back to the diagonalization approach on the basis of a Bogoliubov transformation in Appendix E, which is applied to the renormalized Hamiltonian $\tilde{\mathcal{H}}$ in the superconducting state. Also the pair correlation function $\langle \hat{c}_{-\mathbf{k}\downarrow} \hat{c}_{\mathbf{k}\uparrow} \rangle$ is evaluated in this way which results in a temperature dependence as in BCS superconductors as well.

In Fig. 16, the critical temperature T_c is given as a function of the hole doping δ. The parameter values are again $t' = 0.4t$ and $J = 0.2t$. Note that for small hole doping $\delta \leqslant 0.03$, no superconducting solutions are found. Also this result of the PRM is in good agreement with experiments. In the underdoped region for $\delta > 0.03$, the critical temperature T_c first increases substantially until it arrives a maximum value at about $\delta \approx 0.08$. Above the optimal doping concentration of $\delta = 0.08$, the critical temperature decreases again (overdoped region). Within the parameter range, given in the figure, the T_c behavior agrees very well with experiment. For still larger values of $\delta (\delta > 0.15)$, our PRM result for T_c remains finite. This feature is in disagreement with experiments, where the superconducting phase vanishes above a critical hole concentration. However, this defect of the present approach is by no means surprising. As was discussed in Secs. IV and VI, we have argued from the beginning that the present approach is not applicable for the case of large hole doping. Nevertheless, Fig. 16 demonstrates that we are able to explain the experimental findings at least in the underdoped and in the optimal doping regime. For the present parameter values, the maximum of T_c at optimal doping is approximately given by $T_c \approx 0.06t$. Assuming a bare bandwidth of $8t \approx 10^4$ K, this T_c value corresponds to a critical temperature of order 50–100 K, which is in the correct order of magnitude.

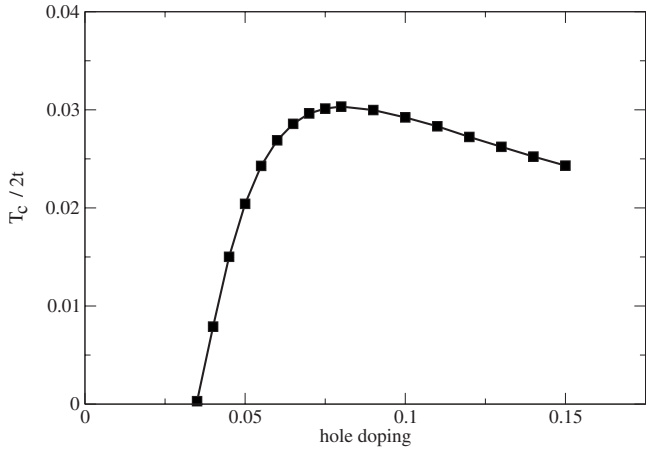

FIG. 16. Critical temperature T_c as a function of the hole doping δ for $t' = 0.4t$ and $J = 0.2t$. No superconducting solution is found for $\delta \leqslant 0.03$. This result explains the vanishing of the superconducting phase in the cuprates at very low doping.

3. Discussion

Next, we want to discuss the origin of the superconducting pairing mechanism. Let us start with the superconducting order parameter $\tilde{\Delta}_{\mathbf{k}}^{(1)}$ after the first renormalization step. According to Eq. (91), we have

$$\tilde{\Delta}_{\mathbf{k}}^{(n=1)} = \Delta_{\mathbf{k},\lambda=0} - \frac{1}{N}\sum_{\mathbf{q}} \frac{3J_{\mathbf{q}}}{4\hat{\omega}_{\mathbf{q},\lambda=0}^2} (\varepsilon_{\mathbf{k},\lambda=0} - \varepsilon_{\mathbf{k}+\mathbf{q},\lambda=0})^2 \times \langle \hat{c}_{-(\mathbf{k}+\mathbf{q})\downarrow} \hat{c}_{\mathbf{k}+\mathbf{q}\uparrow} \rangle. \tag{103}$$

The first term on the right-hand side results from second-order renormalization contributions according to Eq. (86). The numerical evaluation of Eq. (103) shows that it is small compared to the second term. According to Sec. VI, the latter one results from the factorization of the contribution $\sim \dot{\mathbf{S}}_{\mathbf{q}} \dot{\mathbf{S}}_{-\mathbf{q}}$ in the renormalized Hamiltonian $\mathcal{H}_{\lambda=0} = \Sigma_{\mathbf{q}} (J_{\mathbf{q}})/(2\hat{\omega}_{\mathbf{q}}^2) \dot{\mathbf{S}}_{\mathbf{q}} \dot{\mathbf{S}}_{-\mathbf{q}} + \cdots$ after the first renormalization cycle. Therefore, we can conclude from (D2) that the dominant part of the microscopic pairing interaction is given by

$$\mathcal{H}_{(SC)} = \frac{1}{N}\sum_{\mathbf{qk}} \frac{J_{\mathbf{q}}}{4\hat{\omega}_{\mathbf{q}}^2} (\varepsilon_{\mathbf{k}} - \varepsilon_{\mathbf{k}-\mathbf{q}})^2 (\hat{c}_{\mathbf{k}\uparrow}^{\dagger} \hat{c}_{-\mathbf{k}\downarrow}^{\dagger} \hat{c}_{-(\mathbf{k}-\mathbf{q})\downarrow} \hat{c}_{\mathbf{k}-\mathbf{q}\uparrow} + 2\hat{c}_{\mathbf{k}\uparrow}^{\dagger} \hat{c}_{-\mathbf{k}\downarrow}^{\dagger} \hat{c}_{\mathbf{k}-\mathbf{q}\downarrow} \hat{c}_{-(\mathbf{k}-\mathbf{q})\uparrow}). \tag{104}$$

Here, spin-singlet pairing was assumed. Expression (104) is our central result for the superconducting pairing mechanism in the cuprates. In contrast to usual BCS superconductors, where the pairing interaction between Cooper electrons is mediated by phonons, the present result can not be interpreted as an effective interaction of second order in some electron-bath coupling. Note that Eq. (104) results from the part of the exchange $\mathcal{H}_J$ which commutes with $\mathcal{H}_t$. An important feature of the pairing interaction is the oscillation frequency $\hat{\omega}_{\mathbf{q}}^2$ in the denominator of Eq. (104),

$$\hat{\omega}_{\mathbf{q}}^2 = 2P_0(t_{\mathbf{q}=0}^2 - t_{\mathbf{q}}^2) = \hat{\omega}_{-\mathbf{q}}^2 \geqslant 0, \quad t_{\mathbf{q}}^2 = \sum_{l(\neq i)} t_{il}^2 \cos \mathbf{q}(\mathbf{R}_l - \mathbf{R}_i), \tag{105}$$

which enhances the pairing mechanism for small hole doping since $P_0 \sim \delta$. Therefore, the pairing interaction is mediated by oscillating hopping processes between nearest neighbors. This was discussed in detail in Sec. IV A. First, an electron hops to a neighboring site which is empty. In the second step, it hops back to the first site since this site was certainly empty after the first hop. Thereby, the presence of short-range antiferromagnetic correlations in the unperturbed Hamiltonian $\mathcal{H}_0$ is crucial since it prevents the hopping to more distant sites.

In order to derive an approximate gap equation, let us again start from Eq. (103). When we restrict ourselves to a weak coupling theory, the λ dependence of $\varepsilon_{\mathbf{k},\lambda}$ and $\hat{\omega}_{\mathbf{q},\lambda}$ can be neglected,

$$\tilde{\Delta}_{\mathbf{k}}^{(1)} = -\frac{1}{N}\sum_{\mathbf{q}} \frac{3J_{\mathbf{q}}}{4\hat{\omega}_{\mathbf{q}}^2}(\varepsilon_{\mathbf{k}} - \varepsilon_{\mathbf{k}+\mathbf{q}})^2 \langle \hat{c}_{-(\mathbf{k}+\mathbf{q})\downarrow} \hat{c}_{\mathbf{k}+\mathbf{q}\uparrow} \rangle, \tag{106}$$

where the first term from Eq. (103) was already omitted. For a purely qualitative discussion of the gap parameter, let us abandon all higher order renormalization effects, which would be included in the full renormalization scheme of Sec. VI. Inserting the former expression [Eq. (100)] for $\langle \hat{c}_{-\mathbf{k}\downarrow} \hat{c}_{\mathbf{k}\uparrow} \rangle$ into Eq. (106), we find

$$\tilde{\Delta}_{\mathbf{k}}^{(1)} = -\frac{1}{N}\sum_{\mathbf{q}} \frac{3J_{\mathbf{q}}}{4\hat{\omega}_{\mathbf{q}}^2}(\varepsilon_{\mathbf{k}} - \varepsilon_{\mathbf{k}+\mathbf{q}})^2 \tilde{u}_{\mathbf{k}+\mathbf{q}}^2 D^2 \frac{1 - 2f(E_{\mathbf{k}+\mathbf{q}})}{2\sqrt{\varepsilon_{\mathbf{k}+\mathbf{q}}^2 + D^2\tilde{\Delta}_{\mathbf{k}+\mathbf{q}}^2}} \tilde{\Delta}_{\mathbf{k}+\mathbf{q}}, \tag{107}$$

where $E_{\mathbf{k}}$ is again given by $E_{\mathbf{k}} = \sqrt{\varepsilon_{\mathbf{k}}^2 + D^2\tilde{\Delta}_{\mathbf{k}}^2}$, and $f(E_{\mathbf{k}})$ is the Fermi function $f(E_{\mathbf{k}}) = 1/(1 + e^{\beta E_{\mathbf{k}}})$. Moreover, by replacing on the left-hand side also $\tilde{\Delta}_{\mathbf{k}}^{(1)}$ by $\tilde{\Delta}_{\mathbf{k}}$, we arrive at the following approximate gap equation:

$$\tilde{\Delta}_{\mathbf{k}} \approx -\frac{1}{N} D^2 \sum_{\mathbf{q}} \frac{3J_{\mathbf{q}}}{4\hat{\omega}_{\mathbf{q}}^2}(\varepsilon_{\mathbf{k}} - \varepsilon_{\mathbf{k}+\mathbf{q}})^2 \tilde{u}_{\mathbf{k}+\mathbf{q}}^2 \frac{1 - 2f(E_{\mathbf{k}+\mathbf{q}})}{2\sqrt{\varepsilon_{\mathbf{k}+\mathbf{q}}^2 + D^2\tilde{\Delta}_{\mathbf{k}+\mathbf{q}}^2}} \tilde{\Delta}_{\mathbf{k}+\mathbf{q}}. \tag{108}$$

Note that the main features of our numerical results for the full renormalization scheme can already be detected from this equation. Due to the doping dependence of $\tilde{u}_{\mathbf{k}}$, shown in Fig. 9, superconductivity sets in at the same small δ value, at which $\tilde{u}_{\mathbf{k}}$ becomes nonzero. With increasing hole doping, $\tilde{u}_{\mathbf{k}}$ increases, which also leads to a strengthening of the coherent excitation in $\mathfrak{I}G(\mathbf{k},\omega)$. Moreover, superconductivity is favored for low doping due to the factor $\hat{\omega}_{\mathbf{q}}^2 \sim \delta$ in the denominator of Eq. (108). Both features together, i.e., the increase in $\tilde{u}_{\mathbf{k}}$ with δ and $\hat{\omega}_{\mathbf{q}}^2 \sim \delta$ lead to a maximum of T_c at a finite doping value which is seen in Fig. 16. The property $\hat{\omega}_{\mathbf{q}}^2 \sim \delta$ also explains the decrease in T_c in the overdoped region since renormalization processes become weaker for larger δ.

The preference of the PRM to find solutions with d-wave symmetry for the gap parameter can also be understood from gap equation (108). For an explanation, let us start by dividing the sum over $\mathbf{q}$ in Eq. (108) into two parts with $|\varepsilon_{\mathbf{k}+\mathbf{q}}| \leqslant |\tilde{\Delta}_{\mathbf{k}+\mathbf{q}}|$ and $|\varepsilon_{\mathbf{k}+\mathbf{q}}| > |\tilde{\Delta}_{\mathbf{k}+\mathbf{q}}|$. Omitting the second sum, one finds

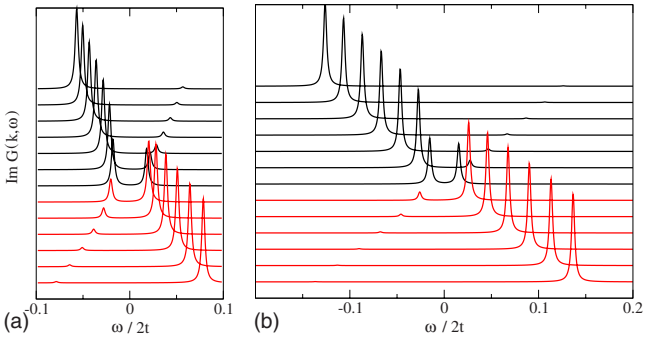

FIG. 17. (Color online) Spectral functions $\mathfrak{I}G(\mathbf{k},\omega)$ in the superconducting phase at optimal doping, $\delta = 0.08$ for two fixed k_x values: (a) $k_x = \pi$ (antinodal region) and (b) $k_x = 5\pi/8$ (in between antinodal and nodal region). By varying k_y, the Fermi surface is crossed. The other parameters are $t' = 0.4t$, $J = 0.2t$, and $T = 0$.

$$\tilde{\Delta}_{\mathbf{k}} \approx -\frac{1}{N} \sum_{\mathbf{q}, |\varepsilon_{\mathbf{k}+\mathbf{q}}| \leqslant |\tilde{\Delta}_{\mathbf{k}+\mathbf{q}}|} \frac{3J_{\mathbf{q}}}{4\hat{\omega}_{\mathbf{q}}^2}(\varepsilon_{\mathbf{k}} - \varepsilon_{\mathbf{k}+\mathbf{q}})^2 \times \tilde{u}_{\mathbf{k}+\mathbf{q}}^2 D^2 \frac{1 - 2f(E_{\mathbf{k}+\mathbf{q}})}{2\sqrt{\varepsilon_{\mathbf{k}+\mathbf{q}}^2 + \tilde{\Delta}_{\mathbf{k}+\mathbf{q}}^2}} \tilde{\Delta}_{\mathbf{k}+\mathbf{q}}. \tag{109}$$

For most values of $\mathbf{k}$, the neglected sum is smaller by a factor of order Δ/t. An exception are $\mathbf{k}$ values close to the Fermi surface $\mathbf{k} \approx \mathbf{k}_F$ [with $|\varepsilon_{\mathbf{k}}| \leqslant O(\Delta_{\mathbf{k}})$], which will be excluded in the following discussion. Here, the sum with $|\varepsilon_{\mathbf{k}+\mathbf{q}}| > |\tilde{\Delta}_{\mathbf{k}+\mathbf{q}}|$ would be larger by a factor of order t/Δ. With respect to Eq. (109), those terms of the $\mathbf{q}$ sum are most important, which have energies $|\varepsilon_{\mathbf{k}+\mathbf{q}}|$ not exceeding $|\tilde{\Delta}_{\mathbf{k}+\mathbf{q}}|$. For $\mathbf{k}$ values on the diagonal, $k_x = k_y$, of the Brillouin zone, it can be seen that $\mathbf{q}$ values with $q_y \approx q_x \pm \pi$ lead to small energies $\varepsilon_{\mathbf{k}+\mathbf{q}} \approx 0$ and thus to the dominant contributions in Eq. (109). Here, the dispersion relation $\varepsilon_{\mathbf{k}} = -2t(\cos k_x a + \cos k_y a)$ was used. However, the prefactor $J_{\mathbf{q}}$ vanishes in this case. This explains the nodal line $k_x = k_y$ and similarly $k_x = -k_y$ of the gap parameter in Fig. 11. However note that the exchange constant $J_{\mathbf{q}}$ changes its sign as a function of $\mathbf{q}$. From this behavior, one can conclude that d-wave symmetry for the order parameter is more favorable than s-wave symmetry.

B. ARPES spectral functions

Finally, let us discuss the ARPES spectral function in the superconducting phase. This quantity is obtained from the dissipative part of the anticommutator Green's function [Eq. (57)].

In Figs. 17–19, our results for the superconducting phase are given which are obtained from the numerical evaluation of Eq. (98). First, in Fig. 17, we have chosen as parameters: $\delta = 0.08$ (optimal doping), $T = 0$, $t' = 0.4t$, and $J = 0.2t$. Two cuts with fixed k_x and varying k_y are shown. Thereby the FS is crossed. In panel (a), where $k_x = \pi$, the spectra belong to $\mathbf{k}$ values in the antinodal region, whereas in (b) $k_x = 5\pi/8$.

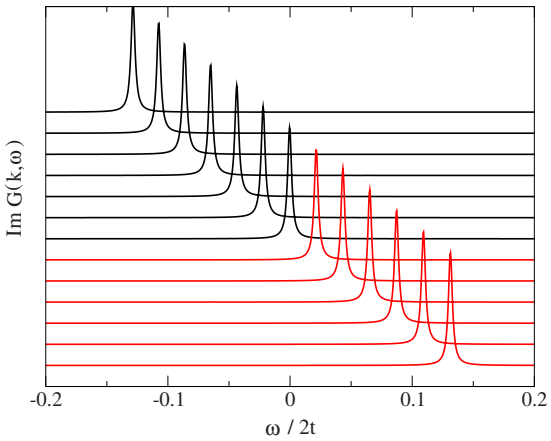

FIG. 18. (Color online) Spectral functions $\Im G(\mathbf{k},\omega)$ as in Fig. 17 for a fixed k_x value, $k_x=\pi/2$. By varying k_y the Fermi surface is crossed in the nodal region.

Here, a **k** region is probed in between the nodal and the antinodal point. The spectra in both panels display peaklike structures in a small energy range around $\omega=0$. Note that all structures are caused alone by the coherent part of $\Im G(\mathbf{k},\omega)$ [first line in Eq. (98)], which consists of two peaks at the positions $\omega=\pm E_{\mathbf{k}}$. For **k** vectors, far away from the FS [top and bottom plots in Figs. 17(a) and 17(b)], a dominating peak at $\omega\approx\tilde{\varepsilon}_{\mathbf{k}}$ is found, which arises from the excitations at $\pm E_{\mathbf{k}}$, depending on the sign of $\tilde{\varepsilon}_{\mathbf{k}}$. By approaching the FS, a secondary peak arises at $\omega\approx-\tilde{\varepsilon}_{\mathbf{k}}$. An expansion of the prefactors in Eq. (98) shows that in each case the secondary peak has a smaller weight of order $(\tilde{\Delta}_{\mathbf{k}}/\tilde{\varepsilon}_{\mathbf{k}})^2$. Only for **k** values on the FS ($\tilde{\varepsilon}_{\mathbf{k}}=0$), the two coherent peaks have equal weight. They are separated by an energy distance, which is given by the gap parameter $(2D\tilde{\Delta}_{\mathbf{k}})$. Note that the gap size is almost the same for the two cases of Fig. 17. A comparison of both panels of Fig. 17 also shows that the secondary peak is more pronounced in the antinodal region than in between the antinodal and nodal regions. Furthermore, the overall dispersion of $\tilde{\varepsilon}_{\mathbf{k}}$ of the primary peak is weaker in the antinodal region than for the case of intermediate k_x values. With respect to the incoherent contributions to $\Im G(\mathbf{k},\omega)$, note that for optimal doping the overall weight of the coherent and of the incoherent excitations are approximately the same. However, the incoherent part of the spectrum is spread over a much larger frequency range. Therefore, in a small ω range, close to the Fermi level, the coherent excitations are dominant.

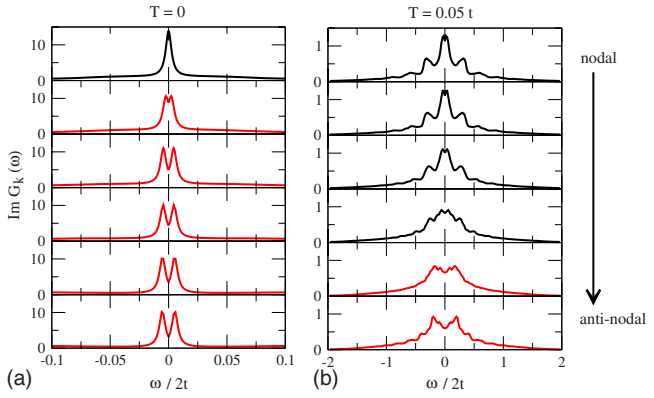

FIG. 19. (Color online) Symmetrized spectral functions $\Im G(\mathbf{k},\omega)$ for **k** values on the FS between the nodal (top) and antinodal point (bottom) for two temperatures (a) in the superconducting phase at $T=0$, and (b) in the pseudogap phase at $T=0.05t$. The critical temperature is $T_c=0.03t$ (underdoped case $\delta=0.05$). The other parameters are the same as in Fig. 17.

In Fig. 18, the spectral function is plotted in the nodal region for fixed $k_x=\pi/2$ and different values of k_y. Thereby, again the FS is crossed. Note that neither a secondary peak nor a superconducting gap is found in the nodal region. Also, the coherent peak moves almost unchanged through the FS, when k_y is varied.

Finally, Fig. 19 shows the results for the symmetrized spectral functions $\Im G(\mathbf{k},\omega)$ for two different temperatures (a) $T=0$ (superconducting phase) and (b) $T=0.05t$ (pseudogap phase). The **k** values proceed on the FS between the nodal (top) and the antinodal (bottom) point. The hole concentration is $\delta=0.05$ (underdoped regime) which leads to a critical temperature $T_c=0.03t$. In the spectra at temperature $T=0$, one recognizes the opening of a superconducting gap for all **k** vectors except at the nodal point. The gap size as a function of the Fermi surface angle ϕ is given by the blue line in Fig. 12. Similar as before, the peaklike structure arises from the coherent excitations in a small ω range around $\omega=0$. For the higher temperature, $T=0.05t$ (pseudogap phase), the system is in the normal state. On a substantial part of the Fermi surface, the spectra now show the typical large spectral weight around $\omega=0$, indicating a Fermi arc of gapless excitations. The Fermi arc extents over a finite **k** range. In contrast to the superconducting case, the spectrum is now dominated by the incoherent excitations. In the antinodal region, they form the pseudogap around $\omega=0$. Note that the pseudogap in Fig. 19(b) is about ten times larger than the superconducting gap at $T=0$ (for the present hole doping $\delta=0.05$). Note that for both temperatures, the spectra are in good qualitative agreement with recent ARPES measurements.[9,11,12]

Let us finally make one remark concerning the linewidth of the coherent peaks. As was already mentioned in Sec. V, from the experimental point of view, we would expect a temperature-dependent broadening of the coherent peaks which is caused by the coupling to other degrees of freedom. Such a broadening was not incorporated in the present approach. Note, however, that a broadening of the spectra is also produced by the incoherent excitations of $\Im G(\mathbf{k},\omega)$. In order to include a temperature-dependent broadening of the coherent excitations, we have added by hand a small linewidth in Fig. 19, which is taken of the order of k_BT.

VIII. CONCLUSIONS

In this paper, we have given a microscopic approach to high-temperature superconductivity at moderate hole doping. Thereby, a recently developed projector-based renormalization method (PRM) was applied to the t-J model in order to investigate the pseudogap as well as the superconducting phase. The pseudogap, which is found in ARPES experi-

ments, can be traced back to incoherent excitations in the one-particle Green's function. It can neither be explained by a competing order nor as a precursor of superconductivity. Instead, the pseudogap phase is an intrinsic property of the cuprates close to half-filling. Our result for the superconducting order parameter shows d-wave symmetry with a coherence length of a few lattice constants which is in agreement with experiments. In contrast to usual BCS superconductors, where the pairing interaction between Cooper electrons is mediated by phonons, the superconducting pairing interaction in the cuprates can not be interpreted as an effective interaction of second order in some electron-bath coupling. Instead, the main contribution to the pairing results from the part of the exchange interaction which commutes with the hopping Hamiltonian $\mathcal{H}_t$. The superconducting state naturally arises from a typical oscillation behavior of the correlated electrons between neighboring lattice sites due to the presence of spin fluctuations. The theoretical results can explain the experimental findings in the underdoped as well as in the optimal doping regime. The obtained value of T_c at optimal doping has the correct order of magnitude.

ACKNOWLEDGMENTS

We would like to acknowledge stimulating and enlightening discussions with J. Fink and A. Hübsch. This work was supported by the DFG through the research program SFB 463.

APPENDIX A: DERIVATION OF THE SPIN SUSCEPTIBILITY $\chi(\mathbf{q},\omega)$

The derivation of the spin susceptibility $\chi(\mathbf{q},\omega)$ in Eq. (24) for the system, described by the Hamiltonian $\mathcal{H}_0=\mathcal{H}_t+\mathcal{H}_J^{(0)}$, is based on the Mori-Zwanzig projection formalism. This formalism allows to derive exact equations of motion for an appropriately chosen set of relevant operator variables $\{A_\alpha\}$,

$$\frac{d}{dt}A_\alpha(t)=i\sum_\beta A_\beta(t)\Omega_{\beta\alpha}-\int_0^t\sum_\beta A_\beta(t-t')\Sigma_{\beta\alpha}(t')dt'+F_\alpha(t), \tag{A1}$$

where the dynamics of the set $A_\alpha(t)$ should be governed by $\mathcal{H}_0$, i.e., $A_\alpha(t)=e^{i/\hbar\mathcal{H}_0t}A_\alpha e^{-i/\hbar\mathcal{H}_0t}$. The quantities $i\omega_{\alpha\beta}$, $\Sigma_{\alpha\beta}(t)$, and $F_\alpha(t)$ are called frequency matrix, self-energy, and random force

$$i\Omega_{\alpha\beta}=\sum_\gamma\chi^{-1}_{\alpha\gamma}(A_\alpha|\dot{A}_\beta),\quad \Sigma_{\alpha\beta}(t)=\sum_\gamma\chi^{-1}_{\alpha\gamma}(\dot{A}_\gamma|\mathsf{Q}e^{i\mathsf{QL}_0\mathsf{Q}t}\mathsf{Q}\dot{A}_\beta),$$
$$F_\alpha(t)=ie^{i\mathsf{QL}_0\mathsf{Q}t}\mathsf{QL}_0A_\alpha. \tag{A2}$$

Here, $\dot{A}_\alpha$ is the time derivative of A_α, defined by $\dot{A}_\alpha=i\mathsf{L}_0A_\alpha$, and $\chi^{-1}_{\alpha\beta}$ is the inverse of the susceptibility matrix $\chi_{\alpha\beta}=(A_\alpha|A_\beta)$. In Eqs. (A2), we have also introduced a scalar product between operator quantities A and B,

$$(A|B)=\int_0^\beta d\lambda\langle A^\dagger e^{-\lambda\mathsf{L}_0}B\rangle_0, \tag{A3}$$

where the expectation value $\langle\cdots\rangle_0$ is formed with $\mathcal{H}_0$ and L_0 is the Liouville operator, which corresponds to $\mathcal{H}_0$. In $\Sigma_{\alpha\beta}(t)$ the quantity Q is a projection operator which projects on the subspace of all operator variables which are "perpendicular" to the set $\{A_\alpha\}$, i.e.,

$$\mathsf{Q}=1-\sum_\alpha|A_\alpha)\chi^{-1}_{\alpha\beta}(A_\beta|. \tag{A4}$$

To use the general projection formalism to derive $\chi(\mathbf{q},\omega)$, we have to choose an appropriate set of relevant operator $\{A_\alpha\}$. In our case, this set is given by $\mathbf{S_q}$ and its time derivative $\dot{\mathbf{S}}_\mathbf{q}$, i.e.,

$$\{A_\alpha\}=\{\mathbf{S_q},\dot{\mathbf{S}}_\mathbf{q}\}. \tag{A5}$$

From Eqs. (A1), one easily derives the following two equations:

$$\frac{d}{dt}\mathbf{S_q}(t)=\dot{\mathbf{S}}_\mathbf{q}(t),$$
$$\frac{d}{dt}\dot{\mathbf{S}}_\mathbf{q}(t)=-\omega_\mathbf{q}^2\mathbf{S_q}(t)-\int_0^t dt'\dot{\mathbf{S}}_\mathbf{q}(t-t')\Sigma_\mathbf{q}(t')+\mathbf{F_q}(t), \tag{A6}$$

where the frequency and the self-energy in the second equation are given by

$$\omega_\mathbf{q}^2=\frac{(\dot{\mathbf{S}}_\mathbf{q}|\dot{\mathbf{S}}_\mathbf{q})}{(\mathbf{S_q}|\mathbf{S_q})},\quad \Sigma_\mathbf{q}(t)=\frac{1}{(\dot{\mathbf{S}}_\mathbf{q}|\dot{\mathbf{S}}_\mathbf{q})}(\ddot{\mathbf{S}}_\mathbf{q}|\mathsf{Q}e^{i\mathsf{QL}_0\mathsf{Q}t}\mathsf{Q}\ddot{\mathbf{S}}_\mathbf{q}) \tag{A7}$$

and the random force is $\mathbf{F_q}(t)=e^{i\mathsf{QL}_0\mathsf{Q}t}\mathsf{Q}\ddot{\mathbf{S}}_\mathbf{q}$. The projector Q projects perpendicular to $\mathbf{S_q}$ and $\dot{\mathbf{S}}_\mathbf{q}$. In deriving Eqs. (A6), we have also used $(S_\mathbf{q}^\nu|\dot{S}_\mathbf{q}^\mu)=i\langle[S_\mathbf{q}^{\nu\dagger},S_\mathbf{q}^\mu]\rangle_0=0$ (for all $\nu,\mu=x,y,z$), which follows from the exact relation $(A|\mathsf{L}_0B)=\langle[A^\dagger,B]\rangle_0$. To find the dynamical susceptibility $\chi(\mathbf{q},\omega)$, we multiply both equations [Eqs. (A6)] with the bra $(\mathbf{S_q}|$ and go over to the Laplace transform. Using $(\mathbf{S_q}|\mathbf{F_q})=0$, we obtain

$$\chi(\mathbf{q},\omega)=\frac{-\omega_\mathbf{q}^2}{\omega^2-\omega_\mathbf{q}^2-\omega\Sigma_\mathbf{q}(\omega)}\chi(\mathbf{q}). \tag{A8}$$

Here, $\chi(\mathbf{q})=(S_\mathbf{q}|S_\mathbf{q})$ is the static spin susceptibility and $\Sigma_\mathbf{q}(\omega)$ is the Laplace transformed self-energy,

$$\Sigma_\mathbf{q}(\omega)=\frac{1}{(\dot{\mathbf{S}}_\mathbf{q}|\dot{\mathbf{S}}_\mathbf{q})}\left(\ddot{\mathbf{S}}_\mathbf{q}|\mathsf{Q}\frac{1}{\omega-\mathsf{QL}_0\mathsf{Q}-i\eta}\mathsf{Q}\ddot{\mathbf{S}}_\mathbf{q}\right). \tag{A9}$$

To proceed, we have to evaluate the second time derivative $\ddot{\mathbf{S}}_\mathbf{q}$

$$\ddot{\mathbf{S}}_\mathbf{q}=-\frac{1}{\sqrt{N}}\sum_{i\neq l}t_{il}^2(e^{i\mathbf{qR}_l}-e^{i\mathbf{qR}_i})(\vec{S}_l\mathcal{P}_0(i)-\vec{S}_i\mathcal{P}_0(l))$$
$$-\frac{1}{2\sqrt{N}}\sum_{\alpha\beta}\sum_{i\neq j}\sum_{j(\neq i\neq l)}t_{il}t_{lj}(e^{i\mathbf{qR}_i}-e^{i\mathbf{qR}_l})$$
$$\times\{\vec{\sigma}_{\alpha\beta}[\hat{c}_{j\alpha}^\dagger\mathcal{D}_\alpha(l)\hat{c}_{i\beta}+\hat{c}_{j,-\alpha}^\dagger S_l^\alpha\hat{c}_{i\beta}]$$
$$+\vec{\sigma}_{\alpha\beta}^*[\hat{c}_{i\beta}^\dagger\mathcal{D}_\alpha(l)\hat{c}_{j\alpha}+c_{i\beta}^\dagger S_l^{-\alpha}\hat{c}_{m,-\alpha}]\}, \tag{A10}$$

where only the dominant part of the hopping Hamiltonian $\mathcal{H}_t$

was taken into account. The first term on the right-hand side of Eq. (A10) enters from a twofold hopping to a neighboring site and back. By replacing the two projectors $\mathcal{P}_0(i)$ and $\mathcal{P}_0(l)$ by their expectation values, we come back to the former equation of motion [Eq. (22)]. Therefore, we can conclude that the frequency term $\omega_{\mathbf{q}}^2$, defined in Eq. (A7), agrees with the former frequency term $\hat{\omega}_{\mathbf{q}}^2$ from Eq. (22),

$$\omega_{\mathbf{q}}^2 = \hat{\omega}_{\mathbf{q}}^2 = 2P_0(t_{\mathbf{q}=0}^2 - t_{\mathbf{q}}^2) \geqslant 0. \tag{A11}$$

The second contribution in Eq. (A10) describes a twofold hopping away from the starting site and agrees with the quantity $\mathsf{Q}\ddot{\mathbf{S}}_{\mathbf{q}}$ in the self-energy,

$$\begin{aligned}\mathsf{Q}\ddot{\mathbf{S}}_{\mathbf{q}} = -\frac{1}{2\sqrt{N}}\sum_{\alpha\beta}\sum_{i\neq j}\sum_{j(\neq i\neq l)} t_{il}t_{lj}(e^{i\mathbf{q}\mathbf{R}_i} - e^{i\mathbf{q}\mathbf{R}_l}) \\ \times \mathsf{Q}\{\vec{\sigma}_{\alpha\beta}[\hat{c}_{j\alpha}^{\dagger}\mathcal{D}_{\alpha}(l)\hat{c}_{i\beta} + \hat{c}_{j,-\alpha}^{\dagger}S_l^{\alpha}\hat{c}_{i\beta}] \\ + \vec{\sigma}_{\alpha\beta}^{*}[\hat{c}_{i\beta}^{\dagger}\mathcal{D}_{\alpha}(l)\hat{c}_{j\alpha} + c_{i\beta}^{\dagger}S_l^{-\alpha}\hat{c}_{m,-\alpha}]\}. \end{aligned} \tag{A12}$$

In order to obtain a rough estimate for the self-energy $\Sigma_{\mathbf{q}}(\omega)$, we neglect the spin flip operators in Eq. (A12) and replace the local projectors $\mathcal{D}_{\alpha}(i)$ and $\mathcal{D}_{\alpha}(l)$ as before by their expectation value D. By introducing Fourier transformed quantities, we find

$$\mathsf{Q}\ddot{\mathbf{S}}_{\mathbf{q}} = \frac{D}{2\sqrt{N}}\sum_{\alpha\beta}\vec{\sigma}_{\alpha\beta}[(\varepsilon_{\mathbf{k}+\mathbf{q}} - \varepsilon_k)^2 - 2(t_{\mathbf{q}=0}^2 - t_{\mathbf{q}}^2)]\mathsf{Q}\hat{c}_{\mathbf{k}+\mathbf{q},\alpha}^{\dagger}\hat{c}_{\mathbf{k}\beta}. \tag{A13}$$

The self-energy then reads

$$\begin{aligned}\Sigma_{\mathbf{q}}(\omega) = \frac{D^2}{(\dot{\vec{S}}_{\mathbf{q}}|\dot{\vec{S}}_{\mathbf{q}})}\frac{1}{4N}\sum_{\mathbf{k}\mathbf{k}'}\sum_{\alpha\beta}\sum_{\alpha'\beta'}\vec{\sigma}_{\alpha\beta}\cdot\vec{\sigma}_{\alpha'\beta'}^{*} \\ \times[(\varepsilon_{\mathbf{k}+\mathbf{q}} - \varepsilon_{\mathbf{k}})^2 - 2(t_{\mathbf{q}=0}^2 - t_{\mathbf{q}}^2)] \\ \times[(\varepsilon_{\mathbf{k}'+\mathbf{q}} - \varepsilon_{\mathbf{k}'})^2 - 2(t_{\mathbf{q}=0}^2 - t_{\mathbf{q}}^2)] \\ \times\left(\hat{c}_{\mathbf{k}+\mathbf{q},\alpha}^{\dagger}\hat{c}_{\mathbf{k}\beta}|\frac{1}{\omega - \mathsf{Q}\mathsf{L}_0\mathsf{Q} - i\eta}\mathsf{Q}\hat{c}_{\mathbf{k}'+\mathbf{q},\alpha'}^{\dagger}\hat{c}_{\mathbf{k}'\beta'}\right).\end{aligned} \tag{A14}$$

In the final step, we factorize the two-particle correlation function in Eq. (A14) in a product of one-particle Green's functions. A straightforward calculation leads for the imaginary part of the self-energy to

$$\begin{aligned}\Im\Sigma_{\mathbf{q}}(\omega) = \frac{D^2}{(\dot{\vec{S}}_{\mathbf{q}}|\dot{\vec{S}}_{\mathbf{q}})}\frac{3}{2N}\sum_{\mathbf{k}}[(\varepsilon_{\mathbf{k}+\mathbf{q}} - \varepsilon_{\mathbf{k}})^2 \\ - 2(t_{\mathbf{q}=0}^2 - t_{\mathbf{q}}^2)]^2\Im M_{\mathbf{k}}(\mathbf{q},\omega),\end{aligned}$$

$$\Im M_{\mathbf{k}}(\mathbf{q},\omega) = \frac{1 - e^{-\beta\omega}}{\beta\omega}\frac{1}{\pi}\int_{-\infty}^{\infty}d\tilde{\omega}\frac{\Im G_{\mathbf{k}}^{(0)}(\omega+\tilde{\omega})}{1 + e^{-\beta(\omega+\tilde{\omega})}}\frac{\Im G_{\mathbf{k}+\mathbf{q}}^{(0)}(\tilde{\omega})}{1 + e^{\beta\tilde{\omega}}}. \tag{A15}$$

Here, $\Im G_{\mathbf{k}}^{(0)}(\omega)$ is the imaginary part of the one-particle Green's function, formed with the Hamiltonian $\mathcal{H}_0$,

$$G_{\mathbf{k}}^{(0)}(\omega) = i\int_0^{\infty}dt\langle[\hat{c}_{\mathbf{k},\alpha}(t),\hat{c}_{\mathbf{k},\alpha}^{\dagger}]_+\rangle_0 e^{-i(\omega - i\eta)t}. \tag{A16}$$

Finally, we have to evaluate the denominator $(\dot{\vec{S}}_{\mathbf{q}}|\dot{\vec{S}}_{\mathbf{q}})$ of $\Sigma_{\mathbf{q}}(\omega)$. Proceeding in analogy to the evaluation of $\Sigma_{\mathbf{q}}(\omega)$, we find

$$(\dot{\mathbf{S}}_{\mathbf{q}}|\dot{\mathbf{S}}_{\mathbf{q}}) = \frac{3}{2N}\sum_{\mathbf{k}}(\varepsilon_{\mathbf{k}+\mathbf{q}} - \varepsilon_{\mathbf{k}})^2(\hat{c}_{\mathbf{k}+\mathbf{q},\alpha}^{\dagger}\hat{c}_{\mathbf{k}\beta}|\hat{c}_{\mathbf{k}+\mathbf{q},\alpha}^{\dagger}\hat{c}_{\mathbf{k}\beta}) \tag{A17}$$

with

$$\begin{aligned}(\hat{c}_{\mathbf{k}+\mathbf{q},\alpha}^{\dagger}\hat{c}_{\mathbf{k}\beta}|\hat{c}_{\mathbf{k}+\mathbf{q},\alpha}^{\dagger}\hat{c}_{\mathbf{k}\beta}) \\ = \int_{-\infty}^{\infty}d\omega\frac{1 - e^{-\beta\omega}}{\beta\omega}\frac{1}{\pi^2}\int_{-\infty}^{\infty}d\tilde{\omega}\frac{\Im G_{\mathbf{k}}^{(0)}(\omega+\tilde{\omega})}{1 + e^{-\beta(\omega+\tilde{\omega})}}\frac{\Im G_{\mathbf{k}+\mathbf{q}}^{(0)}(\tilde{\omega})}{1 + e^{\beta\tilde{\omega}}}.\end{aligned}$$

APPENDIX B: FACTORIZATION OF $\dot{\mathbf{S}}_{\mathbf{q},\lambda}\dot{\mathbf{S}}_{-\mathbf{q},\lambda}$ FOR THE PSEUDOGAP PHASE

The aim of this appendix is to simplify the operator product $\dot{\mathbf{S}}_{\mathbf{q},\lambda}\dot{\mathbf{S}}_{-\mathbf{q},\lambda}$ in the expressions for $\mathcal{H}_{0,\lambda}$ and $\mathcal{H}_{1,\lambda}$ from Sec. IV A,

$$\mathcal{H}_{0,\lambda} = \sum_{\mathbf{q}}\frac{J_{\mathbf{q}}}{2}\left(\mathbf{S}_{\mathbf{q}}\cdot\mathbf{S}_{-\mathbf{q}} + \frac{1}{\omega_{\mathbf{q},\lambda}}\dot{\mathbf{S}}_{\mathbf{q},\lambda}\cdot\dot{\mathbf{S}}_{-\mathbf{q},\lambda}\right),$$

$$\mathcal{H}_{1,\lambda} = \sum_{\mathbf{q}}\frac{J_{\mathbf{q}}}{2}\left(\mathbf{S}_{\mathbf{q}}\cdot\mathbf{S}_{-\mathbf{q}} - \frac{1}{\omega_{\mathbf{q},\lambda}}\dot{\mathbf{S}}_{\mathbf{q},\lambda}\cdot\dot{\mathbf{S}}_{-\mathbf{q},\lambda}\right).$$

This will be done by use of a factorization approximation. Using for the time derivative

$$\dot{\mathbf{S}}_{\mathbf{q},\lambda} = \frac{i}{2\sqrt{N}}\sum_{\alpha\beta}\vec{\sigma}_{\alpha\beta}\sum_{i\neq j}t_{ij,\lambda}(e^{i\mathbf{q}\mathbf{R}_i} - e^{i\mathbf{q}\mathbf{R}_j})\hat{c}_{i\alpha}^{\dagger}\hat{c}_{j\beta}$$

we first can rewrite $\dot{\mathbf{S}}_{\mathbf{q},\lambda}\dot{\mathbf{S}}_{-\mathbf{q},\lambda}$ as

$$\begin{aligned}\dot{\mathbf{S}}_{\mathbf{q},\lambda}\dot{\mathbf{S}}_{-\mathbf{q},\lambda} = \frac{1}{4N}\sum_{\alpha\beta}\sum_{\gamma\delta}(\vec{\sigma}_{\alpha\beta}\cdot\vec{\sigma}_{\delta\gamma})\sum_{i\neq j}t_{ij,\lambda}(e^{i\mathbf{q}\mathbf{R}_i} - e^{i\mathbf{q}\mathbf{R}_j}) \\ \times\sum_{l\neq m}t_{lm,\lambda}(e^{-i\mathbf{q}\mathbf{R}_l} - e^{-i\mathbf{q}\mathbf{R}_m})\hat{c}_{i\alpha}^{\dagger}\hat{c}_{j\beta}\hat{c}_{m\delta}^{\dagger}\hat{c}_{l\gamma}.\end{aligned} \tag{B1}$$

Using a factorization approximation, the four-fermion operator on the right hand side can be reduced to operators $\hat{c}_{\mathbf{k}\sigma}^{\dagger}\hat{c}_{\mathbf{k}\sigma}$ which will lead to a renormalization of $\varepsilon_{\mathbf{k}}$. Thereby, we have to pay attention to the fact that the averaged spin operator vanishes ($\langle\mathbf{S}_i\rangle=0$) outside the antiferromagnetic regime. Moreover, all local indices in the four-fermion term of Eq. (B1) should be different from each other. This follows from the former decomposition of the exchange interaction into eigenmodes of L_t in Sec. IV A, where we have implicitly assumed that the operators $\dot{\mathbf{S}}_{\mathbf{q},\lambda}$ and $\dot{\mathbf{S}}_{-\mathbf{q},\lambda}$ do not overlap in the local space. Otherwise, the decomposition would be much more involved. However, it can be shown that these

"interference" terms only make a minor impact on the results. For the factorization, we find

$$\dot{\mathbf{S}}_{\mathbf{q},\lambda}\dot{\mathbf{S}}_{-\mathbf{q},\lambda} = \frac{3}{4N}\sum_{i\neq j} t_{ij,\lambda}(e^{i\mathbf{q}\mathbf{R}_i} - e^{i\mathbf{q}\mathbf{R}_j}) \sum_{l\neq m} t_{lm,\lambda}(e^{-i\mathbf{q}\mathbf{R}_l} - e^{-i\mathbf{q}\mathbf{R}_m}) \times \left\{ \sum_{\alpha} \langle (\hat{c}_{j\beta}\hat{c}^{\dagger}_{m\beta})_{NL}\rangle (\hat{c}^{\dagger}_{i\alpha}\hat{c}_{l\alpha})_{NL} + \sum_{\beta} \langle (\hat{c}^{\dagger}_{i\alpha}\hat{c}_{l\alpha})_{NL}\rangle \times (\hat{c}_{j\beta}\hat{c}_{m\beta})_{NL} \right\}, \tag{B2}$$

where we have neglected an additional c-number quantity, which enters in the factorization. The attached subscript in $(\cdots)_{NL}$ on the right-hand side indicates that the local sites of the operators inside the brackets are different from each other. Note that sums over spin indices in Eq. (B1) have already been carried out. Fourier transforming Eq. (B2) leads to

$$\dot{\mathbf{S}}_{\mathbf{q},\lambda}\dot{\mathbf{S}}_{-\mathbf{q},\lambda} = -\frac{3}{2N}\sum_{\mathbf{k}\sigma} (\varepsilon_{\mathbf{k},\lambda} - \varepsilon_{\mathbf{k}-\mathbf{q},\lambda})^2 \langle (\hat{c}^{\dagger}_{\mathbf{k}-\mathbf{q}\alpha}\hat{c}_{\mathbf{k}-\mathbf{q}\alpha})_{NL}\rangle \times (\hat{c}^{\dagger}_{\mathbf{k}\sigma}\hat{c}_{\mathbf{k}\sigma})_{NL}, \tag{B3}$$

where we have defined

$$(\hat{c}^{\dagger}_{\mathbf{k}\sigma}\hat{c}_{\mathbf{k}\sigma})_{NL} = \hat{c}^{\dagger}_{\mathbf{k}\sigma}\hat{c}_{\mathbf{k}\sigma} - \frac{1}{N}\sum_{\mathbf{k}'} \hat{c}^{\dagger}_{\mathbf{k}'\sigma}\hat{c}_{\mathbf{k}'\sigma}.$$

Using Eq. (B3) together with Eq. (51), one is led to the renormalization result [Eq. (53)] of $\tilde{\varepsilon}^{(0)}_{\mathbf{k}}$ to first order in J.

In the following, let us simplify the notation and suppress the index λ in $\dot{\mathbf{S}}_{\mathbf{q},\lambda}$, $\varepsilon_{\mathbf{k},\lambda}$, and also in $\hat{\omega}_{\mathbf{q},\lambda}$. With this convention, we shall use factorization (B3) in order to derive renormalization (41) for $\varepsilon_{\mathbf{k},\lambda}$ in second order in J. We start from expression (40) for the renormalized Hamiltonian $\mathcal{H}^{(2)}_{\lambda-\Delta\lambda}$ in second order,

$$\mathcal{H}^{(2)}_{\lambda-\Delta\lambda} = \sum_{\mathbf{q}} J_{\mathbf{q}} \left\{ \Theta(\lambda - |2\hat{\omega}_{\mathbf{q},\lambda}|) - \frac{1}{2} \right\} [X_{\lambda,\Delta\lambda}, \mathcal{A}_{1,\lambda}(\mathbf{q}) + \mathcal{A}^{\dagger}_{1,\lambda}(\mathbf{q})] + \sum_{\mathbf{q}} J_{\mathbf{q}} [X_{\lambda,\Delta\lambda}, \mathcal{A}_{0,\lambda}],$$

$$= \sum_{\mathbf{q}} J_{\mathbf{q}}\Theta_{\mathbf{q}}(\lambda,\Delta\lambda) \left(\frac{3}{4}[X_{\lambda,\Delta\lambda}, \mathbf{S}_{\mathbf{q}}\cdot\mathbf{S}_{-\mathbf{q}}] + \frac{1}{4\hat{\omega}^2_{\mathbf{q}}}[X_{\lambda,\Delta\lambda}, \dot{\mathbf{S}}_{\mathbf{q}}\cdot\dot{\mathbf{S}}_{-\mathbf{q}}] \right), \tag{B4}$$

where in the first line we have already used $[X_{\lambda,\Delta\lambda}, \mathcal{H}_{t,\lambda}] = -\Sigma_{\mathbf{q}} J_{\mathbf{q}}\Theta_{\mathbf{q}}(\lambda,\Delta\lambda)[\mathcal{A}_{1,\lambda}(\mathbf{q}) + \mathcal{A}^{\dagger}_{1,\lambda}(\mathbf{q})]$. Next, we have to evaluate the commutators of $X_{\lambda,\Delta\lambda}$ with $\mathbf{S}_{\mathbf{q}}\cdot\mathbf{S}_{-\mathbf{q}}$ and $\dot{\mathbf{S}}_{\mathbf{q}}\cdot\dot{\mathbf{S}}_{-\mathbf{q}}$. Using $[\dot{S}^{\nu}_{-\mathbf{q}}, S^{\nu}_{\mathbf{q}}] = \frac{i}{4N}\Sigma_{\mathbf{q}\sigma}(2\varepsilon_{\mathbf{k}} - \varepsilon_{\mathbf{k}+\mathbf{q}} - \varepsilon_{\mathbf{k}-\mathbf{q}})\hat{c}^{\dagger}_{\mathbf{k}\sigma}\hat{c}_{\mathbf{k}\sigma}$, $(\nu = x, y, z)$, and Eq. (39), we find

$$[X_{\lambda,\Delta\lambda}, \mathbf{S}_{\mathbf{q}}\cdot\mathbf{S}_{-\mathbf{q}}] = \frac{J_{\mathbf{q}}}{4\hat{\omega}^2_{\mathbf{q}}}\Theta_{\mathbf{q}}(\lambda,\Delta\lambda) \left(\frac{1}{N}\sum_{\mathbf{k}\sigma} (2\varepsilon_{\mathbf{k}} - \varepsilon_{\mathbf{k}+\mathbf{q}} - \varepsilon_{\mathbf{k}-\mathbf{q}}) \times \langle \hat{c}^{\dagger}_{\mathbf{k}\sigma}\hat{c}_{\mathbf{k}\sigma}\rangle \right) \mathbf{S}_{\mathbf{q}}\cdot\mathbf{S}_{-\mathbf{q}} + \frac{J_{\mathbf{q}}}{4\hat{\omega}^2_{\mathbf{q}}}\Theta_{\mathbf{q}}(\lambda,\Delta\lambda) \times \langle \mathbf{S}_{\mathbf{q}}\cdot\mathbf{S}_{-\mathbf{q}}\rangle \frac{1}{N}\sum_{\mathbf{k}\sigma} (2\varepsilon_{\mathbf{k}} - \varepsilon_{\mathbf{k}+\mathbf{q}} - \varepsilon_{\mathbf{k}-\mathbf{q}})\hat{c}^{\dagger}_{\mathbf{k}\sigma}\hat{c}_{\mathbf{k}\sigma},$$

$$[X_{\lambda,\Delta\lambda}, \dot{\mathbf{S}}_{\mathbf{q}}\cdot\dot{\mathbf{S}}_{-\mathbf{q}}] = -\frac{J_{\mathbf{q}}}{4\hat{\omega}^2_{\mathbf{q}}}\Theta_{\mathbf{q}}(\lambda,\Delta\lambda) \left(\frac{1}{N}\sum_{\mathbf{k}\sigma} (2\varepsilon_{\mathbf{k}} - \varepsilon_{\mathbf{k}+\mathbf{q}} - \varepsilon_{\mathbf{k}-\mathbf{q}}) \times \langle \hat{c}^{\dagger}_{\mathbf{k}\sigma}\hat{c}_{\mathbf{k}\sigma}\rangle \right) \dot{\mathbf{S}}_{\mathbf{q}}\cdot\dot{\mathbf{S}}_{-\mathbf{q}} - \frac{J_{\mathbf{q}}}{4\hat{\omega}^2_{\mathbf{q}}}\Theta_{\mathbf{q}}(\lambda,\Delta\lambda) \times \langle \dot{\mathbf{S}}_{\mathbf{q}}\cdot\dot{\mathbf{S}}_{-\mathbf{q}}\rangle \frac{1}{N}\sum_{\mathbf{k}\sigma} (2\varepsilon_{\mathbf{k}} - \varepsilon_{\mathbf{k}+\mathbf{q}} - \varepsilon_{\mathbf{k}-\mathbf{q}})\hat{c}^{\dagger}_{\mathbf{k}\sigma}\hat{c}_{\mathbf{k}\sigma}. \tag{B5}$$

Note that in Eq. (B5) already a factorization approximation was used. With relations (B4) and (B5), we obtain

$$\mathcal{H}^{(2)}_{\lambda-\Delta\lambda} = 3\sum_{\mathbf{q}} \left(\frac{J_{\mathbf{q}}}{4\hat{\omega}^2_{\mathbf{q}}}\right)^2 \Theta_{\mathbf{q}}(\lambda,\Delta\lambda) \left(\left[\frac{1}{N}\sum_{\mathbf{k}\sigma} (2\varepsilon_{\mathbf{k}} - \varepsilon_{\mathbf{k}+\mathbf{q}} - \varepsilon_{\mathbf{k}-\mathbf{q}}) \times \langle \hat{c}^{\dagger}_{\mathbf{k}\sigma}\hat{c}_{\mathbf{k}\sigma}\rangle \right] \mathbf{S}_{\mathbf{q}}\cdot\mathbf{S}_{-\mathbf{q}} + \langle \mathbf{S}_{\mathbf{q}}\cdot\mathbf{S}_{-\mathbf{q}}\rangle \frac{1}{N}\sum_{\mathbf{k}\sigma} (2\varepsilon_{\mathbf{k}} - \varepsilon_{\mathbf{k}+\mathbf{q}} - \varepsilon_{\mathbf{k}-\mathbf{q}})\hat{c}^{\dagger}_{\mathbf{k}\sigma}\hat{c}_{\mathbf{k}\sigma} \right) - \sum_{\mathbf{q}} \left(\frac{J_{\mathbf{q}}}{4\hat{\omega}^2_{\mathbf{q}}}\right)^2 \Theta_{\mathbf{q}}(\lambda,\Delta\lambda) \times \left(\left[\frac{1}{N}\sum_{\mathbf{k}\sigma} (2\varepsilon_{\mathbf{k}} - \varepsilon_{\mathbf{k}+\mathbf{q}} - \varepsilon_{\mathbf{k}-\mathbf{q}}) \langle \hat{c}^{\dagger}_{\mathbf{k}\sigma}\hat{c}_{\mathbf{k}\sigma}\rangle \right] \dot{\mathbf{S}}_{\mathbf{q}}\cdot\dot{\mathbf{S}}_{-\mathbf{q}} + \langle \dot{\mathbf{S}}_{\mathbf{q}}\cdot\dot{\mathbf{S}}_{-\mathbf{q}}\rangle \frac{1}{N}\sum_{\mathbf{k}\sigma} (2\varepsilon_{\mathbf{k}} - \varepsilon_{\mathbf{k}+\mathbf{q}} - \varepsilon_{\mathbf{k}-\mathbf{q}})\hat{c}^{\dagger}_{\mathbf{k}\sigma}\hat{c}_{\mathbf{k}\sigma} \right). \tag{B6}$$

In a final step, we factorize $\sim\dot{\mathbf{S}}_{\mathbf{q}}\cdot\dot{\mathbf{S}}_{-\mathbf{q}}$ according to Eq. (B3),

$$\mathcal{H}^{(2)}_{\lambda-\Delta\lambda} = 3\sum_{\mathbf{q}} \left(\frac{J_{\mathbf{q}}}{4\hat{\omega}^2_{\mathbf{q}}}\right)^2 \Theta_{\mathbf{q}}(\lambda,\Delta\lambda) \left(\left[\frac{1}{N}\sum_{\mathbf{k}\sigma} (2\varepsilon_{\mathbf{k}} - \varepsilon_{\mathbf{k}+\mathbf{q}} - \varepsilon_{\mathbf{k}-\mathbf{q}}) \times \langle \hat{c}^{\dagger}_{\mathbf{k}\sigma}\hat{c}_{\mathbf{k}\sigma}\rangle \right] \mathbf{S}_{\mathbf{q}}\cdot\mathbf{S}_{-\mathbf{q}} + \langle \mathbf{S}_{\mathbf{q}}\cdot\mathbf{S}_{-\mathbf{q}}\rangle \frac{1}{N}\sum_{\mathbf{k}\sigma} (2\varepsilon_{\mathbf{k}} - \varepsilon_{\mathbf{k}+\mathbf{q}} - \varepsilon_{\mathbf{k}-\mathbf{q}})\hat{c}^{\dagger}_{\mathbf{k}\sigma}\hat{c}_{\mathbf{k}\sigma} \right) - \sum_{\mathbf{q}} \left(\frac{J_{\mathbf{q}}}{4\hat{\omega}^2_{\mathbf{q}}}\right)^2 \Theta_{\mathbf{q}}(\lambda,\Delta\lambda) \times \langle \dot{\mathbf{S}}_{\mathbf{q}}\cdot\dot{\mathbf{S}}_{-\mathbf{q}}\rangle \frac{1}{N}\sum_{\mathbf{k}\sigma} (2\varepsilon_{\mathbf{k}} - \varepsilon_{\mathbf{k}+\mathbf{q}} - \varepsilon_{\mathbf{k}-\mathbf{q}})\hat{c}^{\dagger}_{\mathbf{k}\sigma}\hat{c}_{\mathbf{k}\sigma} + \frac{3}{2N}\sum_{\mathbf{q}\sigma} \left(\frac{J_{\mathbf{q}}}{4\hat{\omega}^2_{\mathbf{q}}}\right)^2 \Theta_{\mathbf{q}}(\lambda,\Delta\lambda) \times \left[\frac{1}{N}\sum_{\mathbf{k}'\sigma'} (2\varepsilon_{\mathbf{k}'} - \varepsilon_{\mathbf{k}'+\mathbf{q}} - \varepsilon_{\mathbf{k}'-\mathbf{q}}) \langle \hat{c}^{\dagger}_{\mathbf{k}'\sigma'}\hat{c}_{\mathbf{k}'\sigma'}\rangle \right] \times \sum_{\mathbf{k}\sigma} (\varepsilon_{\mathbf{k}} - \varepsilon_{\mathbf{k}-\mathbf{q}})^2 \langle (\hat{c}^{\dagger}_{\mathbf{k}-\mathbf{q}\alpha}\hat{c}_{\mathbf{k}-\mathbf{q}\alpha})_{NL}\rangle (\hat{c}^{\dagger}_{\mathbf{k}\sigma}\hat{c}_{\mathbf{k}\sigma})_{NL}. \tag{B7}$$

From Eq. (B7), renormalization equation (41) for $\varepsilon_{\mathbf{k},\lambda-\Delta\lambda}$ can immediately be deduced.

APPENDIX C: RENORMALIZATION EQUATIONS FOR FERMION OPERATORS

The aim of this appendix is to derive the renormalization equation for the fermion operator $\hat{c}_{\mathbf{k}\sigma}(\lambda)=e^{X_\lambda}\hat{c}_{\mathbf{k}\sigma}e^{-X_\lambda}$ in second order in $J_\mathbf{q}$. As before, we shall suppress the index λ everywhere in $\dot{\mathbf{S}}_{\mathbf{q},\lambda}$, $\hat{\omega}_{\mathbf{q},\lambda}$, and $\varepsilon_{\mathbf{q},\lambda}$ in order to simplify the notation. Let us start from an *ansatz* for $\hat{c}_{\mathbf{k}\sigma}(\lambda)$ after all excitations with transition energies larger than λ have been integrated out. It reads

$$\hat{c}_{\mathbf{k}\sigma}(\lambda)=u_{\mathbf{k},\lambda}\hat{c}_{\mathbf{k}\sigma}-i\sum_{\mathbf{q}}\Theta(|2\hat{\omega}_\mathbf{q}|-\lambda)\times v_{\mathbf{k},\mathbf{q},\lambda}\frac{J_\mathbf{q}}{4\hat{\omega}_\mathbf{q}^2}[\mathbf{S}_\mathbf{q}\cdot\dot{\mathbf{S}}_{-\mathbf{q}}+\dot{\mathbf{S}}_{-\mathbf{q}}\cdot\mathbf{S}_\mathbf{q},c_{\mathbf{k}\sigma}]. \quad \text{(C1)}$$

In Eq. (C1), the parameters $u_{\mathbf{k},\lambda}$ and $v_{\mathbf{k},q,\lambda}$ account for the λ dependence. Note that the operator structure in Eq. (C1) corresponds to that of the first-order expansion for $\hat{c}_{\mathbf{k}\sigma}(\lambda)\approx\hat{c}_{\mathbf{k}\sigma}+[X_\lambda,\hat{c}_{\mathbf{k}\sigma}]$. Here, X_λ has the same operator form as the generator $X_{\lambda,\Delta\lambda}$ in Eq. (38). Due to construction, the $\mathbf{q}$ sum in Eq. (C1) only runs over $\mathbf{q}$ values with excitation energies $|2\hat{\omega}_\mathbf{q}|$ larger than λ. This is assured by the Θ function in Eq. (C1). For simplicity, in the following we agree upon to incorporate the Θ function in $v_{\mathbf{k},q,\lambda}$. Thus, we can write

$$\hat{c}_{\mathbf{k}\sigma}(\lambda)=u_{\mathbf{k},\lambda}\hat{c}_{\mathbf{k}\sigma}-i\sum_{\mathbf{q}}v_{\mathbf{k},\mathbf{q},\lambda}\frac{J_\mathbf{q}}{4\hat{\omega}_\mathbf{q}^2}\{([\mathbf{S}_\mathbf{q},c_{\mathbf{k}\sigma}]\cdot\dot{\mathbf{S}}_{-\mathbf{q}}+\dot{\mathbf{S}}_{-\mathbf{q}}\cdot[\mathbf{S}_\mathbf{q},c_{\mathbf{k}\sigma}])+(\mathbf{S}_\mathbf{q}\cdot[\dot{\mathbf{S}}_{-\mathbf{q}},c_{\mathbf{k}\sigma}]+[\dot{\mathbf{S}}_{-\mathbf{q}},c_{\mathbf{k}\sigma}]\cdot\mathbf{S}_\mathbf{q})\}. \quad \text{(C2)}$$

For the additional renormalization from λ to the reduced cutoff $\lambda-\Delta\lambda$, we have

$$\hat{c}_{\mathbf{k}\sigma}(\lambda-\Delta\lambda)=e^{X_{\lambda,\Delta\lambda}}\hat{c}_{\mathbf{k}\sigma}(\lambda)e^{-X_{\lambda,\Delta\lambda}}=u_{\mathbf{k},\lambda}e^{X_{\lambda,\Delta\lambda}}\hat{c}_{\mathbf{k}\sigma}e^{-X_{\lambda,\Delta\lambda}}-i\sum_{\mathbf{q}}v_{\mathbf{k},\mathbf{q},\lambda}\frac{J_\mathbf{q}}{4\hat{\omega}_\mathbf{q}^2}e^{X_{\lambda,\Delta\lambda}}\times[\mathbf{S}_\mathbf{q}\cdot\dot{\mathbf{S}}_{-\mathbf{q}}+\dot{\mathbf{S}}_{-\mathbf{q}}\cdot\mathbf{S}_\mathbf{q},c_{\mathbf{k}\sigma}]e^{-X_{\lambda,\Delta\lambda}}, \quad \text{(C3)}$$

where $X_{\lambda,\Delta\lambda}$ is the generator from Eq. (38),

$$X_{\lambda,\Delta\lambda}=-i\sum_{\mathbf{q}}\frac{J_\mathbf{q}}{4\hat{\omega}_\mathbf{q}}\Theta_\mathbf{q}(\lambda,\Delta\lambda)(\mathbf{S}_\mathbf{q}\dot{\mathbf{S}}_{-\mathbf{q}}+\dot{\mathbf{S}}_\mathbf{q}\mathbf{S}_{-\mathbf{q}}).$$

First, let us expand the term $\sim u_{\mathbf{k},\lambda}$ in Eq. (C3),

$$e^{X_{\lambda,\Delta\lambda}}\hat{c}_{\mathbf{k}\sigma}e^{-X_{\lambda,\Delta\lambda}}=\hat{c}_{\mathbf{k}\sigma}+[X_{\lambda,\Delta\lambda},\hat{c}_{\mathbf{k}\sigma}]+\frac{1}{2}[X_{\lambda,\Delta\lambda},[X_{\lambda,\Delta\lambda},\hat{c}_{\mathbf{k}\sigma}]]+\cdots. \quad \text{(C4)}$$

Here, we can combine the second term in Eq. (C3) with the second part in Eq. (C2),

$$\hat{c}_{\mathbf{k}\sigma}(\lambda-\Delta\lambda)=(u_{\mathbf{k},\lambda}+\cdots)\hat{c}_{\mathbf{k}\sigma}-i\sum_{\mathbf{q}}(v_{\mathbf{k},\mathbf{q},\lambda}+u_{\mathbf{k},\lambda}\Theta_\mathbf{q}(\lambda,\Delta\lambda)+\cdots)\frac{J_\mathbf{q}}{4\hat{\omega}_\mathbf{q}^2}[\mathbf{S}_\mathbf{q}\cdot\dot{\mathbf{S}}_{-\mathbf{q}}+\dot{\mathbf{S}}_{-\mathbf{q}}\cdot\mathbf{S}_\mathbf{q},c_{\mathbf{k}\sigma}]+\cdots, \quad \text{(C5)}$$

where the dots $(+\cdots)$ mean additional contributions from higher-order commutators with $X_{\lambda,\Delta\lambda}$. On the other hand, $\hat{c}_{\mathbf{k}\sigma}(\lambda-\Delta\lambda)$ should have the same form as ansatz (C1), when λ is replaced by $\lambda-\Delta\lambda$,

$$\hat{c}_{\mathbf{k}\sigma}(\lambda-\Delta\lambda)=u_{\mathbf{k},\lambda-\Delta\lambda}\hat{c}_{\mathbf{k}\sigma}-i\sum_{\mathbf{q}}v_{\mathbf{k},\mathbf{q},\lambda-\Delta\lambda}\times\frac{J_\mathbf{q}}{4\hat{\omega}_\mathbf{q}^2}[\mathbf{S}_\mathbf{q}\cdot\dot{\mathbf{S}}_{-\mathbf{q}}+\dot{\mathbf{S}}_{-\mathbf{q}}\cdot\mathbf{S}_\mathbf{q},c_{\mathbf{k}\sigma}]. \quad \text{(C6)}$$

The comparison of Eqs. (C6) and (C5) immediately leads to renormalization equation (61) for $v_{\mathbf{k},\mathbf{q},\lambda}$,

$$v_{\mathbf{k},\mathbf{q},\lambda-\Delta\lambda}=v_{\mathbf{k},\mathbf{q},\lambda}+u_{\mathbf{k},\lambda}\Theta_\mathbf{q}(\lambda,\Delta\lambda), \quad \text{(C7)}$$

where we have restricted ourselves to the lowest order contributions in $X_{\lambda,\Delta\lambda}$. Furthermore, we have exploited the very weak λ dependency of $\varepsilon_{\mathbf{k},\lambda}$ and $\hat{\omega}_{\mathbf{q},\lambda}$.

The renormalization equation for the second parameter $u_{\mathbf{k},\lambda}$ requires the evaluation of higher-order commutators in Eq. (C3). Alternatively, we can start from anticommutator relation (3)

$$[\hat{c}^\dagger_{\mathbf{k}\sigma}(\lambda),\hat{c}_{\mathbf{k}\sigma}(\lambda)]_+=\frac{1}{N}\sum_i e^{X_\lambda}\mathcal{D}_\sigma(i)e^{-X_\lambda}=\frac{1}{N}\sum_i\mathcal{D}_\sigma(i)$$

with $\mathcal{D}_\sigma(i)=1-n_{1,-\sigma}$, where in the last relation $[X_\lambda,\Sigma_i\mathcal{D}_\sigma(i)]=0$ was used. When we take the average, we obtain

$$\langle[\hat{c}^\dagger_{\mathbf{k}\sigma}(\lambda),\hat{c}_{\mathbf{k}\sigma}(\lambda)]_+\rangle=\langle\mathcal{D}_\sigma(i)\rangle=:D. \quad \text{(C8)}$$

In order to evaluate the anticommutator in Eq. (C8), we have to insert the former ansatz [Eq. (C2)] for $\hat{c}_{\mathbf{k}\sigma}(\lambda)$. Here, we make an additional approximation by taking into account only the two first terms in Eq. (C2). The remaining terms have explicit spin operators $\mathbf{S}_\mathbf{q}$. In the commutator of Eq. (C8), they lead to additional contributions with one or two spin operators. Outside the antiferromagnetic phase, no magnetic order is present and also spin correlations are weak. Therefore, it seems reasonable to neglect these terms. Thus, we can approximate $\hat{c}_{\mathbf{k}\sigma}(\lambda)$ by

$$\hat{c}_{\mathbf{k}\sigma}(\lambda)=u_{\mathbf{k},\lambda}\hat{c}_{\mathbf{k}\sigma}-i\sum_{\mathbf{q}}v_{\mathbf{k},\mathbf{q},\lambda}\times\frac{J_\mathbf{q}}{4\hat{\omega}_\mathbf{q}^2}([\mathbf{S}_\mathbf{q},c_{\mathbf{k}\sigma}]\cdot\dot{\mathbf{S}}_{-\mathbf{q}}+\dot{\mathbf{S}}_{-\mathbf{q}}\cdot[\mathbf{S}_\mathbf{q},c_{\mathbf{k}\sigma}]),$$

$$=u_{\mathbf{k},\lambda}\hat{c}_{\mathbf{k}\sigma}+\frac{1}{2N}\sum_{\mathbf{q}}v_{\mathbf{k},\mathbf{q},\lambda}\frac{J_\mathbf{q}}{4\hat{\omega}_\mathbf{q}^2}\sum_{\alpha\beta\gamma}(\vec{\sigma}_{\alpha\beta}\cdot\vec{\sigma}_{\sigma\gamma})\times\sum_{\mathbf{k}'}(\varepsilon_{\mathbf{k}'}-\varepsilon_{\mathbf{k}'+\mathbf{q}})\hat{c}^\dagger_{\mathbf{k}'+\mathbf{q}\alpha}\hat{c}_{\mathbf{k}'\beta}\hat{c}_{\mathbf{k}+\mathbf{q}\gamma}. \quad \text{(C9)}$$

Inserting Eq. (C9) and $\hat{c}^{\dagger}_{\mathbf{k}\sigma}(\lambda)$ into Eq. (C8), we obtain

$$D = |u_{\mathbf{k},\lambda}|^2 D + \frac{1}{(2N)^2}\sum_{\mathbf{q}'\mathbf{q}} v^{*}_{\mathbf{k},\mathbf{q}',\lambda} v_{\mathbf{k},\mathbf{q},\lambda} \frac{J_{\mathbf{q}'}}{4\hat{\omega}^2_{\mathbf{q}'}} \frac{J_{\mathbf{q}}}{4\hat{\omega}^2_{\mathbf{q}}} \sum_{\alpha',\beta',\gamma'} \sum_{\alpha,\beta,\gamma} (\vec{\sigma}_{\beta'\alpha'}\cdot\vec{\sigma}_{\gamma'\sigma})(\vec{\sigma}_{\alpha\beta}\cdot\vec{\sigma}_{\sigma\gamma}) \times \sum_{\mathbf{k}',\mathbf{k}''} (\varepsilon_{\mathbf{k}''} - \varepsilon_{\mathbf{k}''+\mathbf{q}'})(\varepsilon_{\mathbf{k}'} - \varepsilon_{\mathbf{k}'+\mathbf{q}}) \langle [\hat{c}^{\dagger}_{\mathbf{k}+\mathbf{q}'\gamma'} \hat{c}^{\dagger}_{\mathbf{k}''\beta'} \hat{c}_{\mathbf{k}''+\mathbf{q}'\alpha'}, \hat{c}^{\dagger}_{\mathbf{k}'+\mathbf{q}\alpha} \hat{c}_{\mathbf{k}'\beta} \hat{c}_{\mathbf{k}+\mathbf{q}\gamma}]_+ \rangle. \tag{C10}$$

To find the renormalization equation for $u_{\mathbf{k},\lambda-\Delta\lambda}$, we use the same equation, thereby replacing λ by $\lambda-\Delta\lambda$. We then obtain

$$\begin{aligned} D = |u_{\mathbf{k},\lambda-\Delta\lambda}|^2 D &+ \frac{1}{(2N)^2}\sum_{\mathbf{q}'\mathbf{q}} (v^{*}_{\mathbf{k},\mathbf{q}',\lambda} + u^{*}_{\mathbf{k},\lambda}\Theta_{\mathbf{q}'}(\lambda,\Delta\lambda))(v_{\mathbf{k},\mathbf{q},\lambda} \\ &+ u_{\mathbf{k},\lambda}\Theta_{\mathbf{q}}(\lambda,\Delta\lambda)) \frac{J_{\mathbf{q}'}}{4\hat{\omega}^2_{\mathbf{q}'}} \frac{J_{\mathbf{q}}}{4\hat{\omega}^2_{\mathbf{q}}} \times \sum_{\alpha',\beta',\gamma'} \sum_{\alpha,\beta,\gamma} (\vec{\sigma}_{\beta'\alpha'}\cdot\vec{\sigma}_{\gamma'\sigma}) \\ &\times (\vec{\sigma}_{\alpha\beta}\cdot\vec{\sigma}_{\sigma\gamma}) \times \sum_{\mathbf{k}',\mathbf{k}''} (\varepsilon_{\mathbf{k}''} - \varepsilon_{\mathbf{k}''+\mathbf{q}'})(\varepsilon_{\mathbf{k}'} - \varepsilon_{\mathbf{k}'+\mathbf{q}}) \\ &\times \langle [\hat{c}^{\dagger}_{\mathbf{k}+\mathbf{q}'\gamma'} \hat{c}^{\dagger}_{\mathbf{k}''\beta'} \hat{c}_{\mathbf{k}''+\mathbf{q}'\alpha'}, \hat{c}^{\dagger}_{\mathbf{k}'+\mathbf{q}\alpha} \hat{c}_{\mathbf{k}'\beta} \hat{c}_{\mathbf{k}+\mathbf{q}\gamma}]_+ \rangle, \end{aligned} \tag{C11}$$

where we have inserted the former renormalization result [Eq. (C7)] for $v_{\mathbf{k},q,\lambda-\Delta\lambda}$. Restricting ourselves to the lowest-order contributions in $J_{\mathbf{q}}$, we can subtract Eq. (C10) from Eq. (C11) and obtain the renormalization equation which connects $u_{\mathbf{k},\lambda-\Delta\lambda}$ with $u_{\mathbf{k},\lambda}$,

$$\begin{aligned} |u_{\mathbf{k},\lambda-\Delta\lambda}|^2 D = |u_{\mathbf{k},\lambda}|^2 D &- \frac{1}{(2N)^2}\sum_{\mathbf{q}'\mathbf{q}} \frac{J_{\mathbf{q}'}}{4\hat{\omega}^2_{\mathbf{q}'}} \frac{J_{\mathbf{q}}}{4\hat{\omega}^2_{\mathbf{q}}} \sum_{\alpha',\beta',\gamma'} \sum_{\alpha,\beta,\gamma} (\vec{\sigma}_{\beta'\alpha'}\cdot\vec{\sigma}_{\gamma'\sigma}) \\ &\times (\vec{\sigma}_{\alpha\beta}\cdot\vec{\sigma}_{\sigma\gamma}) \times \{|u_{\mathbf{k},\lambda}|^2 \Theta_{\mathbf{q}'}(\lambda,\Delta\lambda)\Theta_{\mathbf{q}}(\lambda,\Delta\lambda) \\ &+ [u_{\mathbf{k},\lambda} v^{*}_{\mathbf{k},\mathbf{q}',\lambda} \Theta_{\mathbf{q}}(\lambda,\Delta\lambda) + u^{*}_{\mathbf{k},\lambda} v_{\mathbf{k},\mathbf{q},\lambda} \Theta_{\mathbf{q}'}(\lambda,\Delta\lambda)]\} \\ &\times \sum_{\mathbf{k}',\mathbf{k}''} (\varepsilon_{\mathbf{k}''} - \varepsilon_{\mathbf{k}''+\mathbf{q}'})(\varepsilon_{\mathbf{k}'} - \varepsilon_{\mathbf{k}'+\mathbf{q}}) \\ &\times \langle [\hat{c}^{\dagger}_{\mathbf{k}+\mathbf{q}'\gamma'} \hat{c}^{\dagger}_{\mathbf{k}''\beta'} \hat{c}_{\mathbf{k}''+\mathbf{q}'\alpha'}, \hat{c}^{\dagger}_{\mathbf{k}'+\mathbf{q}\alpha} \hat{c}_{\mathbf{k}'\beta} \hat{c}_{\mathbf{k}+\mathbf{q}\gamma}]_+ \rangle. \end{aligned} \tag{C12}$$

What remains is to evaluate the commutator in Eq. (C12). In a final factorization approximation, we find

$$\begin{aligned} |u_{\mathbf{k},\lambda-\Delta\lambda}|^2 = |u_{\mathbf{k},\lambda}|^2 &- \frac{1}{(2N)^2}\sum_{\mathbf{q}} \left(\frac{J_{\mathbf{q}}}{4\hat{\omega}^2_{\mathbf{q}}}\right)^2 \sum_{\alpha,\beta,\gamma} |\vec{\sigma}_{\alpha\beta}\cdot\vec{\sigma}_{\sigma\gamma}|^2 \\ &\times \Theta_{\mathbf{q}}(\lambda,\Delta\lambda)\{|u_{\mathbf{k},\lambda}|^2 + (u_{\mathbf{k},\lambda} v^{*}_{\mathbf{k},\mathbf{q},\lambda} + u^{*}_{\mathbf{k},\lambda} v_{\mathbf{k},\mathbf{q},\lambda})\} \\ &\times \sum_{\mathbf{k}'} (\varepsilon_{\mathbf{k}'} - \varepsilon_{\mathbf{k}'+\mathbf{q}})^2 \{n_{\mathbf{k}+\mathbf{q}}(n_{\mathbf{k}'} + D) + n_{\mathbf{k}'+\mathbf{q}}(m_{\mathbf{k}'} \\ &- n_{\mathbf{k}+\mathbf{q}})\} + \frac{1}{(2N)^2}\sum_{\mathbf{q}'\mathbf{q}} \frac{J_{\mathbf{q}'}}{4\hat{\omega}^2_{\mathbf{q}'}} \frac{J_{\mathbf{q}}}{4\hat{\omega}^2_{\mathbf{q}}} \sum_{\alpha,\beta,\gamma} (\vec{\sigma}_{\gamma\alpha}\cdot\vec{\sigma}_{\beta\sigma}) \\ &\times (\vec{\sigma}_{\alpha\beta}\cdot\vec{\sigma}_{\sigma\gamma}) \times \{|u_{\mathbf{k},\lambda}|^2 \Theta_{\mathbf{q}'}(\lambda,\Delta\lambda)\Theta_{\mathbf{q}}(\lambda,\Delta\lambda) \\ &+ [u_{\mathbf{k},\lambda} v^{*}_{\mathbf{k},\mathbf{q}',\lambda} \Theta_{\mathbf{q}}(\lambda,\Delta\lambda) + u^{*}_{\mathbf{k},\lambda} v_{\mathbf{k},\mathbf{q},\lambda} \Theta_{\mathbf{q}'}(\lambda,\Delta\lambda)]\} \\ &\times (\varepsilon_{\mathbf{k}+\mathbf{q}} - \varepsilon_{\mathbf{k}+\mathbf{q}+\mathbf{q}'})(\varepsilon_{\mathbf{k}+\mathbf{q}'} - \varepsilon_{\mathbf{k}+\mathbf{q}'+\mathbf{q}})\{n_{\mathbf{k}+\mathbf{q}'}(n_{\mathbf{k}+\mathbf{q}} \\ &+ D) + n_{\mathbf{k}+\mathbf{q}+\mathbf{q}'}(m_{\mathbf{k}+\mathbf{q}} - n_{\mathbf{k}+\mathbf{q}'})\}. \end{aligned} \tag{C13}$$

Summing over the spin indices and exploiting that $u_{\mathbf{k},\lambda}$ and $v_{\mathbf{k},\mathbf{q},\lambda}$ are real, we arrive at expression (60).

APPENDIX D: FACTORIZATION OF $\dot{\mathbf{S}}_{\mathbf{q},\lambda}\dot{\mathbf{S}}_{-\mathbf{q},\lambda}$ FOR THE SUPERCONDUCTING PHASE

The aim of this appendix is to simplify the operator product $\dot{\mathbf{S}}_{\mathbf{q},\lambda}\dot{\mathbf{S}}_{-\mathbf{q},\lambda}$ for the superconducting phase, which enters expressions (85) for $\mathcal{H}_{0,\lambda}$ and $\mathcal{H}_{1,\lambda}$. Neglecting in the notation again the index λ, we start from the expression

$$\begin{aligned} \dot{\mathbf{S}}_{\mathbf{q}}\dot{\mathbf{S}}_{-\mathbf{q}} = \frac{1}{4N}\sum_{\alpha\beta}\sum_{\gamma\delta} &(\vec{\sigma}_{\alpha\beta}\cdot\vec{\sigma}_{\delta\gamma}) \\ &\times \sum_{i\neq j} t_{ij}(e^{i\mathbf{q}\mathbf{R}_i} - e^{i\mathbf{q}\mathbf{R}_j}) \\ &\times \sum_{l\neq m} t_{lm}(e^{-i\mathbf{q}\mathbf{R}_l} - e^{-i\mathbf{q}\mathbf{R}_m}) \hat{c}^{\dagger}_{i\alpha}\hat{c}_{j\beta}\hat{c}^{\dagger}_{m\delta}\hat{c}_{l\gamma}. \end{aligned} \tag{D1}$$

Note that the four-fermion operator on the right-hand side can be factorized in two different ways: One can either reduce it to operators $\hat{c}^{\dagger}_{\mathbf{k}\sigma}\hat{c}_{\mathbf{k}\sigma}$ or to operators $\hat{c}^{\dagger}_{\mathbf{k}\sigma}\hat{c}^{\dagger}_{-\mathbf{k},-\sigma}$ and $\hat{c}_{-\mathbf{k},-\sigma}\hat{c}_{\mathbf{k},\sigma}$. The first factorization type was discussed in Appendix B and leads to a renormalization of $\varepsilon_{\mathbf{k}}$. Here, we are interested in a factorization which renormalizes the superconducting order parameter $\Delta_{\mathbf{k}}$. Thereby, we have to pay attention to the fact that the averaged spin operator vanishes $\langle \mathbf{S}_i \rangle = 0$ outside the antiferromagnetic regime. Moreover, all local indices in the four-fermion term of Eq. (D1) should be different from each other. This follows from the former decomposition of the exchange interaction into eigenmodes of L_l, where we have implicitly assumed that the operators $\dot{\mathbf{S}}_{\mathbf{q}}$ and $\dot{\mathbf{S}}_{-\mathbf{q}}$ do not overlap in the local space. Otherwise, the decomposition would be much more involved. However, it can be shown that these interference terms only make a minor impact on the results.

By assuming spin-singlet pairing, we obtain from Eq. (D1),

$$\dot{\mathbf{S}}_{\mathbf{q}}\dot{\mathbf{S}}_{-\mathbf{q}}|_{(\mathrm{sc})} = \frac{1}{2N}\sum_{\mathbf{k}} (\varepsilon_{\mathbf{k}} - \varepsilon_{\mathbf{k}-\mathbf{q}})^2 (\hat{c}^{\dagger}_{\mathbf{k}\uparrow}\hat{c}^{\dagger}_{-\mathbf{k}\downarrow}\hat{c}_{-(\mathbf{k}-\mathbf{q})\downarrow}\hat{c}_{\mathbf{k}-\mathbf{q}\uparrow} + 2\hat{c}^{\dagger}_{\mathbf{k}\uparrow}\hat{c}^{\dagger}_{-\mathbf{k}\downarrow}\hat{c}_{\mathbf{k}-\mathbf{q}\downarrow}\hat{c}_{-(\mathbf{k}-\mathbf{q})\uparrow}). \quad \text{(D2)}$$

According to Sec. VI A, expression (D2) leads to the main part of the superconducting pair interaction. In a factorization approximation, the two contributions in Eq. (D2) can be combined to

$$\dot{\mathbf{S}}_{\mathbf{q}}\dot{\mathbf{S}}_{-\mathbf{q}}|_{(\mathrm{sc})} = \frac{3}{2N}\sum_{\mathbf{k}} (\varepsilon_{\mathbf{k}} - \varepsilon_{\mathbf{k}-\mathbf{q}})^2 \times \{\langle \hat{c}_{-(\mathbf{k}-\mathbf{q})\downarrow}\hat{c}_{\mathbf{k}-\mathbf{q}\uparrow}\rangle \hat{c}^{\dagger}_{\mathbf{k}\uparrow}\hat{c}^{\dagger}_{-\mathbf{k}\downarrow} + h.c.\}. \quad \text{(D3)}$$

Using Eq. (D3), one is led to the renormalization result [Eq. (91)] for $\tilde{\varepsilon}^{(0)}_{\mathbf{k}}$ and $\tilde{\Delta}^{(0)}_{\mathbf{k}}$ to first order in J.

The above factorization can also be used to derive second-order renormalization contribution (86) to $\Delta_{\mathbf{k},\lambda-\Delta\lambda}$. With expression (D2), we can first simplify the second-order renormalization $\mathcal{H}^{(2)}_{\lambda-\Delta\lambda}$ of $\mathcal{H}_{\lambda-\Delta\lambda}$. In analogy to the results of Appendix B, we arrive at

$$\begin{aligned}
\mathcal{H}^{(2)}_{\lambda-\Delta\lambda} = {} & 3\sum_{\mathbf{q}} \left(\frac{J_{\mathbf{q}}}{4\hat{\omega}^2_{\mathbf{q}}}\right)^2 \Theta_{\mathbf{q}}(\lambda,\Delta\lambda)\left(\left[\frac{1}{N}\sum_{\mathbf{k}\sigma}(2\varepsilon_{\mathbf{k}} - \varepsilon_{\mathbf{k}+\mathbf{q}} - \varepsilon_{\mathbf{k}-\mathbf{q}})\langle \hat{c}^{\dagger}_{\mathbf{k}\sigma}\hat{c}_{\mathbf{k}\sigma}\rangle\right]\mathbf{S}_{\mathbf{q}}\cdot\mathbf{S}_{-\mathbf{q}} + \langle \mathbf{S}_{\mathbf{q}}\cdot\mathbf{S}_{-\mathbf{q}}\rangle \frac{1}{N}\sum_{\mathbf{k}\sigma}(2\varepsilon_{\mathbf{k}} - \varepsilon_{\mathbf{k}+\mathbf{q}} - \varepsilon_{\mathbf{k}-\mathbf{q}})\hat{c}^{\dagger}_{\mathbf{k}\sigma}\hat{c}_{\mathbf{k}\sigma}\right) \\
& - \sum_{\mathbf{q}} \left(\frac{J_{\mathbf{q}}}{4\hat{\omega}^2_{\mathbf{q}}}\right)^2 \Theta_{\mathbf{q}}(\lambda,\Delta\lambda)\langle \dot{\mathbf{S}}_{\mathbf{q}}\cdot\dot{\mathbf{S}}_{-\mathbf{q}}\rangle \frac{1}{N}\sum_{\mathbf{k}\sigma}(2\varepsilon_{\mathbf{k}} - \varepsilon_{\mathbf{k}+\mathbf{q}} - \varepsilon_{\mathbf{k}-\mathbf{q}})\hat{c}^{\dagger}_{\mathbf{k}\sigma}\hat{c}_{\mathbf{k}\sigma} \\
& + \frac{3}{2N}\sum_{\mathbf{q}\sigma} \left(\frac{J_{\mathbf{q}}}{4\hat{\omega}^2_{\mathbf{q}}}\right)^2 \Theta_{\mathbf{q}}(\lambda,\Delta\lambda)\left[\frac{1}{N}\sum_{\mathbf{k}'\sigma'}(2\varepsilon_{\mathbf{k}'} - \varepsilon_{\mathbf{k}'+\mathbf{q}} - \varepsilon_{\mathbf{k}'-\mathbf{q}})\langle \hat{c}^{\dagger}_{\mathbf{k}'\sigma'}\hat{c}_{\mathbf{k}'\sigma'}\rangle\right] \\
& \times \sum_{\mathbf{k}\sigma} (\varepsilon_{\mathbf{k}} - \varepsilon_{\mathbf{k}-\mathbf{q}})^2 \langle (\hat{c}^{\dagger}_{\mathbf{k}-\mathbf{q}\alpha}\hat{c}_{\mathbf{k}-\mathbf{q}\alpha})_{NL}\rangle (\hat{c}^{\dagger}_{\mathbf{k}\sigma}\hat{c}_{\mathbf{k}\sigma})_{NL} - \frac{1}{2N}\sum_{\mathbf{q}\sigma}\left(\frac{J_{\mathbf{q}}}{4\hat{\omega}^2_{\mathbf{q}}}\right)^2 \Theta_{\mathbf{q}}(\lambda,\Delta\lambda)\left[\frac{1}{N}\sum_{\mathbf{k}'\sigma'}(2\varepsilon_{\mathbf{k}'} - \varepsilon_{\mathbf{k}'+\mathbf{q}} - \varepsilon_{\mathbf{k}'-\mathbf{q}})\langle \hat{c}^{\dagger}_{\mathbf{k}'\sigma'}\hat{c}_{\mathbf{k}'\sigma'}\rangle\right] \\
& \times \sum_{\mathbf{k}} (\varepsilon_{\mathbf{k}} - \varepsilon_{\mathbf{k}-\mathbf{q}})^2 \langle (\hat{c}_{\mathbf{k}-\mathbf{q}\downarrow}\hat{c}_{\mathbf{k}-\mathbf{q}\uparrow})\rangle (\hat{c}^{\dagger}_{\mathbf{k}\uparrow}\hat{c}^{\dagger}_{\mathbf{k}\downarrow} + h.c.). \quad \text{(D4)}
\end{aligned}$$

From Eq. (D4), the second-order renormalization to $\Delta_{\mathbf{k},\lambda-\Delta\lambda}$ can immediately be deduced.

APPENDIX E: BOGOLIUBOV TRANSFORMATION FOR THE SUPERCONDUCTING HAMILTONIAN $\tilde{\mathcal{H}}$

The aim of this appendix is to diagonalize the renormalized Hamiltonian $\tilde{\mathcal{H}}$ for the superconducting phase. According to Eq. (92), the Hamiltonian $\tilde{\mathcal{H}}$ reads

$$\tilde{\mathcal{H}} = \sum_{\mathbf{k}\sigma} \tilde{\varepsilon}_{\mathbf{k}}\hat{c}^{\dagger}_{\mathbf{k}\sigma}\hat{c}_{\mathbf{k}\sigma} - \sum_{\mathbf{k}} (\tilde{\Delta}_{\mathbf{k}}\hat{c}^{\dagger}_{\mathbf{k},\uparrow}\hat{c}^{\dagger}_{-\mathbf{k},\downarrow} + \tilde{\Delta}^{*}_{\mathbf{k}}\hat{c}_{-\mathbf{k},\downarrow}\hat{c}_{\mathbf{k},\uparrow}) + \tilde{E}. \quad \text{(E1)}$$

Due to the presence of the Hubbard operators in Eq. (E1), the usual Bogoliubov transformation can only be applied approximately. Let us start by introducing new fermion operators,

$$\alpha^{\dagger}_{\mathbf{k}} = \mathsf{U}_{\mathbf{k}}\hat{c}^{\dagger}_{\mathbf{k},\uparrow} - \mathsf{V}_{\mathbf{k}}\hat{c}_{-\mathbf{k},\downarrow},$$

$$\beta^{\dagger}_{\mathbf{k}} = \mathsf{U}_{\mathbf{k}}\hat{c}^{\dagger}_{-\mathbf{k},\downarrow} + \mathsf{V}_{\mathbf{k}}\hat{c}_{\mathbf{k},\uparrow}. \quad \text{(E2)}$$

We require that $\alpha^{\dagger}_{\mathbf{k}}$ and $\beta^{\dagger}_{\mathbf{k}}$ are eigenmodes of $\tilde{\mathcal{H}}$,

$$\tilde{\mathsf{L}}\alpha^{\dagger}_{\mathbf{k}} = E_{\mathbf{k}}\alpha^{\dagger}_{\mathbf{k}}, \quad \tilde{\mathsf{L}}\beta^{\dagger}_{\mathbf{k}} = E_{\mathbf{k}}\beta^{\dagger}_{\mathbf{k}}. \quad \text{(E3)}$$

In order to find equations for $\mathsf{U}_{\mathbf{k}}$ and $\mathsf{V}_{\mathbf{k}}$, let us insert expression (E2) for $\alpha^{\dagger}_{\mathbf{k}}$ into the first equation of Eq. (E3),

$$\mathsf{U}_{\mathbf{k}}\tilde{\mathsf{L}}\hat{c}^{\dagger}_{\mathbf{k},\uparrow} - \mathsf{V}_{\mathbf{k}}\tilde{\mathsf{L}}\hat{c}_{-\mathbf{k},\downarrow} = E_{\mathbf{k}}(\mathsf{U}_{\mathbf{k}}\hat{c}^{\dagger}_{\mathbf{k},\uparrow} - \mathsf{V}_{\mathbf{k}}\hat{c}_{-\mathbf{k},\downarrow}). \quad \text{(E4)}$$

The two commutators on the left-hand side of Eq. (E4) will be evaluated separately. For the first one, $\tilde{\mathsf{L}}\hat{c}_{\mathbf{k}\sigma} = [\tilde{\mathcal{H}}, \hat{c}^{\dagger}_{\mathbf{k},\uparrow}]$, we obtain

$$\tilde{\mathsf{L}}\hat{c}^{\dagger}_{\mathbf{k},\uparrow} = \tilde{\mathsf{L}}_t\hat{c}^{\dagger}_{\mathbf{k},\uparrow} - \sum_{\mathbf{k}'} \tilde{\Delta}^{*}_{\mathbf{k}'}[\hat{c}_{-\mathbf{k}',\downarrow}\hat{c}_{\mathbf{k}',\uparrow},\hat{c}^{\dagger}_{\mathbf{k},\uparrow}].$$

Here, the Liouville operator $\tilde{\mathsf{L}}_t$ corresponds to the commutator with the hopping Hamiltonian $\tilde{\mathcal{H}}_t = \Sigma_{\mathbf{k}}\tilde{\varepsilon}_{\mathbf{k}}\hat{c}^{\dagger}_{\mathbf{k}\sigma}\hat{c}_{\mathbf{k}\sigma}$, which agrees with the fully renormalized Hamiltonian $\tilde{\mathcal{H}}$ in the normal state investigated in Sec. IV. Therefore, we can use $\tilde{\mathsf{L}}_t\hat{c}^{\dagger}_{\mathbf{k},\uparrow} = \tilde{\varepsilon}_{\mathbf{k}}\hat{c}^{\dagger}_{\mathbf{k}\sigma}$ and find using anticommutator relation (3)

$$\tilde{\mathsf{L}}\hat{c}^{\dagger}_{\mathbf{k},\uparrow} = \tilde{\varepsilon}_{\mathbf{k}}\hat{c}^{\dagger}_{\mathbf{k},\uparrow} - \frac{1}{\sqrt{N}}\sum_{i\neq j} \tilde{\Delta}^{*}_{i,j}(e^{-i\mathbf{k}\mathbf{R}_j}\mathcal{D}_{\uparrow}(j)\hat{c}_{i,\downarrow} - e^{-i\mathbf{k}\mathbf{R}_i}S^{-}_i\hat{c}_{j,\uparrow}). \quad \text{(E5)}$$

The quantity $\tilde{\Delta}^{*}_{i,j}$ is defined by $\tilde{\Delta}^{*}_{i,j} = \frac{1}{N}\Sigma_{\mathbf{k}}\tilde{\Delta}^{*}_{\mathbf{k}}e^{i\mathbf{k}(\mathbf{R}_i - \mathbf{R}_j)}$, and $\mathcal{D}_{\sigma}(j) = 1 - n_{j,-\sigma} = \mathcal{P}_0 + \hat{n}_{i\sigma}$ was already given in Eq. (4). The main contribution to the second term in Eq. (E5) is caused by the following process: First, two holes are generated at sites i and j before the hole at j is annihilated again by a local creation operator in $\hat{c}^{\dagger}_{\mathbf{k}\uparrow}$. The arising local projector $\mathcal{D}_{\sigma}(i)$

will be approximated by its average $D=\langle \mathcal{D}_\sigma(j)\rangle = 1-\langle n_{j,-\sigma}\rangle$. Thus, we obtain

$$\tilde{L}\hat{c}^\dagger_{\mathbf{k},\uparrow} = \tilde{\varepsilon}_\mathbf{k}\hat{c}^\dagger_{\mathbf{k},\uparrow} - \frac{D}{\sqrt{N}}\sum_{i\neq j}\tilde{\Delta}^*_{i,j}e^{-i\mathbf{k}\mathbf{R}_j}\hat{c}_{i,\downarrow},$$

$$= \tilde{\varepsilon}_\mathbf{k}\hat{c}^\dagger_{\mathbf{k},\uparrow} - D\tilde{\Delta}^*_\mathbf{k}c_{-\mathbf{k},\downarrow}, \tag{E6}$$

where $\tilde{\Delta}^*_{i,j}$ was Fourier back transformed to $\tilde{\Delta}^*_\mathbf{k}$. A corresponding contribution from the last term in Eq. (E5) vanishes since $\langle S_i^-\rangle = 0$ outside the antiferromagnetic regime. The evaluation of the second commutator in Eq. (E4) can be done in analogy to result (E6),

$$\tilde{L}\hat{c}_{-\mathbf{k},\downarrow} = -\tilde{\varepsilon}_\mathbf{k}\hat{c}_{-\mathbf{k},\downarrow} - D\tilde{\Delta}_\mathbf{k}c^\dagger_{\mathbf{k},\uparrow}. \tag{E7}$$

Inserting Eqs. (E6) and (E7) into Eq. (E4) leads to the following two equations for $\mathsf{U}_\mathbf{k}$ and $\mathsf{V}_\mathbf{k}$:

$$\mathsf{U}_\mathbf{k}(\tilde{\varepsilon}_\mathbf{k} - E_\mathbf{k}) + \mathsf{V}_\mathbf{k}D\tilde{\Delta}_\mathbf{k} = 0,$$

$$-\mathsf{U}_\mathbf{k}D\tilde{\Delta}^*_\mathbf{k} + \mathsf{V}_\mathbf{k}(\tilde{\varepsilon}_\mathbf{k} + E_\mathbf{k}) = 0. \tag{E8}$$

The eigenvalue $E_\mathbf{k}$ for this system of equations is easily obtained,

$$E_\mathbf{k} = \sqrt{\tilde{\varepsilon}^2_\mathbf{k} + D^2|\tilde{\Delta}_\mathbf{k}|^2}. \tag{E9}$$

The expectation value $\langle \hat{c}^\dagger_{\mathbf{k},\uparrow}\hat{c}_{-\mathbf{k},\downarrow}\rangle_{\tilde{\mathcal{H}}}$, formed with the superconducting Hamiltonian $\tilde{\mathcal{H}}$, is found by solving Eqs. (E2) for $\hat{c}^\dagger_{\mathbf{k},\uparrow}$ and $\hat{c}_{-\mathbf{k},\downarrow}$. Using property (E3), one finds

$$\langle \hat{c}^\dagger_{\mathbf{k},\uparrow}\hat{c}^\dagger_{-\mathbf{k},\downarrow}\rangle_{\tilde{\mathcal{H}}} = \frac{D^2\tilde{\Delta}^*_\mathbf{k}}{2E_\mathbf{k}}\left(1 - \frac{2}{1+e^{\beta E_\mathbf{k}}}\right). \tag{E10}$$

[1] J. G. Bednorz and K. A. Müller, Z. Phys. B: Condens. Matter **64**, 189 (1986).
[2] J. Corson, R. Mallozzi, J. Orenstein, J. N. Eckstein, and I. Bozovic, Nature (London) **398**, 221 (1999).
[3] V. J. Emery and S. A. Kivelson, Nature (London) **374**, 434 (1995).
[4] D. Pines, Pure Appl. Chem. **282-287**, 273 (1997).
[5] M. Randeria, arXiv:cond-mat/9710223 (unpublished).
[6] C. M. Varma, Phys. Rev. B **55**, 14554 (1997).
[7] M. R. Norman *et al.*, Nature (London) **392**, 157 (1998).
[8] K. M. Shen, F. Ronning, D. H. Lu, F. Baumberger, N. J. C. Ingle, W. S. Lee, W. Meevasana, Y. Kohsaka, M. Azuma, M. Takano, H. Takagi, and Z.-X. Shen, Science **307**, 901 (2005).
[9] A. Kanigel *et al.*, Nat. Phys. **2**, 447 (2006).
[10] K. Terashima, H. Matsui, T. Sato, T. Takahashi, M. Kofu, and K. Hirota, Phys. Rev. Lett. **99**, 017003 (2007).
[11] A. Kanigel, U. Chatterjee, M. Randeria, M. R. Norman, S. Souma, M. Shi, Z. Z. Li H. Raffy, and J. C. Campuzano, Phys. Rev. Lett. **99**, 157001 (2007).
[12] A. Kanigel, U. Chatterjee, M. Randeria, M. R. Norman, G. Koren, K. Kadowaki, and J. C. Campuzano, Phys. Rev. Lett. **101**, 137002 (2008).
[13] J. Chang *et al.*, New J. Phys. **10**, 103016 (2008).
[14] H. Ding, T. Yokoya, J. C. Campuzano, T. Takahashi, M. Randeria, M. R. Norman, T. Mochikuparallel, K. Kadowakiparallel, and J. Giapintzakis, Nature (London) **382**, 51 (1996).
[15] A. G. Loeser, Z.-X. Shen, D. S. Dessau, D. S. Marshall, C. H. Park, P. Fournier, and A. Kapitulnik, Science **273**, 325 (1996).
[16] K. W. Becker, A. Hübsch, and T. Sommer, Phys. Rev. B **66**, 235115 (2002); for a review see A. Hübsch, S. Sykora, and K. W. Becker, arXiv:0809.3360 (unpublished).
[17] A. Hübsch and K. W. Becker, Eur. Phys. J. B **33**, 391 (2003).
[18] P. Fazekas in *Lecture Notes on Electron Correlations and Magnetism* (World Scientific, Singapore, 1999).
[19] K. Seiler, C. Gros, T. M. Rice, K. Ueda, and D. Vollhardt, J. Low Temp. Phys. **64**, 195 (1986).
[20] J. L. Tallon and J. W. Loram, Physica C **349**, 53 (2001).
[21] J. Bardeen, L. N. Cooper, and J. R. Schrieffer, Phys. Rev. **108**, 1175 (1957).